

Time series analysis of selected geothermal spring temperature recordings

Prepared by:

Poyan Nikrou¹, Juliet Newson² & Robert McKibbin¹

¹Massey University

²The University of Auckland

For:

Waikato Regional Council

Private Bag 3038

Waikato Mail Centre

HAMILTON 3240

May 2013

Document #: 2395548

Peer reviewed by:
Katherine Luketina

Date May 2013

Approved for release by:
Dr Edmund Brown

Date May 2013

Disclaimer

This technical report has been prepared for the use of Waikato Regional Council as a reference document and as such does not constitute Council's policy.

Council requests that if excerpts or inferences are drawn from this document for further use by individuals or organisations, due care should be taken to ensure that the appropriate context has been preserved, and is accurately reflected and referenced in any subsequent spoken or written communication.

While Waikato Regional Council has exercised all reasonable skill and care in controlling the contents of this report, Council accepts no liability in contract, tort or otherwise, for any loss, damage, injury or expense (whether direct, indirect or consequential) arising out of the provision of this information or its use by you or any other party.

Time series analysis of selected geothermal spring temperature recordings

Poyan Nikrou¹, Juliet Newson² & Robert McKibbin³

**A report under Contract No RIG376
between Waikato Regional Council and Massey University**

¹ Massey University

² The University of Auckland

³ Massey University

ABSTRACT

The aim of this study was to examine spring temperature time-series data recorded from two geothermal pools, the Waiotapu Geyser in Waiotapu and the Soda Fountain in Orakei Korako. There are five sets of temperature recordings on the Soda Fountain and four on the Waiotapu Geyser; each dataset is 45 days long with temperature recorded every 2 minutes. Both springs show cyclic behaviour in their temperature recordings. The Waiotapu Geyser shows a distinct cyclic pattern throughout some periods followed by periods of constant temperature (around 80 °C), whereas the Soda fountain shows persistent cyclic patterns at all times.

The effects of rainfall, air pressure, air temperature and seismic activity were analysed in order to ascertain whether there are any relationships between the spring temperatures and any of these factors. Air temperature, rainfall and seismic events did not appear to have much impact on the Waiotapu geyser throughout the period analysed. However, it was found that variations in air pressure could set off or inhibit eruptions at the Waiotapu Geyser as well as affecting its eruption frequency. Generally during periods of high air pressure the geyser did not erupt and its temperature was constant. However, as the air pressure dropped, the geyser began to erupt; further lowering of the air pressure had the effect of making eruptions more frequent. It was speculated that variations in air pressure lead to variations in the filling/heating rates of the Waiotapu Geyser and hence its eruption frequency. These speculations were tested against the data and some evidence was found to support the speculations; however, the evidence was not very strong and rested on the set of assumptions made.

The Soda Fountain, on the other hand, did not seem to be affected by rainfall, air pressure, air temperature or seismic activity throughout the period analysed. This spring did however show a persistent one to two-hourly temperature cycle.

Recommendations for future monitoring, based on lessons learnt from this data analysis are: ensuring continuous data collection rather than discrete datasets; co-recording of water level or pressure data; and multi-level temperature measurements in the spring feed channel.

TABLE OF CONTENTS

1	INTRODUCTION.....	1
1.1	Cyclic activity in geothermal springs.....	3
2	WAIOTAPU GEYSER	9
2.1	Introduction	9
2.2	Description.....	9
2.3	The Data.....	12
2.4	Examining the effects of climate factors.....	17
2.5	Seismic events and spring temperature.....	20
2.6	Fourier analysis	22
2.7	Frequency and air pressure	26
2.8	Waiotapu Geyser: Summary and conclusions.....	47
3	SODA FOUNTAIN	49
3.1	Introduction	49
3.2	Description.....	49
3.3	The Data.....	52
3.4	Examining the effects of climate factors.....	56
3.5	Seismic activity.....	59
3.6	Fourier Analysis.....	62
3.7	Air pressure and the temperature cycle	69
3.8	Soda Fountain: Conclusion	74
4	DISCUSSION AND RECOMMENDATIONS FOR FUTURE MONITORING.....	75
5	REFERENCES.....	75

1 INTRODUCTION

New Zealand's regional councils monitor selected geothermal springs in order to fulfil their legislative responsibility for management of New Zealand's geothermal resource. The subject of this study is data collected from geothermal features as part of the Waikato Regional Council Geothermal Feature Monitoring Program. The data was collected from the Waiotapu Geyser (WRC ID 72_3007) at the Waiotapu Thermal Area, and the Soda Fountain Pool (WRC ID 3065_22) at Orakei Korako. Both Waiotapu and Orakei Korako are located in the Taupo Volcanic Zone (TVZ) of the North Island, New Zealand (Figure 1), and are high-temperature, two-phase, liquid-dominated geothermal systems.

Most temperature monitoring is 'spot' or a single measurement per visit, which results in data points three months to one year apart. However the data presented here is temperature time series data from two boiling or near-boiling springs. Each time series is 45 days long, and the time between data collection points is two minutes.

The aim of this study is to conduct a quantitative analysis of this data, which was initially described in the 2010 and 2011 Geothermal Features Monitoring Reports (Newson, 2011). A preliminary analysis was presented at the International Union of Geodesy and Geophysics General Assembly in 2011 (Newson and Netten, 2011).

The data presented and analysed here is a small sample of the geyser monitoring records collected by Waikato Regional Council since 1995, which is available from the Council on request.

The two springs which are the subject of this study exhibit cyclic temperature variation. The first high-temperature spring, the Waiotapu Geyser, has a mean temperature over the recording time of 86.76°C, and shows times of strong cyclic activity that continues for two to six days, with intervening times of non-cyclic behaviour. Data from this spring has a distinctive 'shape' of the temperature cycle which appears to be independent of frequency. The second, the Soda Fountain at Orakei Korako, exhibits cyclic temperature variation over the entire data collection interval. The pools also exhibit water-level changes, although unfortunately these were not recorded due to equipment limitations.

The processes that cause temperature variations in the Waiotapu Geyser and the Soda Fountain are unknown, however it is possible that these regular temperature variations are sensitive to system disturbance by climatic or seismic events. In addition to characterising the spring temperature data, publicly-available environmental data (climatic and seismic) has been used to investigate whether there is a correlation between this and the spring temperature.

This study here is a qualitative and quantitative analysis of the data from the two springs described above. Avenues of investigation were:

- A relation between climate data (rainfall, air pressure, and air temperature) and spring temperature.
- A relation between seismic events and spring temperature.
- Whether there are dominant frequencies in the cyclic data.

- A detailed examination of the relationship between spring activity and air pressure.

The report concludes with a discussion of the lessons from this study and recommendations for future monitoring programmes.

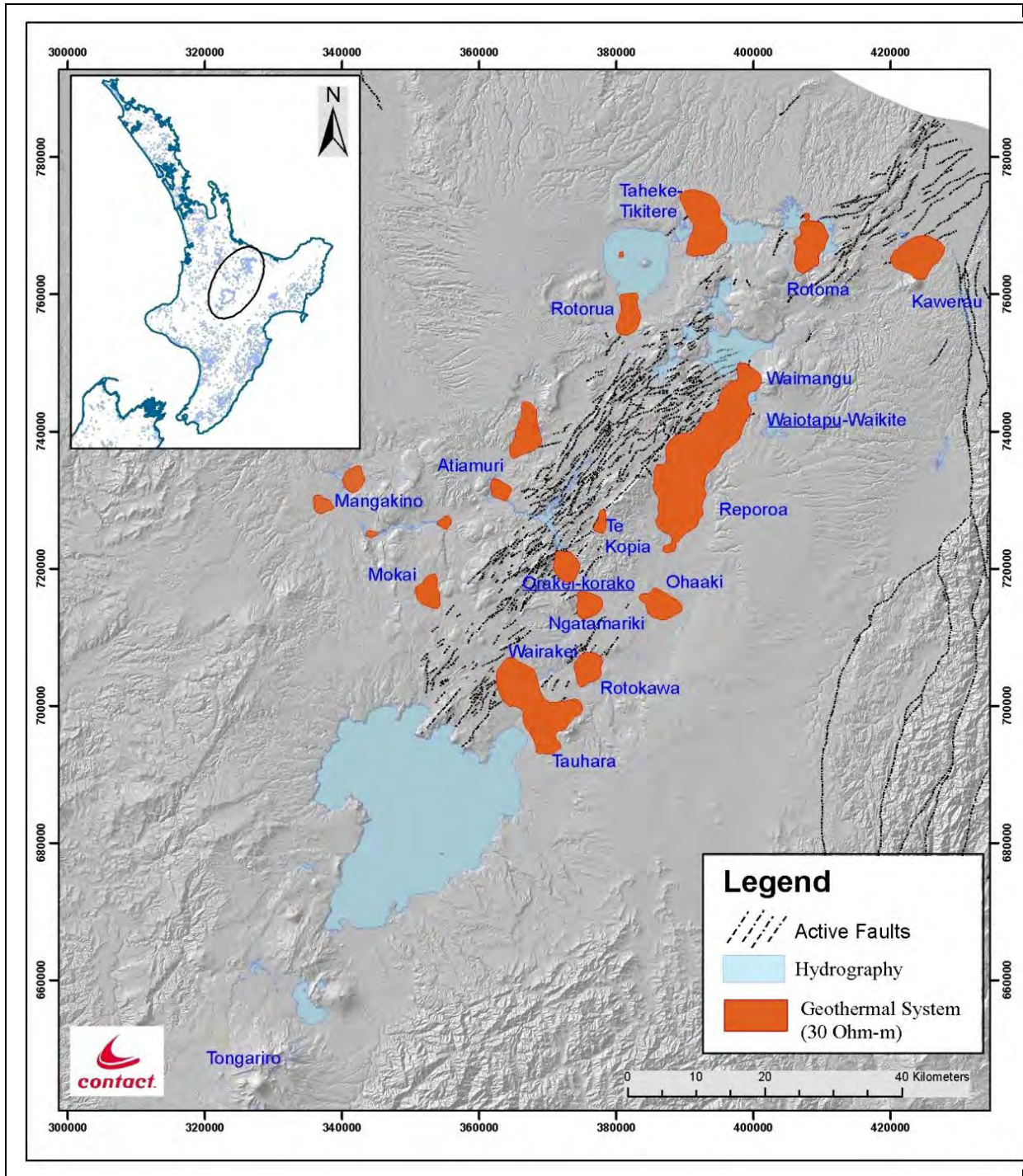


Figure 1. The Taupo Volcanic Zone. The geothermal systems are identified by the outline of the ground resistivity at approximately 500 m depth. Waiotapu is part of the greater Waimangu–Reporoa system.

1.1 Cyclic activity in geothermal springs

This study is concerned only with geothermal springs which discharge liquid water, or a mixture of water and steam, from a point source, and that show a cyclic nature in their activity. It is reasonable to assume that the periodic behaviour of all geothermal pools with respect to temperature, water level, outflow, or activity, are related to the same mechanisms. Thus the periodic behaviour of geysers is due to the same factors as a near-boiling pool with periodic changes in water level. The strength of the response is due to the particular parameters of the system and the magnitude of the inputs. In this section we give a brief review of examples of periodicity; a simple conceptual model of geyser 'plumbing'; temperature – time series from a laboratory model of a geyser; and factors which may influence periodicity. This is intended to give a context to discussions and analysis of the Waiotapu Geyser and Soda Fountain data.

1.1.1 Examples

The most spectacular example of periodicity are large geysers, such as at Whakarewarewa, Rotorua, New Zealand, which periodically and spectacularly discharge water and steam then become quiescent again. However, there are many examples of smaller pools which erupt predominantly liquid to heights of a few metres; for instance Taumatapuhipuhi at Tokaanu, New Zealand, has been observed to erupt hot water to a height of approximately 1.2 m with a period of 2 to 5 minutes (Newson, 2011). The Waiotapu Geyser has also been observed to erupt to a height of one metre or less (see Figure 10).

However, other geothermal springs also have cyclic activity, although they are not described as "geysers" in the traditional sense. Keam (pers. comm.) describes Inferno Crater at Waimangu New Zealand as a "crypto-geyser". This large ~60 m diameter hydrothermal eruption crater is completely occupied by a geothermal pool whose water level rises and falls 8 m over a period of 6–10 weeks; in addition, the level of the water in the pool is inversely related to the water level in the adjacent crater (Frying Pan Flat) (Scott, 1994). Other pools show a cyclic variation in the degree of activity; for example, Manaroa spring at Waikite, New Zealand, boils continuously, but with more vigorous activity and up-doming of the water surface every 30 to 60 seconds (Newson, 2011).

Some springs are known to periodically overflow, for instance, the Soda Fountain Spring at Orakei Korako (one of the two springs featured in this study) (Newson, 2011). While the Soda Fountain inflow does not always break the surface of the water (erupt), it displays more vigorous activity prior to and during overflow. The Soda Fountain is known to exhibit geysering, although this has not been observed by the authors.

The most visible manifestation of periodic behaviour is the variation in water level and/or mass flow from geothermal springs. In conceptual models of geysers, the eruption, or increase in mass flow from the geyser, is due to boiling in the immediate subsurface (Saptadji, 1995; Bryan, 2008). For the duration of the eruption the steam pushes the overlying column of water above the level of the pool, or ground level. Laboratory results from Saptadji (1995) show that the start of eruption is correlated with maximum water temperature. Temperature records from Inferno Crater also show that the temperature variation is positively correlated with water level (Scott, 1994). This study is concerned

with temperature records only; however, the assumption is made that temperature high will coincide with an increase in spring water level or outflow; or with an actual eruption.

1.1.2 Conceptual Model

Ingebritsen & Rojstaczer (1996) describe two conceptual models of geysers which only invoke a permeability contrast in the subsurface. Figure 2 "shows two conceptual models of geyser systems: the classic model of a more-or-less open chamber constricted at the top [Figure 2a] and an alternative model that depicts a fracture zone surrounded by a less permeable rock matrix [Figure 2b] ... they [both] share the essential characteristic of having a permeable conduit surrounded by less permeable and (presumably) less compliant rock."

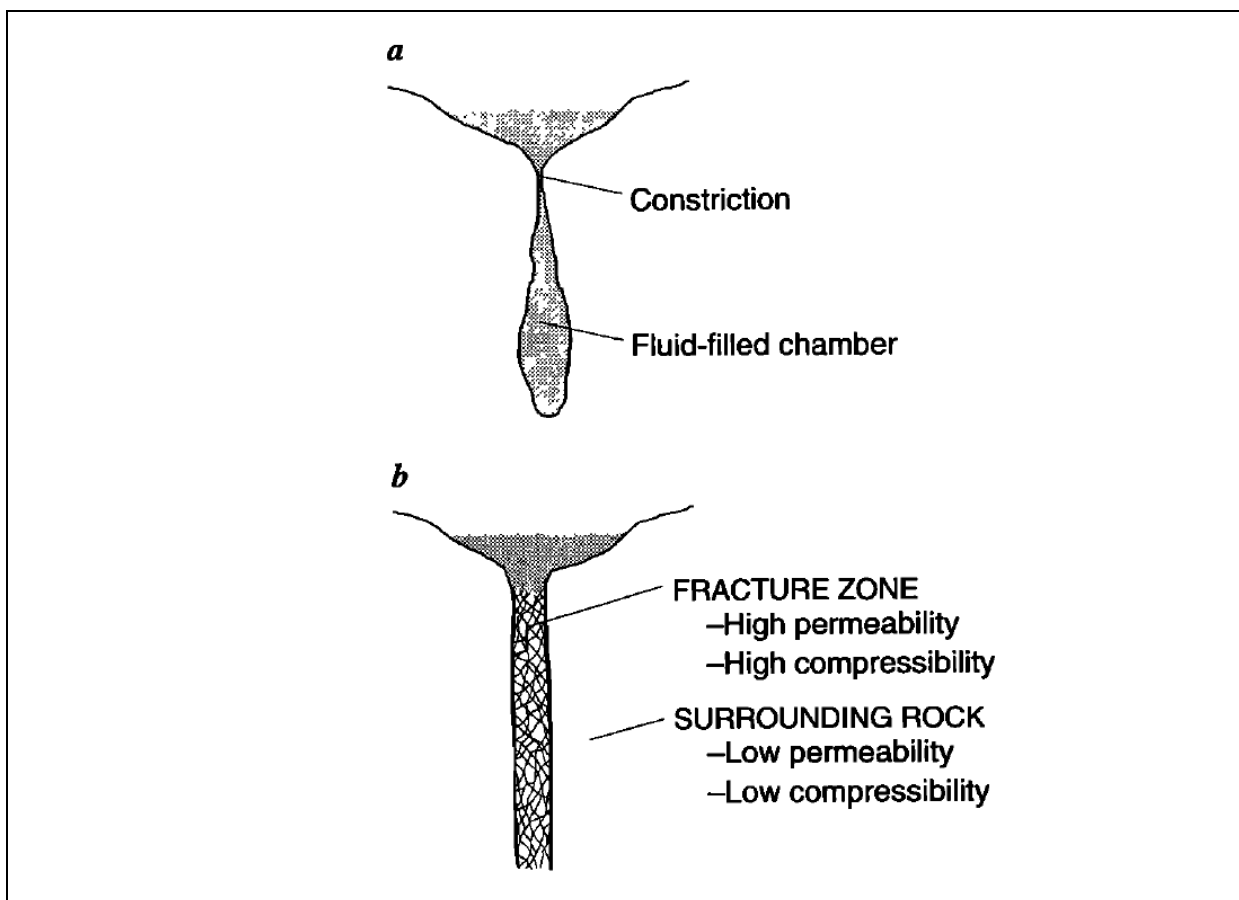


Figure 2. Image taken from Ingebritsen & Rojstaczer (1996).

a) classical 'chamber' or constricted pipe model;

b) 'fracture zone' conceptual model.

In both the models the geyser channel is more permeable than the surrounding rock.

1.1.3 Laboratory model

The advantage of laboratory work is that it enables data collection from all parts of a geysering system. Saptadji (1995) presents temperature-time series from the top, centre, and bottom of the vertical feed channel of a geysering system built in a laboratory. This is potentially useful to compare with data gathered from the present study, as it may be of some use in a qualitative understanding or interpretation, and also in guiding decisions on future data collection. A diagram

of the model is shown in Figure 3. This consists of a chamber with a water source and a heat source, with a vertical channel to the surface, and a collection dish, equivalent to a pool.

The processes involved in one cycle of heating and eruption are shown schematically in Figure 4. The resulting temperature-time series over three cycles are shown in Figure 5; it shows that the inflow rate of cold water is greatest after an eruption and then levels off. When the water boils and reaches its maximum temperature, the eruption begins. After the eruption, cold water flows in at a higher rate, cooling down the geyser; when the geyser is refilled, the inflow rate of cold water decreases and hence allows the geyser to heat up again for another eruption.

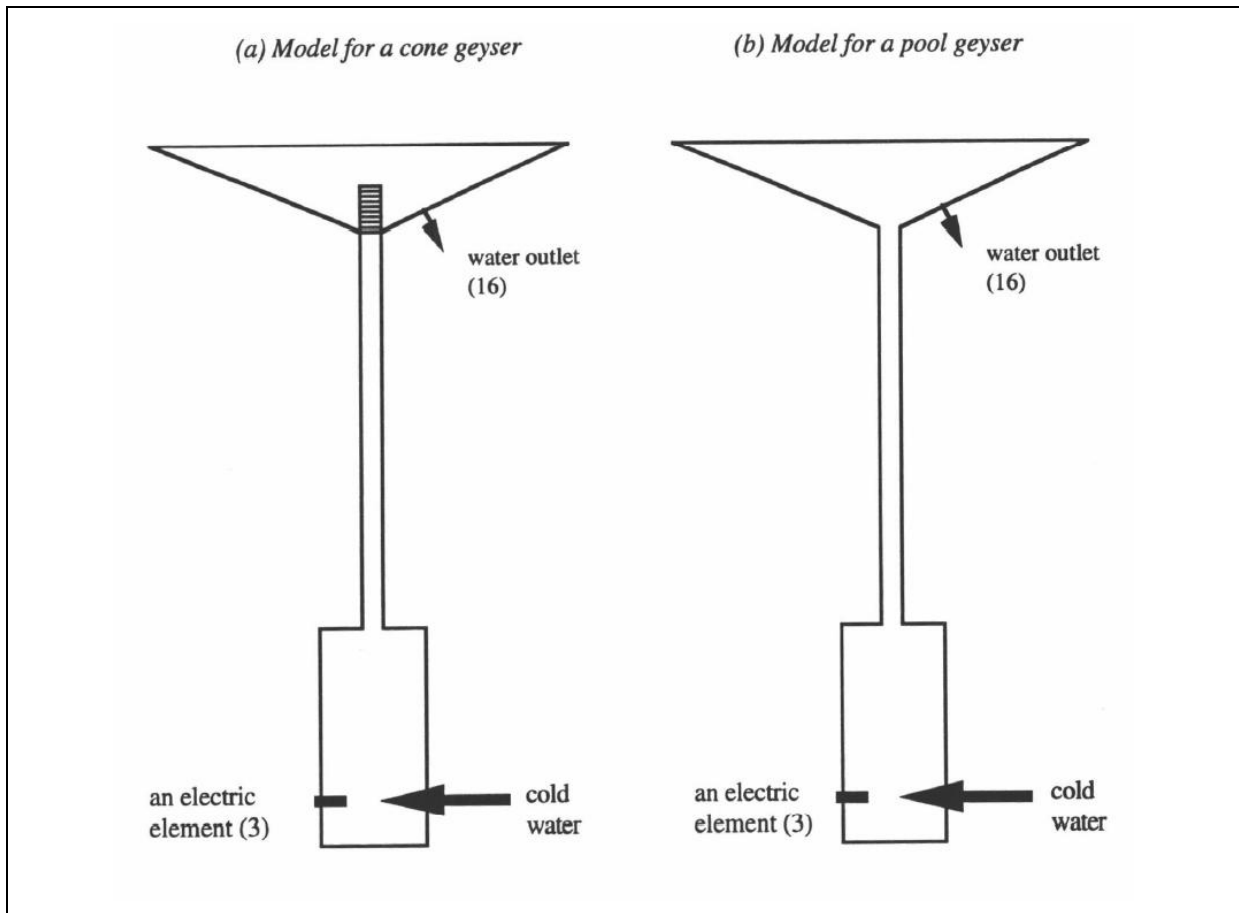


Figure 3. Image take from Saptadji (1995): examples of laboratory geyser models.

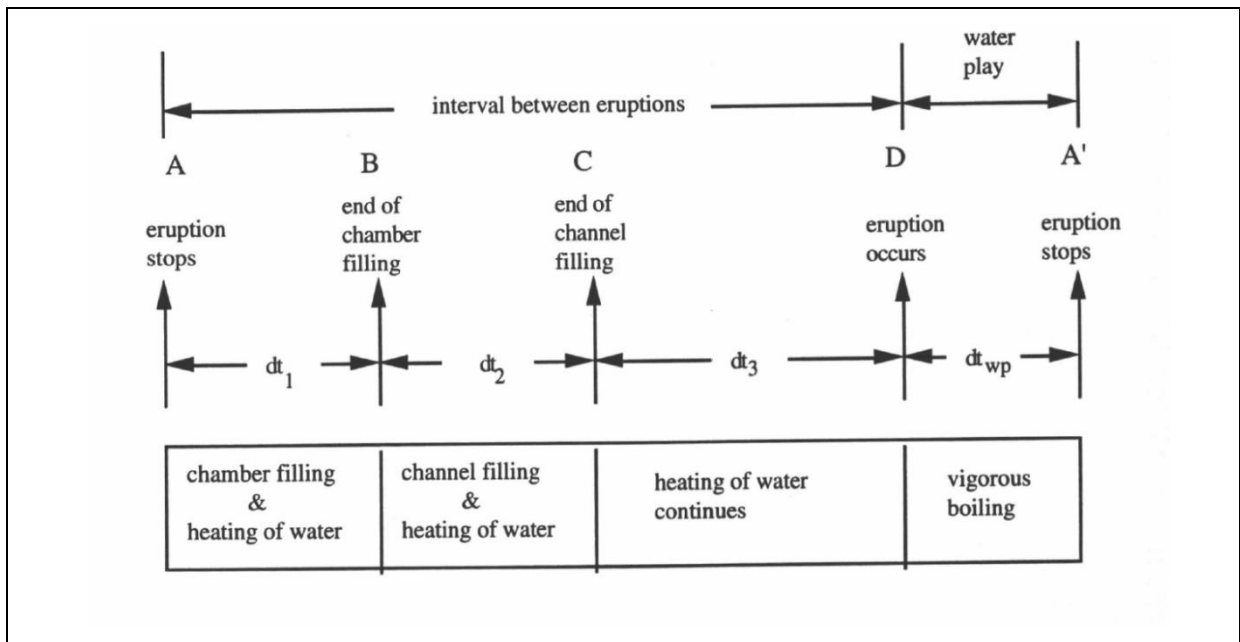


Figure 4. Image taken from Saptadji (1995): a breakdown of the geysering process.

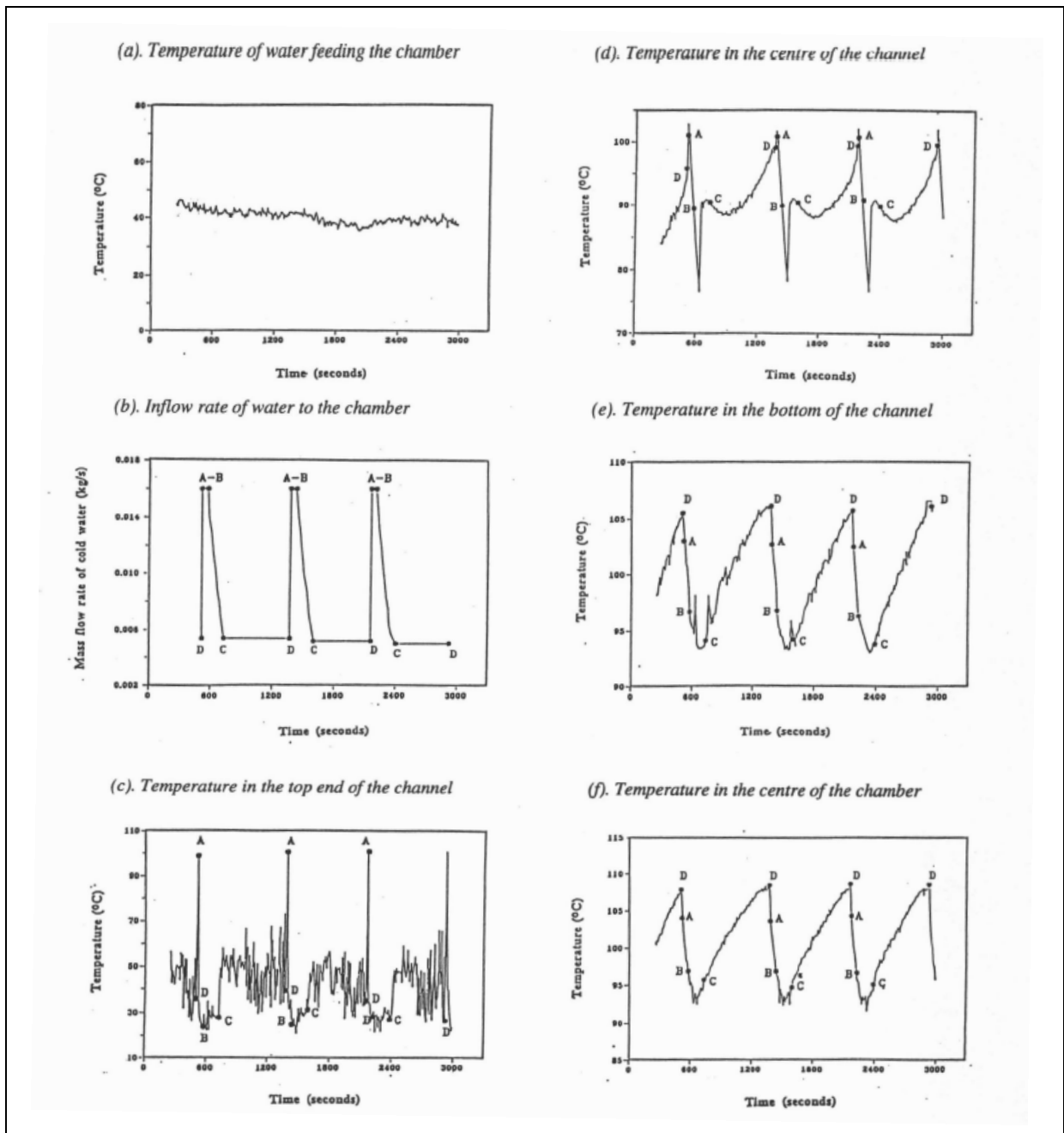


Figure 5. Data obtained from a laboratory column geyser. Inflow rate and temperatures for the model of an overflowing column geyser. (a) Temperature of water feeding the geyser. (b) Inflow rate of water to the chamber. (c) Temperature at the top of the channel. (d) Temperature in the vertical centre of the channel. (e) Temperature at the bottom of the channel. (f) Temperature in the centre of the chamber. A-B=filling of the chamber, B-C=filling of the channel, C-D=heating of the chamber to eruption, D=eruption begins, A=eruption stops. Image and caption text taken from Saptadji (1995).

1.1.4 Influences on periodicity in geothermal features

Even famously regular geysers such as Old Faithful of Yellowstone exhibit variations in their eruption intervals. "Over various time scales, eruption interval has been shown to vary with small strains (typically less than 1 *g*-strain) induced by variations in atmospheric loading, Earth tides, and seismic events" (Ingebritsen & Rojstaczer, 1993).

Husen *et al.* (2008) found that, following the 2002 M 7.9 Denali fault earthquake, despite the large distance of 3,100 km from the epicentre, there were clear changes in geyser activity observed in the Yellowstone National Park area. "Several geysers altered their eruption frequency within hours after the arrival of large-amplitude surface waves from the Denali fault earthquake" (Husen *et al.*, 2004). They interpreted these observations as being "induced by dynamic stresses associated with the arrival of large-amplitude surface waves" while they also suggested that in a "hydrothermal system dynamic stresses can locally alter permeability by unclogging existing fractures, thereby changing geyser activity" (Husen *et al.*, 2004).

Rojstaczer *et al.* (2003) analysed field data from the Upper Geyser Basin, Yellowstone: "geyser [eruption] frequency is less sensitive to elastic deformation than might be surmised from a review of the literature. Earth-tide influences are not identifiable in any of the geysers we monitored. Though atmospheric-pressure influences are observed, only long-period variations of the order of 5 mbars or greater seem to influence geyser frequency. Long-distance interconnections between geysers are common and add to the difficulty of identifying strain influences. Additional variations in geyser periodicity may be governed by the internal dynamics of the geysers rather than external influences" (Rojstaczer *et al.*, 2003).

Hurwitz *et al.* (2008) used instrumental GEI data and demonstrated, through time-series analysis, "that geysers respond to both long-term precipitation trends and to the seasonal hydrologic cycle" (Hurwitz *et al.*, 2008).

Sensitivity analyses conducted using a mathematical model (Saptadji *et al.*, 1994) on several geysers around New Zealand showed that the eruption frequency was positively correlated with the inflow rate of the hot water, atmospheric pressure, temperature of the hot/cold water and negatively correlated with the pressure in the cold water zone and the inflow rate of cold water. The modelling results showed that the geysers studied were all very sensitive to changes in the rate and temperature of the inflow of hot water.

Ingebritsen & Rojstaczer (1996), carried out numerical simulations, based on the conceptual model described in Figure 2. They found that

- eruption frequency and discharge are highly sensitive to the intrinsic permeabilities of the geyser conduit and the surrounding rock matrix;
- "simulated time series of geyser discharge are chaotic, but integrated quantities such as eruption frequency and mass discharge per eruption are free of chaos";
- "Coseismic and postseismic changes in geyser frequency might be explained in terms of permeability changes caused by strong ground motion";
- "as barometric pressure increases, then, fluid pressure increases in the geyser conduit associated with the increased surface load would be larger than those in the matrix, so that recharge rates and geyser activity would be reduced" (Ingebritsen & Rojstaczer, 1996).

2 WAIOTAPU GEYSER

2.1 Introduction

The Waiotapu Geyser is a small, intermittently-geysering spring in the Waiotapu Thermal Area. It is described below in Section 2.2.

The four temperature time series datasets collected from the Waiotapu Geyser (Section 2.3) have been compared to climate data and seismic data in Sections 2.4 and 2.5.

A Fourier analysis (Section 2.6) identifies dominant frequencies in the data. Section 2.7 contains a detailed analysis of the correlation of the Waiotapu Geyser temperature behaviour and air pressure.

2.2 Description

The Waiotapu geothermal system is the largest in terms of surface extent and heat flow (17 km² and 600 MW, respectively) of the 20 major geothermal systems in the Taupo Volcanic Zone, New Zealand (Hedenquist, 1991). Thermal features comprise near-neutral pH chloride springs (often boiling), acid sulphate springs, mud pools and mixed waters, the latter including both bicarbonate-chloride and acid sulphate-chloride springs (Hedenquist, 1991). The Waiotapu Geyser (see Figure 6 to Figure 10) can be classified as a near-neutral pH mixed chloride-bicarbonate spring.

The Waiotapu Geyser is a pool geyser which has some visible liquid water at all times. Following an eruption some of the discharge water finds its way back into the geyser while some overflows and spills away. Unfortunately water level data has not been collected as part of this study. A small stream flows past the geyser (see Figure 8 and Figure 9). The direction of the overflow can be seen in Figure 9. The Geyser is surrounded by silica sinter and geyserite (a 'knobbly' form of sinter caused by splashing of hot silica-saturated geothermal water). It occasionally splashes and erupts, overflows without splashing, or the water level just rises and falls. The eruption height is generally less than one metre.

A video recording showing the eruption of the Waiotapu Geyser can be found on:
<http://www.youtube.com/watch?v=fePZtxnqrmA>.



Figure 6. The Waiotapu Geyser. The knobby texture on the surrounding sinter is geysierite. This is evidence of repeated splashing of silica-saturated water.

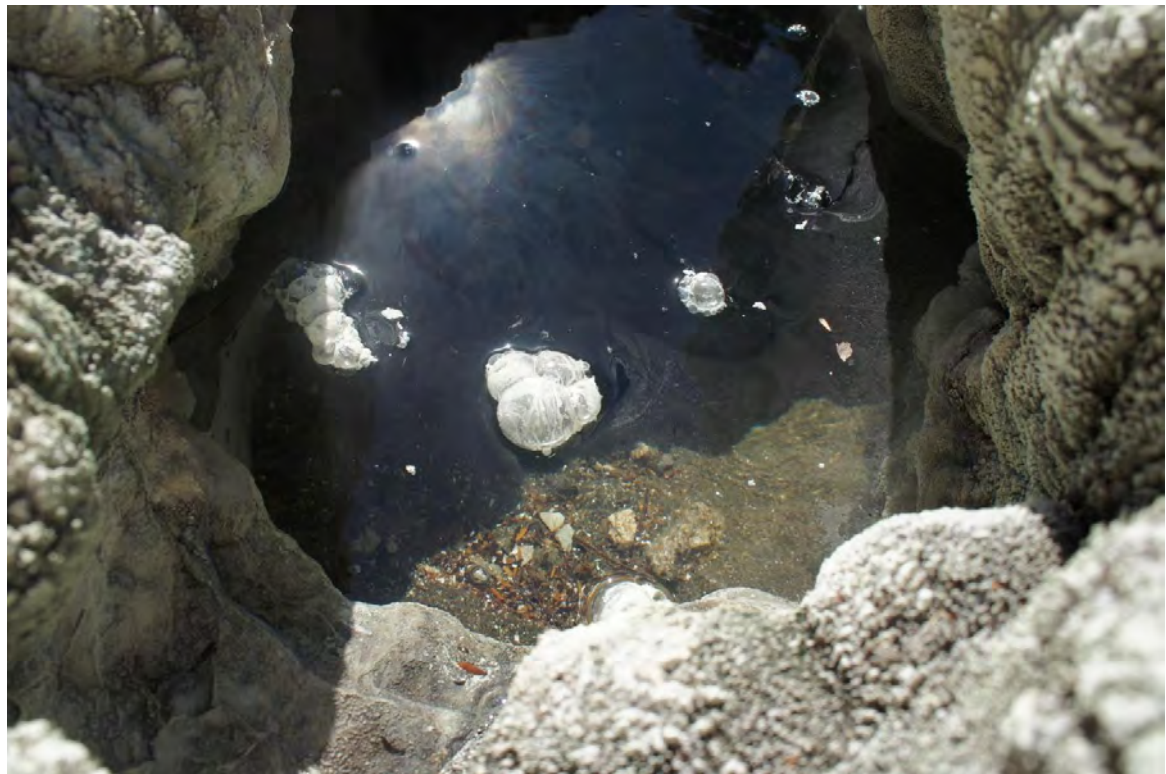


Figure 7. A close up of the Geyser.



Figure 8. Stream passing by the Waiotapu Geyser.



Figure 9. An overview of the area surrounding the Geysir.



Figure 10. Close-up of the Waiotapu Geyser in action.

2.3 The Data

There were four datasets collected from the Waiotapu Geyser: each dataset is 45 days long with temperatures recorded every 2 minutes. A Temprecord Scientific Recorder datalogger was used (<http://www.temprecord.com>). Unfortunately the exact depth of the temperature probe was never recorded, but it was thought to be approximately 0.6 m below the water level of the pool. Figure 11 contains the spring temperature time series plots for the four datasets.

An examination of the graphs in Figure 11 shows periods of relatively constant temperature followed by periods of temperature variation showing a distinct and repetitive cycle with an amplitude of $\sim 18^{\circ}\text{C}$ (with the exception of a some irregularities which will be discussed below).

Figure 12, (a) and (b) show a typical intervals of cyclic activity and quiescence, respectively. Figure 12 (b) (displaying a period of nearly constant temperature) shows no distinctive pattern. The temperature range is about 3.5°C , which is not very large compared to the range of the temperature in the cyclic interval in Figure 12 (a).

Figure 13 (a) and (b) show cyclic and quiet temperature data, respectively, for one day.

Three other features of the data are:

- Periods of cyclic activity where the temperature oscillates between 80 and 20 °C, for instance around 01/07/2010. The cause of this is not known, but it is possible that it may be due to the water level rising and falling past the probe level.
- Two low temperature episodes to approximately 30 °C between 22/01/2011 and 06/02/2011. The rapid decrease in temperature is followed by a gradual recovery similar to a geothermal well temperature recovery. This is discussed in the following section, with respect to rainfall.
- Temperature oscillations of ~10 °C around 45 to 55 °C in the last half of dataset 5. It is not known if these are real and the spring became much cooler than shown in all the previous records, or if the datalogger was failing.

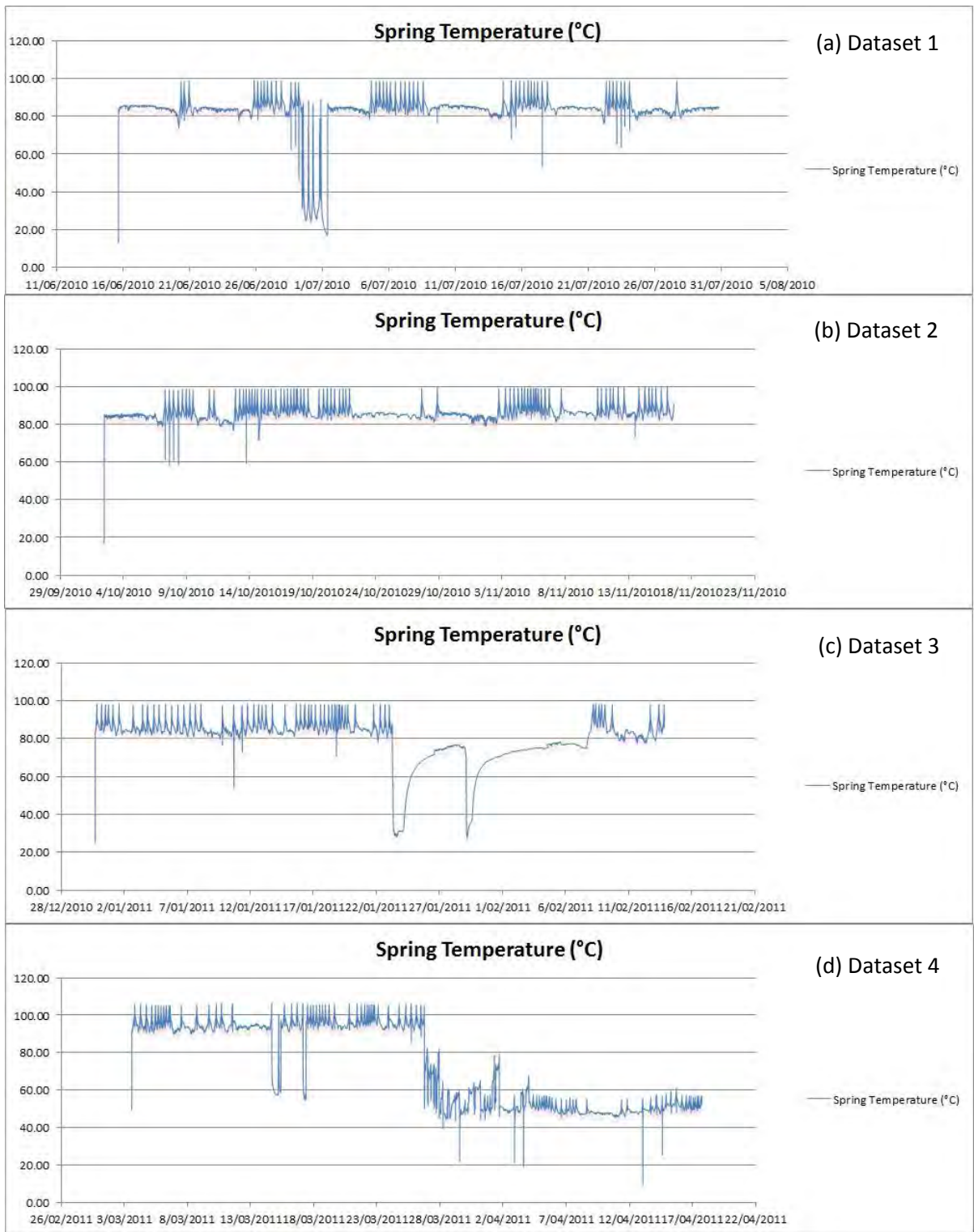


Figure 11. The temperature time-series plots for the Waitotapu Geyser. (a) Dataset 1. (b) Dataset 2. (c) Dataset 3. (d) Dataset 4.

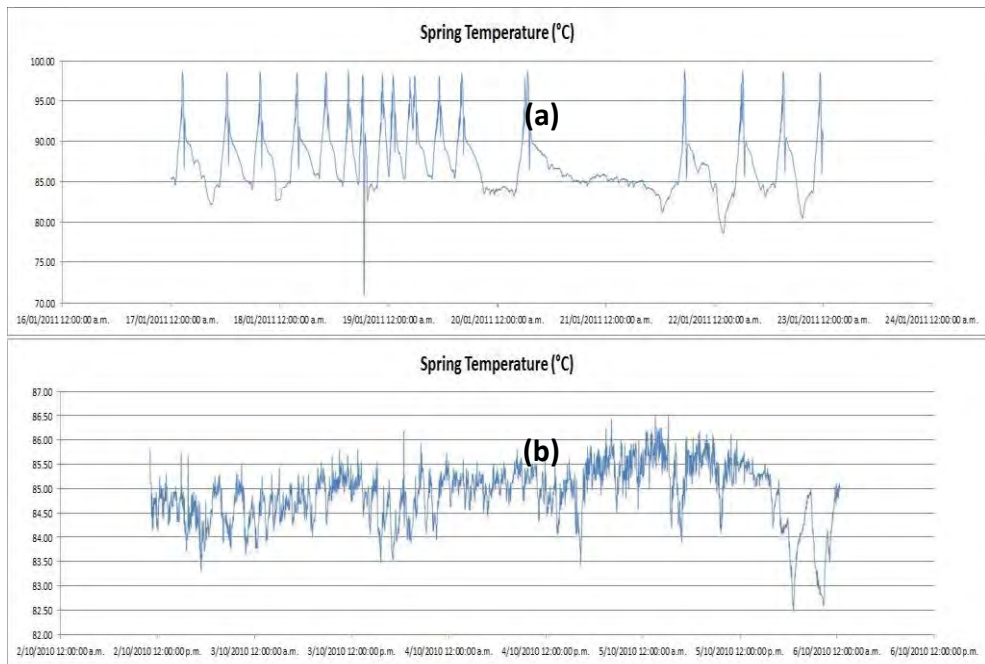


Figure 12. The upper graph (a) shows a typical cyclic period while the lower graph (b) shows a typical period of inactivity .

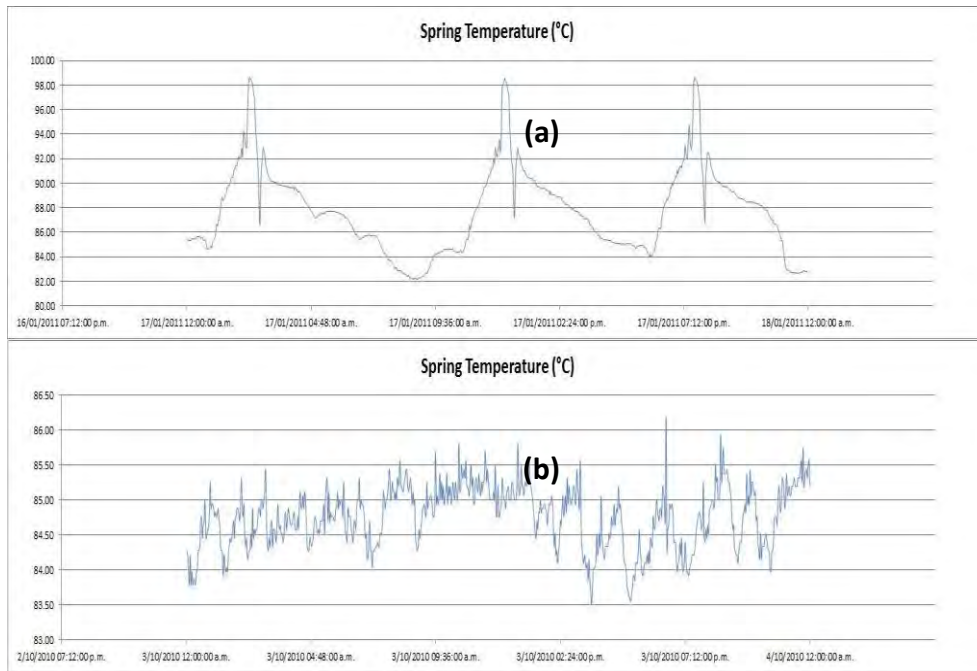


Figure 13. The upper graph (a) shows a typical day with cyclic activity, while the lower graph (b) shows a typical day with inactivity.

2.4 Examining the effects of climate factors

Rainfall, air pressure and air temperature data obtained from the National Institute of Water and Atmospheric Research (NIWA: <http://www.niwa.co.nz>) (Taupo AWS station) were analysed in order to find some relationship between these variables and spring temperature. Note that the air temperature data presented here is an average of the hourly high and lows taken from the NIWA database.

Figure 14 and Figure 15 give a general plot of the different variables along with spring temperature to identify any apparent relationships. From Figure 14, there would seem to be a relationship between spring temperature and air pressure; periods of higher air pressure generally correspond to periods of inactivity, while periods of low air pressure correspond to periods of cyclic activity in the spring temperature.

On the other hand, there does not appear to be any apparent relationship between spring temperature and air temperature.

It is not clear whether there is any consistent relationship between rainfall and spring temperature (Figure 15). One thing worth noting is that, for Dataset 3 between 17/01/2011 and 01/02/2011, the temperature drops sharply then gradually increases before dropping sharply again and increasing gradually again. These 'recovery curves' correspond to periods of high rainfall and we suggest this is due to the nearby stream overflowing into the geyser and cooling it down; after each overflow, the geyser's temperature goes through a recovery period to bring the system back into its original state.

The nature of the datasets makes it difficult to identify any relationship to environmental input other than very short term. It is possible that there may be longer-term correspondence between seasonal climate variation and spring activity. This would be difficult or impossible to identify with the datasets in this study.

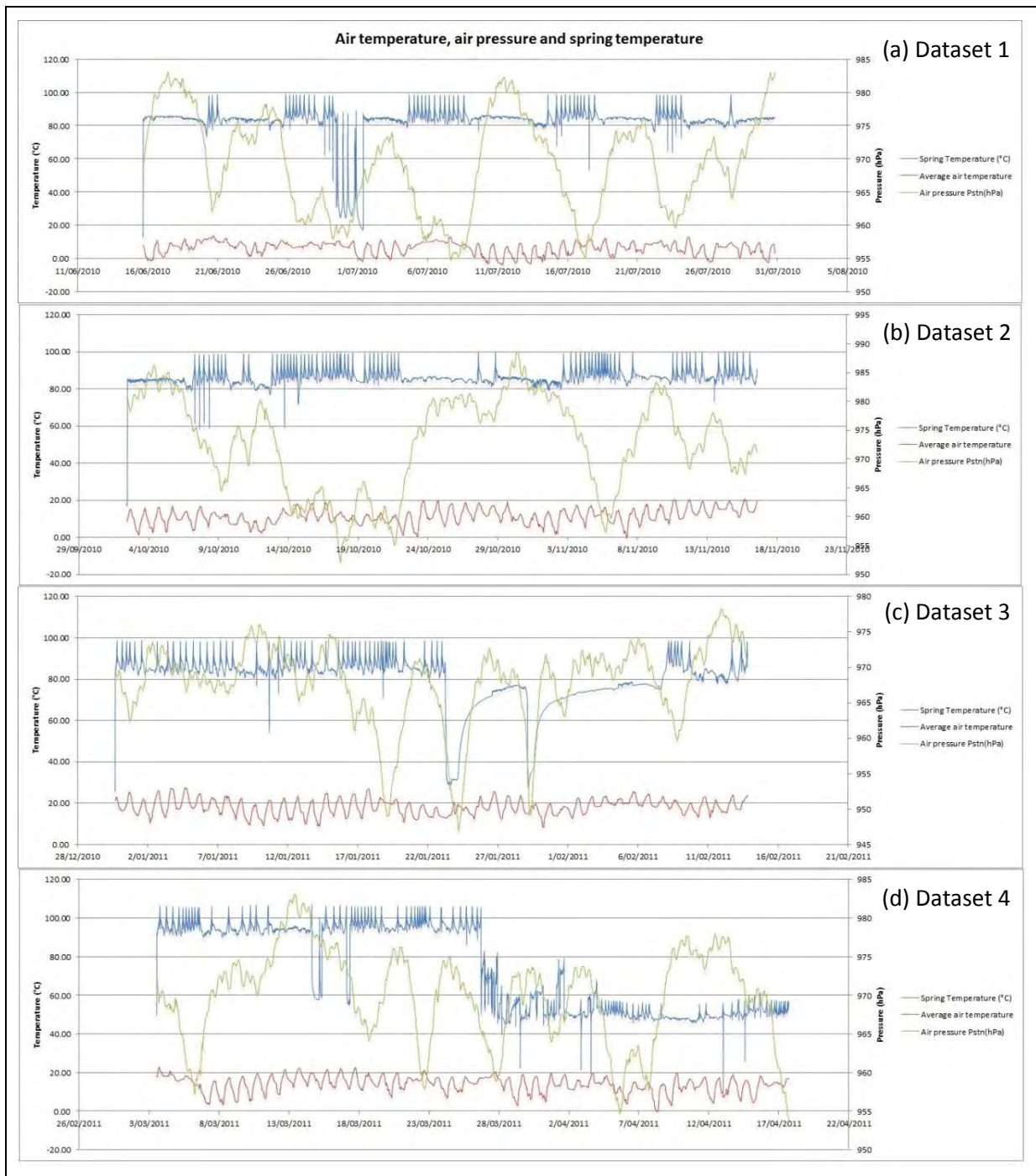


Figure 14. Spring temperature is plotted along with air pressure and air temperature. The red line is the air temperature, the green line is air pressure and the blue line is spring temperature. Pressure (right axis) is measured in hectaPascals while temperature (left axis) is measured in degrees Celsius (°C).
 (a) Dataset 1. (b) Dataset 2. (c) Dataset 3. (d) Dataset 4.



Figure 15. Spring temperature ($^{\circ}\text{C}$) in blue and rainfall (mm) in purple.
 (a) Dataset 1. (b) Dataset 2. (c) Dataset 3. (d) Dataset 4.

2.5 Seismic events and spring temperature

Seismic data obtained from GeoNet – Quake Search is presented in this section along with spring temperature. Figure 16 to Figure 19 below show the plots for seismic activity and spring temperature for the four datasets. Spring temperature (the blue line) is plotted against the right vertical axis and the magnitude of the seismic event (black circles) is plotted on the left vertical axis. The darkness of the circles indicate the distance of the seismic event from the Waiotapu Geyser: the darker the circles the closer the seismic event. The plots appear not to show any kind of relationship; it is not clear if there is a change in the geyser's behaviour after any specific event(s). Either seismic events have had no impact on the geyser throughout the period considered, or the effects were so small that they are not noticeable. In addition, due to the sparse sensor network, the location data for earthquakes is not sufficiently accurate to attempt any detailed correlation of spring activity with proximity to seismic events (F. Sepulveda, pers. comm.).

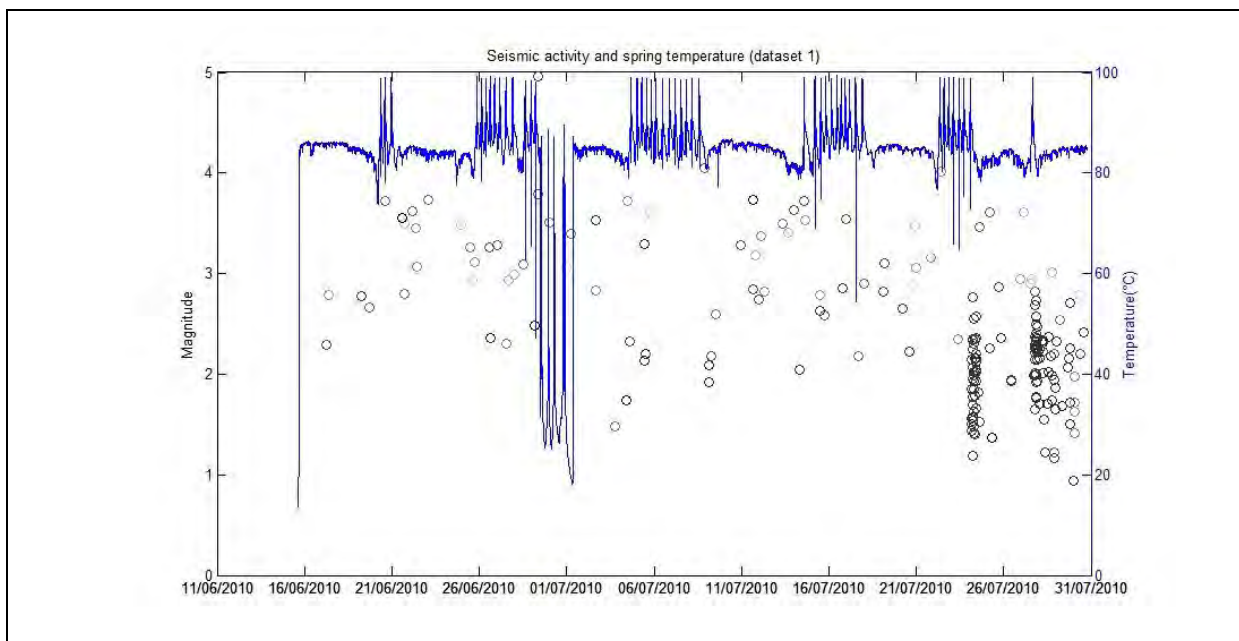


Figure 16. Seismic activity and spring temperature, Dataset 1. Spring temperature: blue line; seismic activity: black circles. Darker circles indicate that the seismic event was closer to the Waiotapu Geyser.

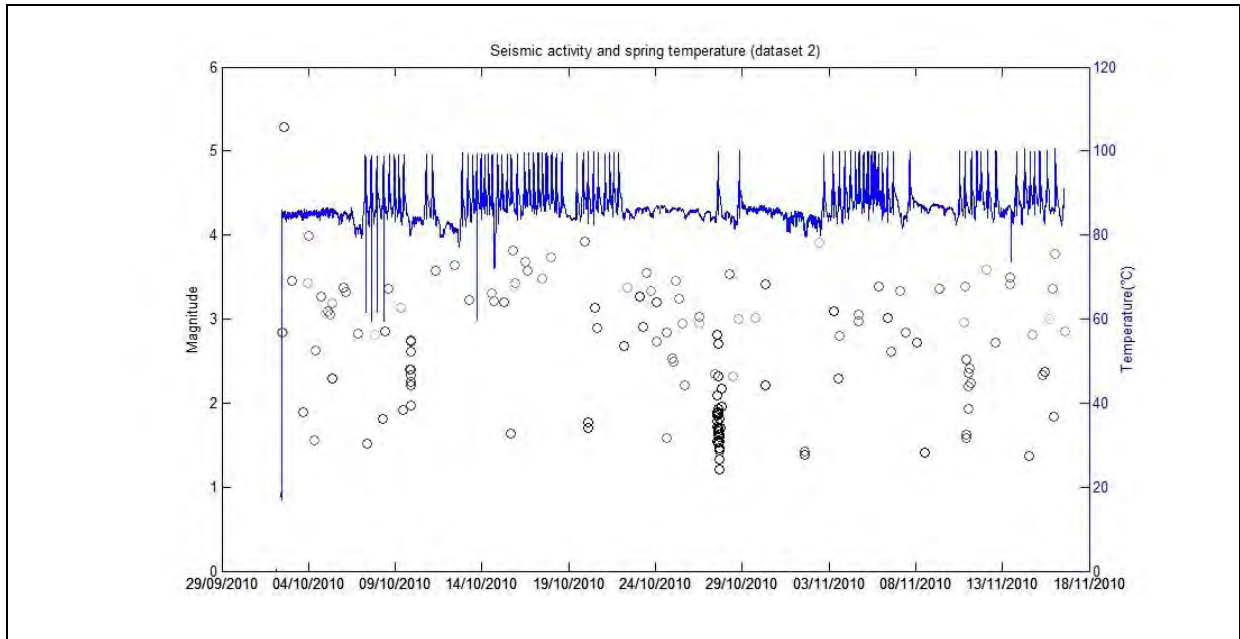


Figure 17. Seismic activity and spring temperature, Dataset 2. Spring temperature: blue line; seismic activity: black circles. Darker circles indicate that the seismic event was closer to the Waiotapu Geysir.

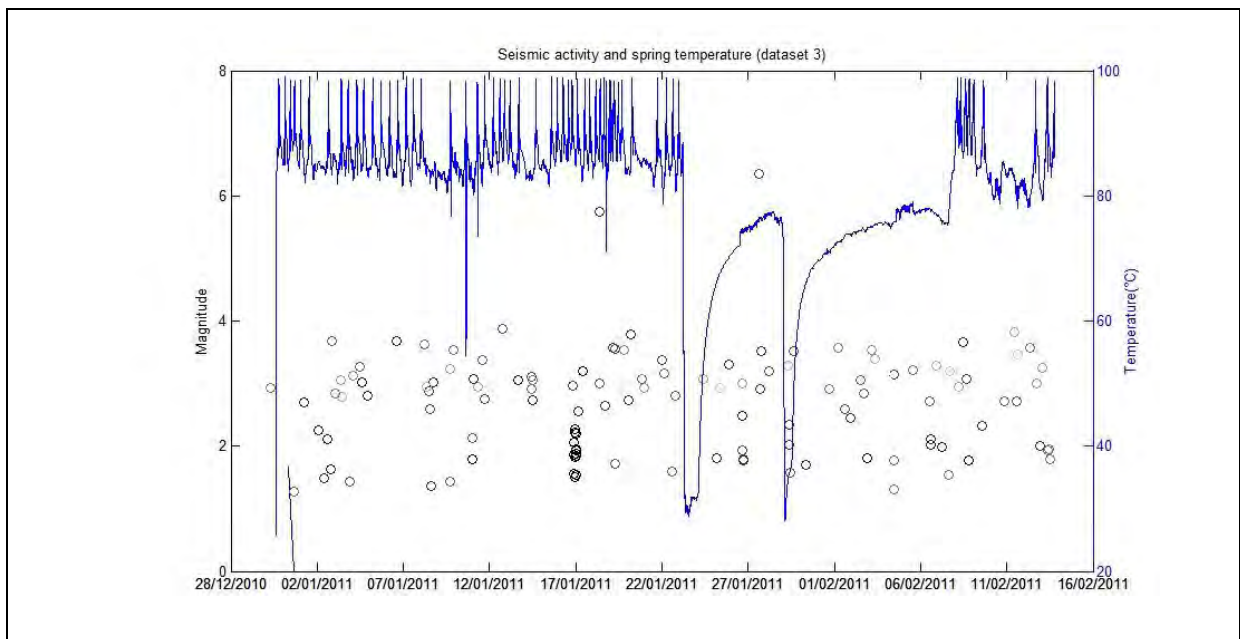


Figure 18. Seismic activity and spring temperature, Dataset 3. Spring temperature: blue line; seismic activity: black circles. Darker circles indicate that the seismic event was closer to the Waiotapu Geysir.

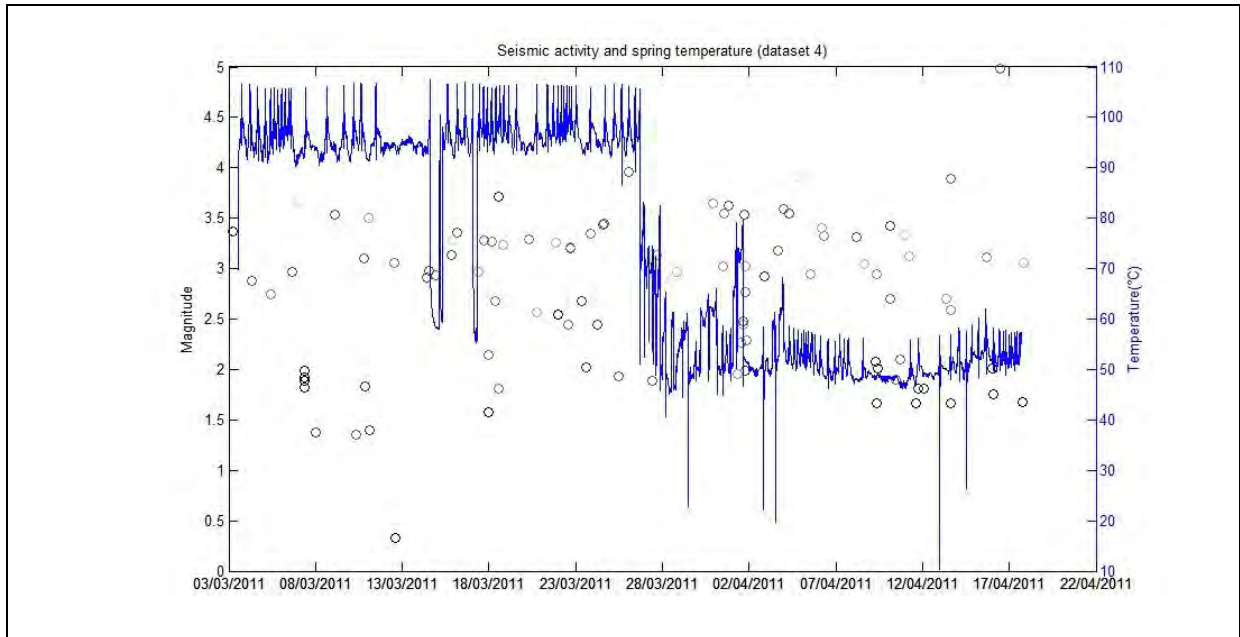


Figure 19. Seismic activity and spring temperature, Dataset 4. Spring temperature: blue line; seismic activity: black circles. Darker circles indicate that the seismic event was closer to the Waiotapu Geysers.

2.6 Fourier analysis

In this section the frequency components of the data are analysed using a Discrete Fourier Transform (carried out numerically using the software package MATLAB). Since the data seems to contain intervals of periodic behaviour, some of these intervals are analysed separately in order to try and find variations in frequency throughout the datasets.

The four-day period 5/07/2010 12:01:38 a.m. to 8/07/2010 11:59:38 p.m. (Figure 20) from the first dataset is analysed first, since it presents one of the first consistent periodic patterns in the data; the dominant frequency is about 3 cycles per day. Next analysed is the six-day period 13/10/2010 12:00:19 a.m. to 18/10/2010 11:58:19 p.m. from the second dataset. The dominant frequency seems to be at about 3.5 cycles per day (Figure 21).

For the four-day period 3/11/2010 12:00:19 a.m. to 6/11/2010 11:58:19 p.m. (Figure 22), the dominant frequency is around 3.25 cycles per day. The nine-day period 31/12/2010 12:00:06 a.m. to 8/01/2011 11:58:06 p.m. shows a dominant frequency of 2.1 cycles per day (Figure 23).

The dominant frequency is 3.6 cycles per day during the four-day period 16/01/2011 12:00:06 a.m. to 19/01/2011 11:58:06 p.m. (Figure 24), while 4.1 cycles per day is the dominant frequency during the three-day period 17/03/2011 08:01:25 a.m. to 19/03/2011 11:59:25 p.m. (Figure 25).

Note that for Figure 20 to Figure 25, the upper graphs are plots of the temperature ($^{\circ}\text{C}$) against time in days. The lower left graph gives the frequency spectrum, where frequency is in cycles per day. The bottom right graph shows the dominant frequency by "zooming in" on the frequency spectrum. Note that the mean is removed from the temperature in this analysis.

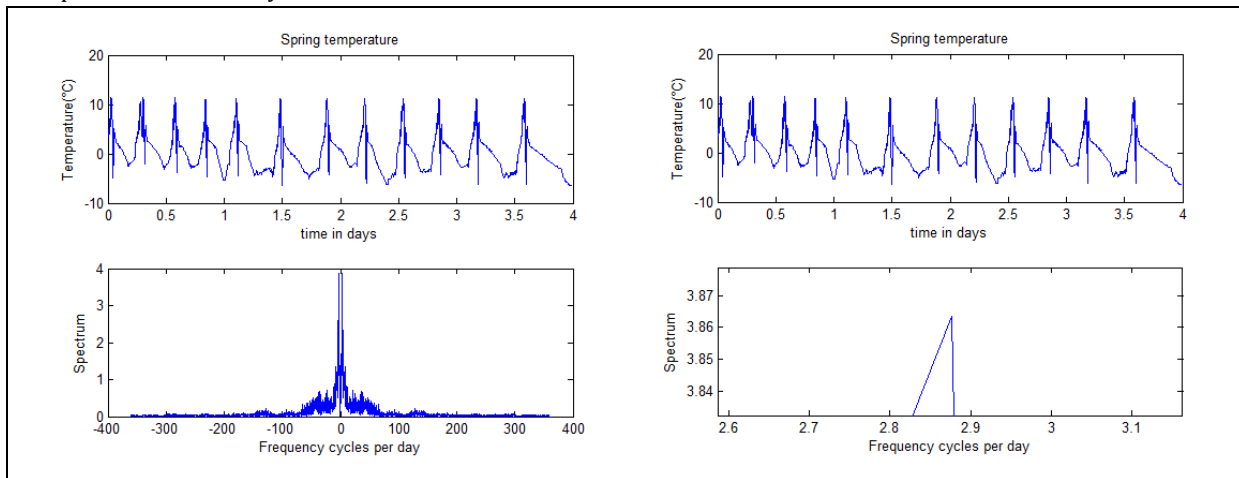


Figure 20. 5/07/2010 12:01:38 a.m. to 8/07/2010 11:59:38 p.m. from Dataset 1. The dominant frequency is close to 3 cycles per day.

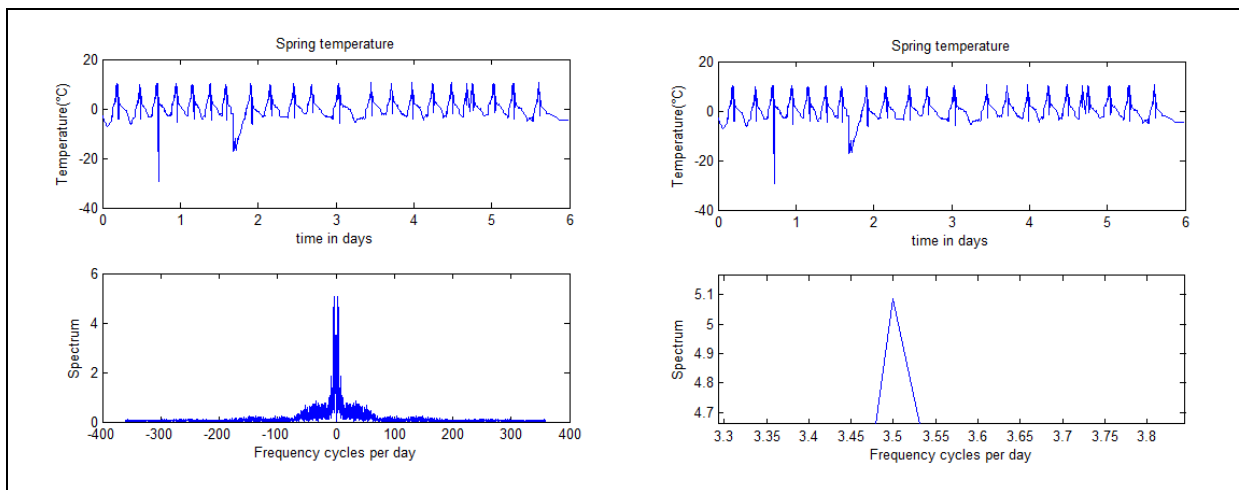


Figure 21. 13/10/2010 12:00:19 a.m. to 18/10/2010 11:58:19 p.m. from Dataset 2. The dominant frequency is about 3.5 cycles per day.

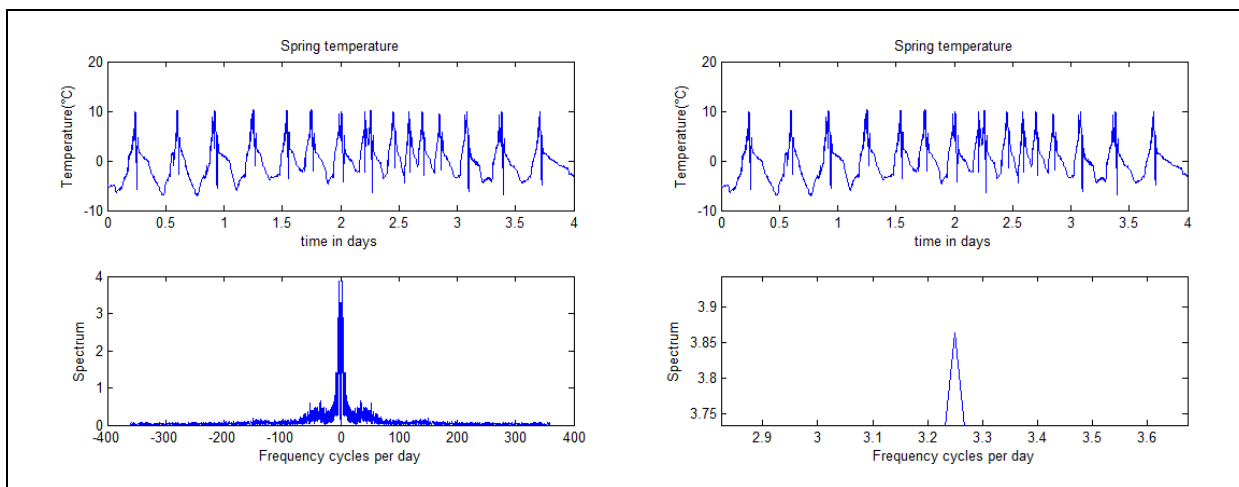


Figure 22. 3/11/2010 12:00:19 a.m. to 6/11/2010 11:58:19 p.m. from Dataset 2. The dominant frequency is about 3.25 cycles per day.

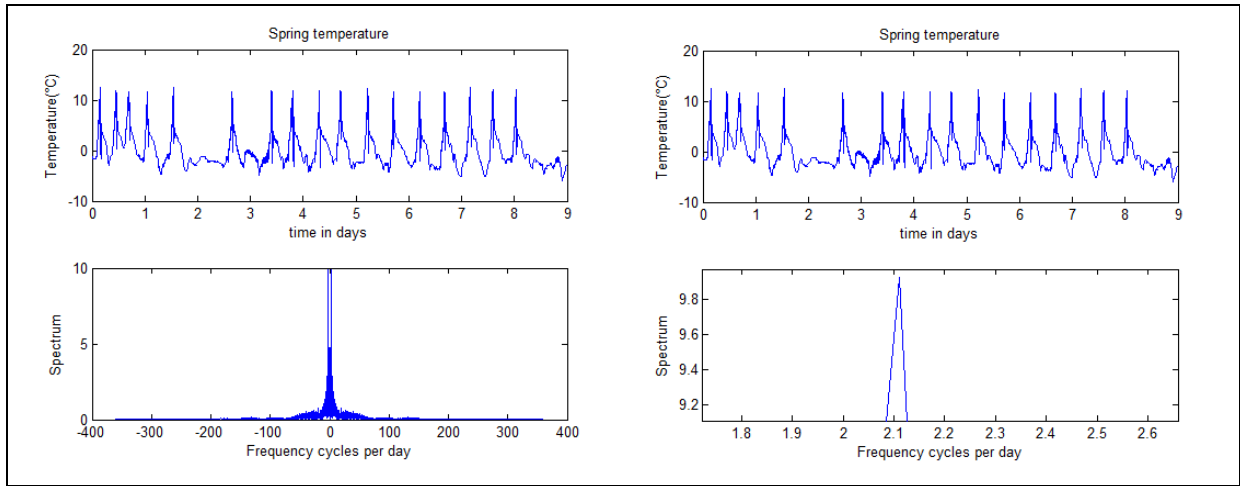


Figure 23. 31/12/2010 12:00:06 a.m. to 8/01/2011 11:58:06 p.m. from Dataset 3. The dominant frequency is 2.1 cycles per day.

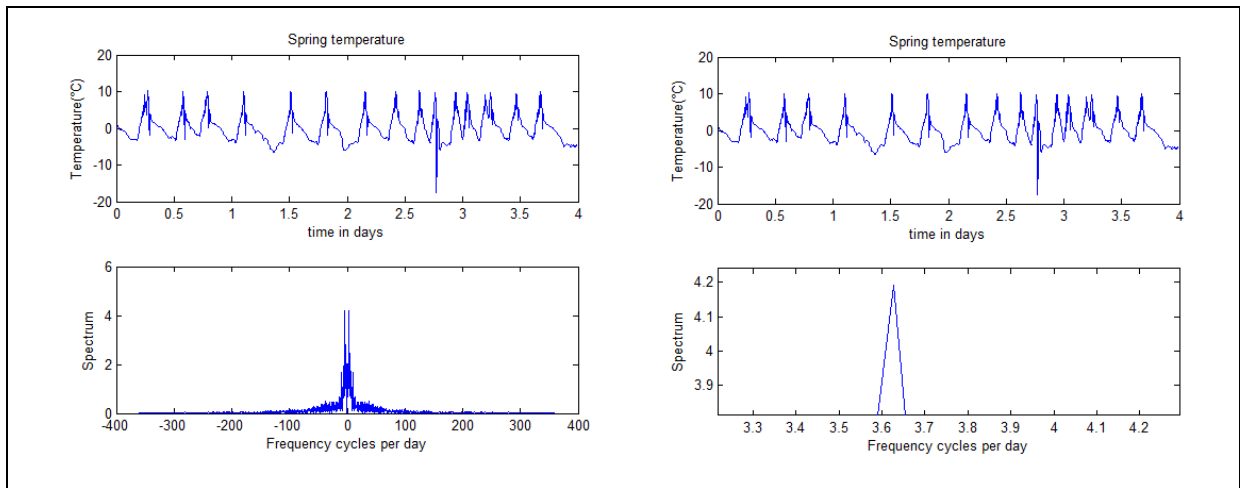


Figure 24. 16/01/2011 12:00:06 a.m. to 19/01/2011 11:58:06 p.m. from Dataset 3. The dominant frequency is 3.65 cycles per day.

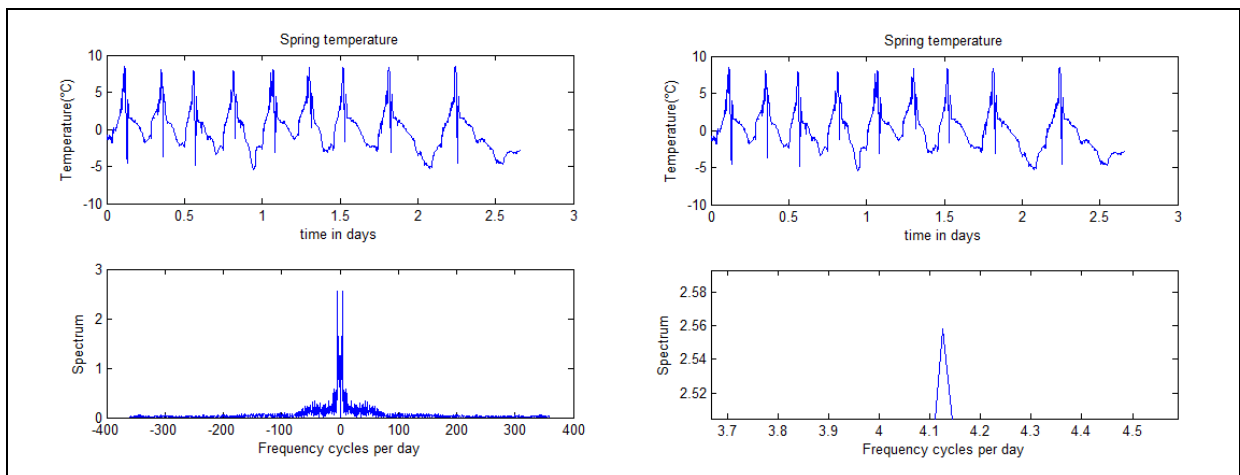


Figure 25. 17/03/2011 08:01:25 a.m. to 19/03/2011 11:59:25 p.m. from Dataset 4. The dominant frequency is about 4.1 cycles per day.

From the above analysis it is clear that the cyclic pattern in the data, when present, has a variable frequency, in the range of 2–4 cycles per day.

Next the air temperature variations during the data collection periods are considered. The same display format as the previous Discrete Fourier Transform on spring temperature is used. We apply a Discrete Fourier Transform to air-temperature data throughout the same time intervals as Datasets 1 to 4 in turn, and list the results in Figure 26 to Figure 29 below.

Fourier analysis of the air-temperature data shows that air temperature has a cycle length of 1 day as one would expect. When displaying cyclic behaviour the spring has a cycle length of about 2 to 4 cycles per day but the air temperature is consistently displaying a cycle length of 1 day. So any relationship between the two variables is not expected.

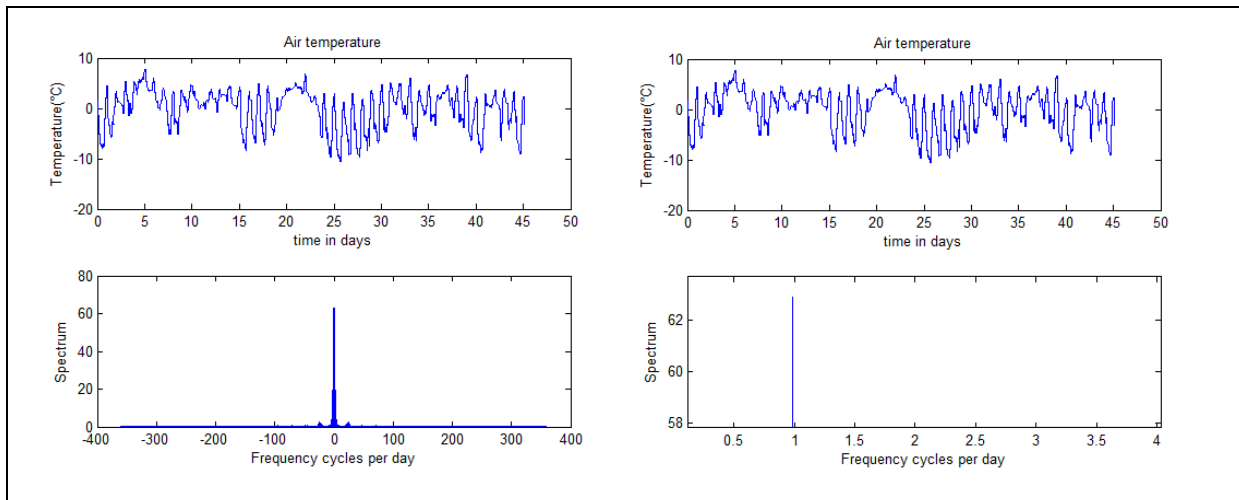


Figure 26. Time interval of Dataset 1. The upper graphs are plots of air-temperature ($^{\circ}\text{C}$) against time in days. The lower left graph gives the frequency spectrum, where frequency is in cycles per day. The graph on the bottom right shows the dominant frequency by zooming in onto the frequency spectrum; the dominant frequency is at about 1 cycle per day. (Note that the mean is removed from the temperature in this analysis.)

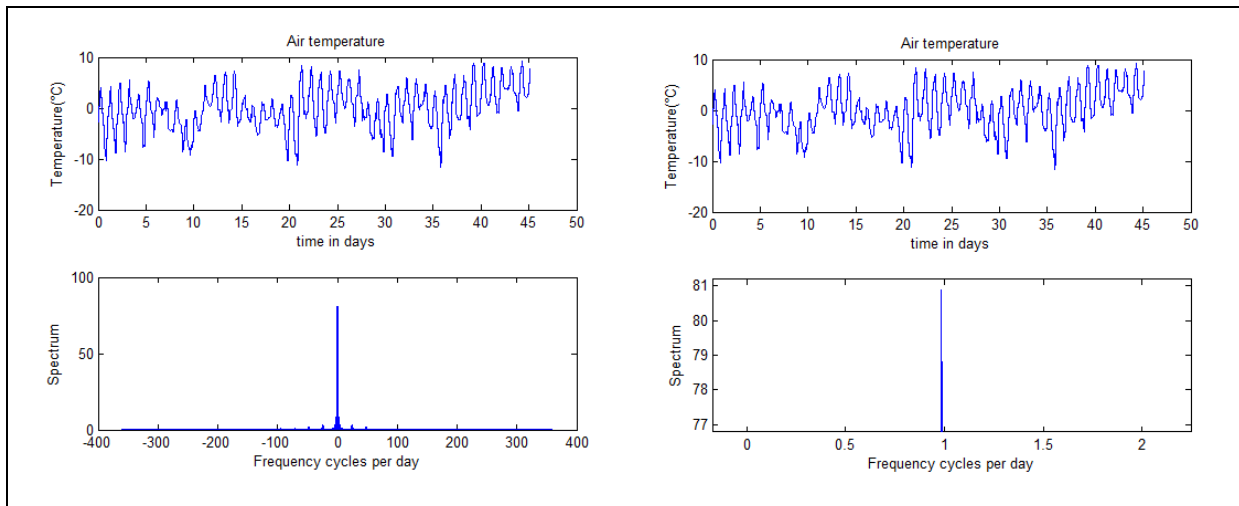


Figure 27. Time interval of Dataset 2. Dominant frequency of 1 cycle per day.

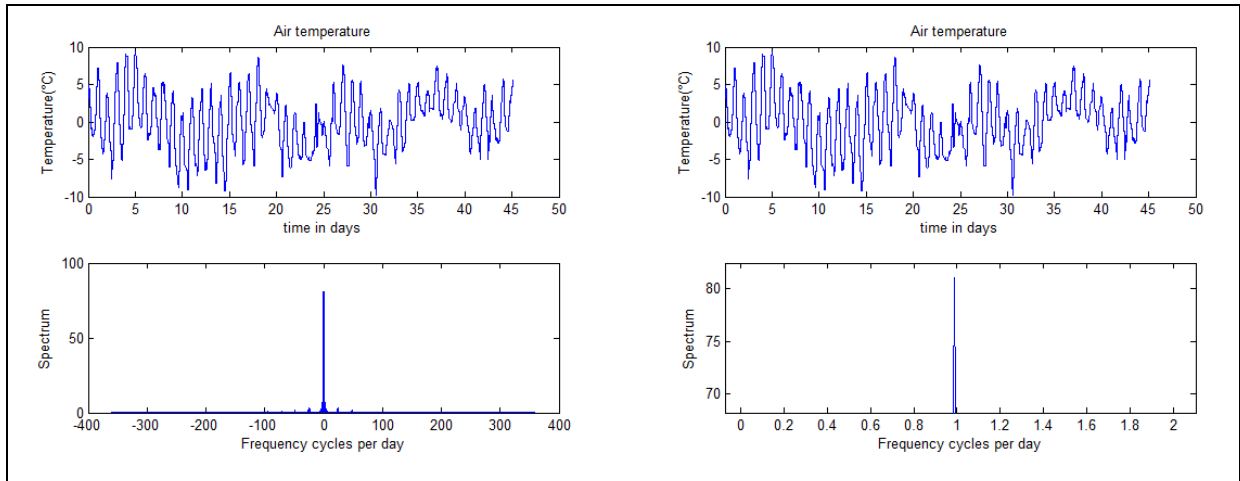


Figure 28. Time interval of Dataset 3. Dominant frequency of 1 cycle per day.

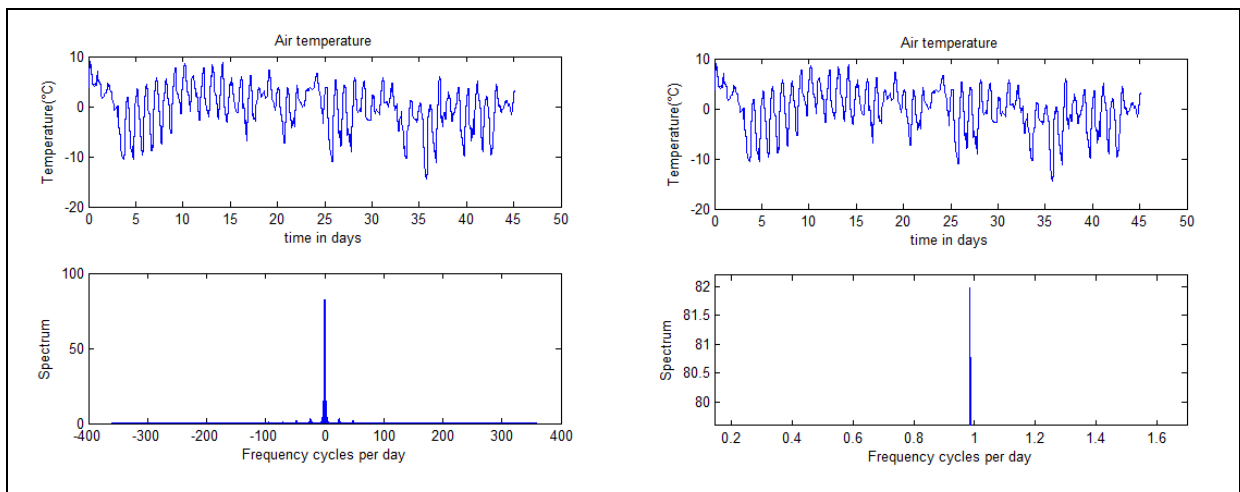


Figure 29. Time interval of Dataset 4. Dominant frequency of 1 cycle per day.

2.7 Frequency and air pressure

So far it has been observed that the spring temperature has indicated two distinct types of activity: a quiescent mode and a cyclic mode. Fourier analysis in the previous section showed that when in this cyclic mode, the frequency of the cycles varies from one cyclic period to the next.

Figure 14 seems to indicate a close relationship between air pressure and spring temperature. It appears that the two modes in the data are somehow driven by air pressure; when the air pressure is lowered the spring shifts into cyclic mode and when the air pressure increases sufficiently the quiescent mode is observed.

A close look at Figure 30 reveals that the frequency of the temperature cycle also seems to depend (inversely) on air pressure. Higher pressure seems to be correlated with a lower frequency and *vice versa*. So, it appears as though air pressure has two effects on spring behaviour:

1. switching the cyclic mode on and off (a threshold effect);
2. increasing/decreasing the frequency of the cycles once in this cyclic mode.

To test this idea daily spring-temperature cycle frequencies were estimated and plotted against average daily air-pressure figures; see Figure 31 and Figure 32 below.

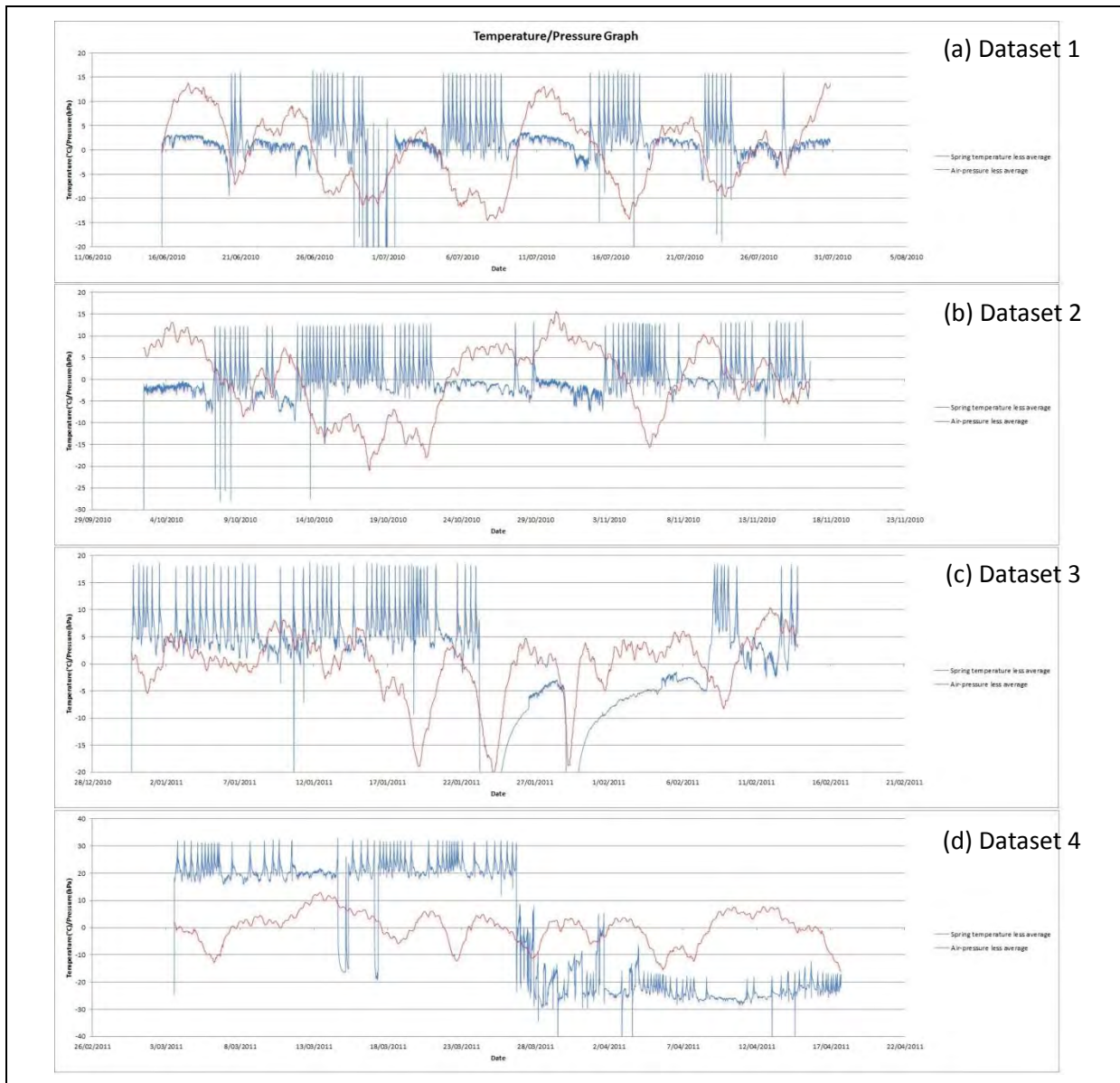


Figure 30. The blue line represents spring temperature and the red line is air-pressure. The vertical axis records pressure (hPa) and temperature (°C) (on the same axis), while on the horizontal axis we have time. (Means have been removed from both variables.) (a) Dataset 1. (b) Dataset 2. (c) Dataset 3. (d) Dataset 4.

The daily spring-temperature cycle frequencies were estimated by looking at the spring temperature plots for each day in turn and simply counting the number of times the cycle seemed to repeat itself in a given day. This was done for the all datasets with the irregular periods mentioned before being ignored. Quiescent periods were given a frequency of zero. Although the method used here to estimate daily frequency seems somewhat arbitrary, the pattern of a typical cycle is prominent enough to allow one to make good estimates of the daily frequencies with reasonable accuracy in order to come up with some crude estimates.

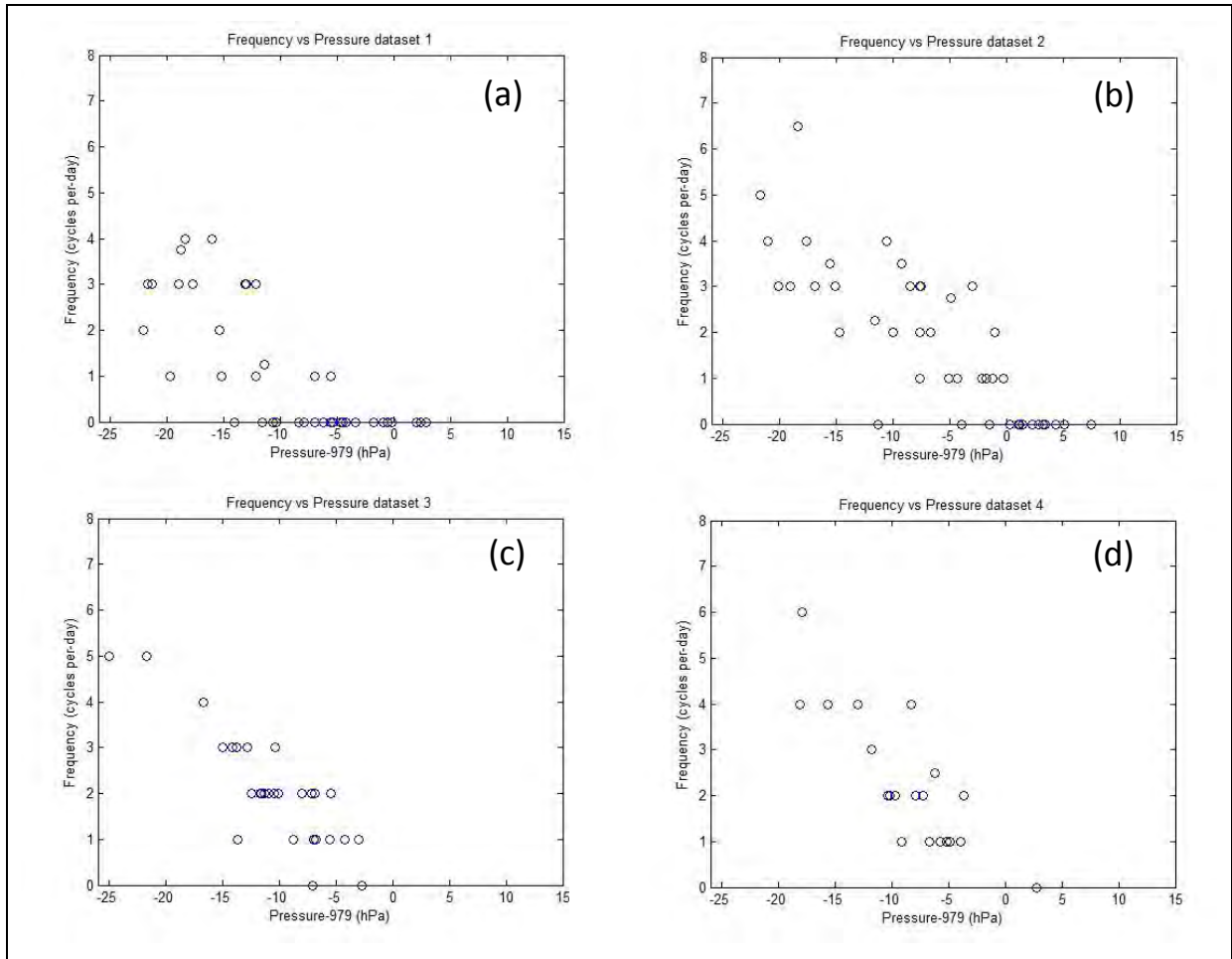


Figure 31. Estimated daily frequencies of the temperature cycles plotted against average daily air pressure (centred at 979 hPa; this pressure is chosen as a tentative threshold) for Datasets 1 to 4. A frequency of zero corresponds to a state of inactivity. (a) Dataset 1. (b) Dataset 2. (c) Dataset 3. (d) Dataset 4.

Figure 31 shows frequency (cycles per day) against air pressure (centred at 979 hPa) as scatter plots for all of the four datasets. The value of 979 hPa was chosen as a possible "threshold" for switching the cyclic mode on and off.

Looking at each of the four scatter plots in isolation one could come up with different values for a possible threshold making it difficult to be certain as to where to draw the line. Although above the chosen threshold there is always inactivity, below this level there are quite a few periods of inactivity also. There are clearly other factors which are coming into play here that are unaccounted for and a pressure threshold, if it exists, may depend on these factors.

All four graphs seem to indicate a negative relationship between frequency and pressure which confirms the initial idea.

Figure 32 is the frequency against pressure plot for all four datasets combined. This graph again appears to confirm the idea that frequency depends inversely on pressure. The correlation coefficient between frequency and pressure is -0.682 (calculated using MINITAB statistical software).

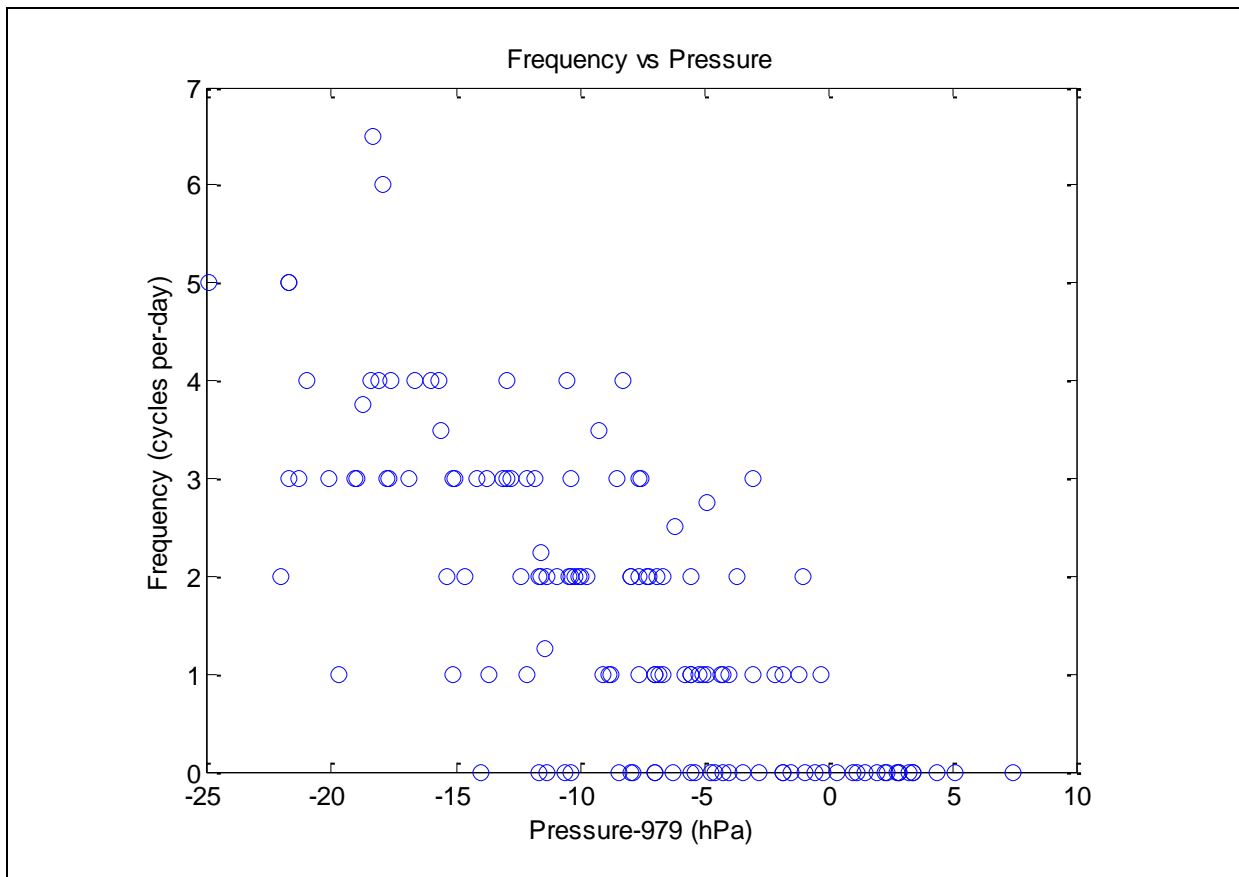


Figure 32. The estimated daily frequencies of the temperature cycles for all four data-sets are combined and plotted against average daily air-pressure during each day (again pressure is centred at 979 hPa). The figure seems to suggest a negative relationship.

From Figure 32 one can identify 3 key areas on the frequency vs pressure plot. When pressure is above the chosen threshold of 979 hPa the frequency is always zero; for pressure between 964 and 979 hPa the frequency is sometimes zero and sometimes non-zero; and when the air-pressure drops below 964 hPa the eruption frequency is always non-zero.

So, while there is not a single value for a threshold which switches the behaviour between cyclic and quiescent, we can think of the pressure threshold as a value past which the frequency is always zero and below which frequency can be both zero and non-zero. If the idea of a threshold is to be imposed on this dataset at a value of 979 hPa then at any time when the pressure is greater than 979 hPa (greater than zero on Figure 32), the frequency can be assumed to be zero.

We now examine what happens when pressure is less than 979 hPa (less than zero on Figure 32). The relationship between frequency and pressure looks to be approximately linear (on the interval we are considering anyway), so we can try to fit a linear regression model for data points with pressure less than 979 hPa. For the regression analysis (see Figure 33), Minitab statistical software was used. The following regression equation is obtained "**Frequency = 0.174 – 0.172 Pressure**". So, within our set of observations, when the air pressure drops by about 5.8 hPa, frequency increases by approximately 1 cycle per day (on average). Note that the standard error of the estimate is 1.08892 cycles per day which is relatively large so the linear model may not very useful for making accurate predictions about the frequency.

Referring to Figure 33, the linear regression has a value $R^2 = 46.5\%$, so only about half of the variability in frequency can be explained by air pressure. Consequently there must be other factors affecting the frequency which are not taken account of here. In this case, the linear model is not overly useful in making predictions due to the large standard error. This analysis does show that pressure and frequency are related, however there are clearly other factors which we have not taken into account that are resulting in this imperfect correlation.

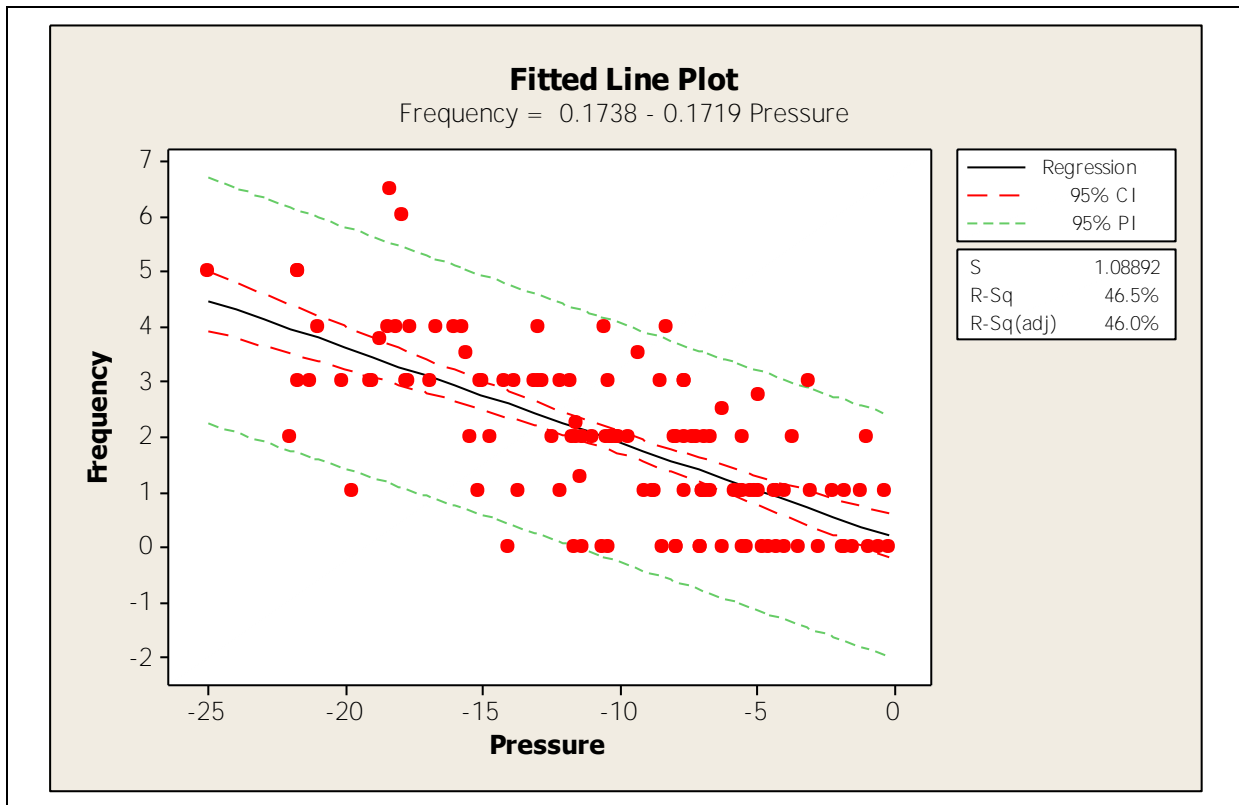


Figure 33. This figure shows the regression line for frequency as a linear function of pressure. The 95% confidence and prediction intervals are plotted also. The standard error (S) and the R-squared (R-sq) values are presented in the side table.

Below, regression analysis data along with other information is presented (from MINITAB).

Regression Analysis: Frequency versus Pressure

The regression equation is

$$\text{Frequency} = 0.174 - 0.172 \text{ Pressure}$$

Predictor	Coef	SE Coef	T	P
Constant	0.1738	0.1989	0.87	0.384
Pressure	-0.17187	0.01705	-10.08	0.000

Standard error = 1.08892 R-Sq = 46.5% R-Sq(adj) = 46.0%

Analysis of Variance

Source	DF	SS	MS	F	P
Regression	1	120.50	120.50	101.62	0.000
Residual Error	117	138.73	1.19		
Total	118	259.23			

Correlations: Pressure, Frequency

Pearson correlation of Pressure and Frequency = -0.682

P-Value = 0.000

Descriptive Statistics: Pressure

Variable	N	Mean	Variance
Pressure	119	-10.087	34.571

2.7.1 The eruption cycle

One prominent feature of the dataset is that when in cyclic mode, a distinct and repetitive pattern can be observed, where the cycle is sometimes stretched or squeezed but nevertheless retains its basic shape.

A typical cycle (see Figure 34 below) consists of a relatively sharp rise in temperature which peaks at about 100°C then drops suddenly by about 20°C before rising rather sharply to about half its original height; it then gradually decreases to around the same level it was originally. The cycle then repeats itself.

Now, recall the generic description for the eruption cycle of geysers: an eruption starts with the water inside the geyser heating up and boiling; after the eruption ends the rate of inflow of cold water into the geyser increases, cooling down and refilling the geyser. The cycle then repeats itself by the geyser heating up again and boiling. With this conceptual idea of the eruption mechanism in mind, it is reasonable to assume that the cyclic behaviour observed in the spring temperature is due to the geyser erupting. The temperature heats up to around 100°C and stays there for about 7–15 minutes which is likely to be the eruption time of the geyser (as the water would be boiling at this stage); after the eruption we observe a drop in temperature which would be due to the rate of inflow of the cold water increasing to replace the lost (hotter) water.

When not in this cyclic mode, the temperature is fairly constant and below boiling, which is telling us that the geyser is not erupting during such an interval.

Then the following conclusion can be drawn about the shape of the graph: the peak in each cycle is the eruption which lasts roughly about 10 minutes, then the drop in the temperature is caused by the inflow of cold water which levels off to a minimum as the geyser fills up and the inflow rate of cold water decreases. At this stage the temperature reaches a low as the geyser is filled and hence the inflow rate of the cold water becomes constant and very small which allows the geyser to heat up again for another eruption (see Figure 34 and 36).

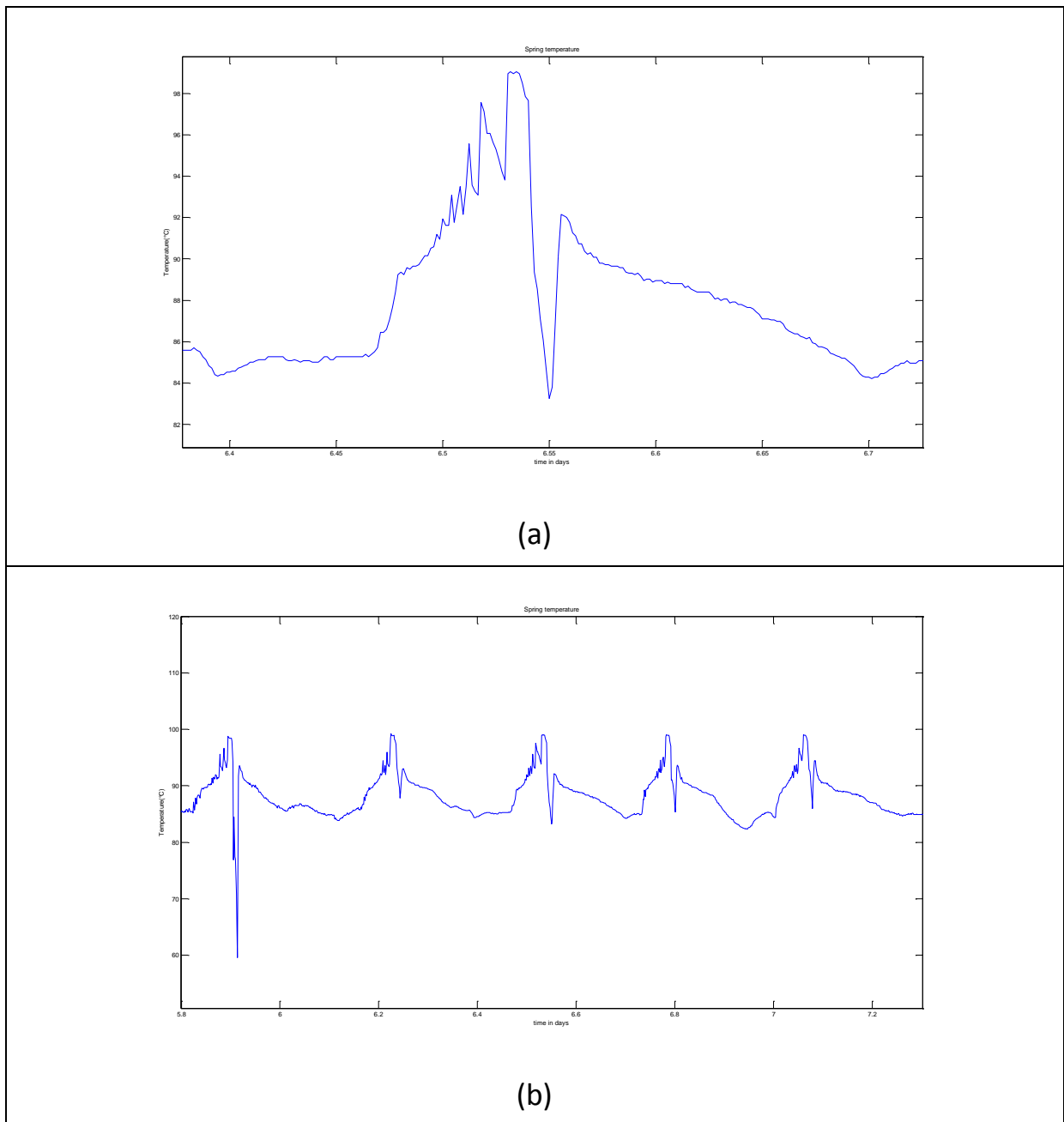


Figure 34. (a) One typical temperature cycle. (b) Repetition of the cycle..

Notice that there is a sudden drop in temperature after an eruption followed by a sharp rise (see Figure 34). One possible explanation for this downward spike may be that the water level drops slightly below the point where the data-logger has been inserted after an eruption due to the loss of water. At this stage we may be observing a combination of air, water and stream temperature. After the water level increases back up to cover the data-logger we would observe an increase in temperature but as the overall water temperature is still dropping due to the refilling process we would observe a gradual decrease in temperature after the upward spike.

In Figure 5 we observed a similar shape in the temperature curves for the laboratory geyser. Saptadji (1995) explains that the sudden falling and rising of the temperature after an eruption was due to the water level falling below the probe point for a short period. The same idea is used to

draw a similar conclusion here. Hence the sharp downward spike after an eruption will be treated as an irregularity and ignored.

This is just one possible explanation for this observation; however there could be other explanations also, such as the recharge point(s) being very close to the data-logger.

2.7.2 Possible effects of air pressure on the geyser

In this section we speculate as to why there are periods when the geyser is erupting and periods when it is not erupting and, during the periods when it is erupting, why it is that the frequency of the eruption cycle varies.

In light of the analysis so far, the obvious driving force (and the only one we have identified so far) behind the eruptions and their frequency would seem to be air pressure.

There may be several possible explanations as to how air pressure is driving geyser activity. One is that there is a relationship between air pressure and the rate at which the cold water flows into the geyser (refilling rate) and/or the rate at which the geyser is heated (heating rate). This could be the case if the pressure in the sources of cold/hot water are independent of air pressure. For this kind of mechanism to have an effect on geyser activity the geyser would need to be reasonably sensitive to changes in refilling/heating rates, since the changes in these rates due to air pressure fluctuations are likely to be quite small.

Faster refilling and heating rates could then contribute to shorter time-intervals between eruptions. On the other hand if air pressure is very high and reduces the heating rate to a low enough level then the geyser may not be able to heat up enough to cause an eruption.

We can try and test this idea on the data but a few assumptions need to be made first. We need to identify definite points on the graphs where we can say that: (1) an eruption has started, (2) the eruption has ended and hence refilling has started and (3) the geyser has been re-filled and is ready to be heated again for another eruption (this is similar to the breakdown in Figure 4). Because it is hard to identify start and end points of an eruption, the eruption is treated as an instantaneous event which occurs when the temperature reaches its maximum point during any cycle. Next we assume that when the temperature reaches the minimum point after an eruption (ignoring the initial downward spike as discussed previously) that the geyser has been filled and is ready to be heated again to another eruption (the temperature curves of the laboratory models in Figure 5 were the basis for these assumptions). Figure 35 depicts the general idea behind our assumptions.

We define "refill time" as the length of the refill phase which is the period from the peak of a cycle to the bottom of the cycle as shown in Figure 35. The "heating time" is defined similarly as the length of the heating phase which is the period from the bottom of a cycle to the peak of the next cycle.

Note that heating takes place continuously throughout time (and hence during the refilling phase also), however what we refer to as the "heating time" in this analysis is the time taken to bring the geyser to an eruption after the geyser has been refilled. The reason we call this heating time is due to the fact that once the geyser has been filled with water the inflow rate of cold water is constant

and very small, so during this time interval the main variable to consider is the heating rate; a higher heating rate would cause the geyser to erupt sooner after refilling.

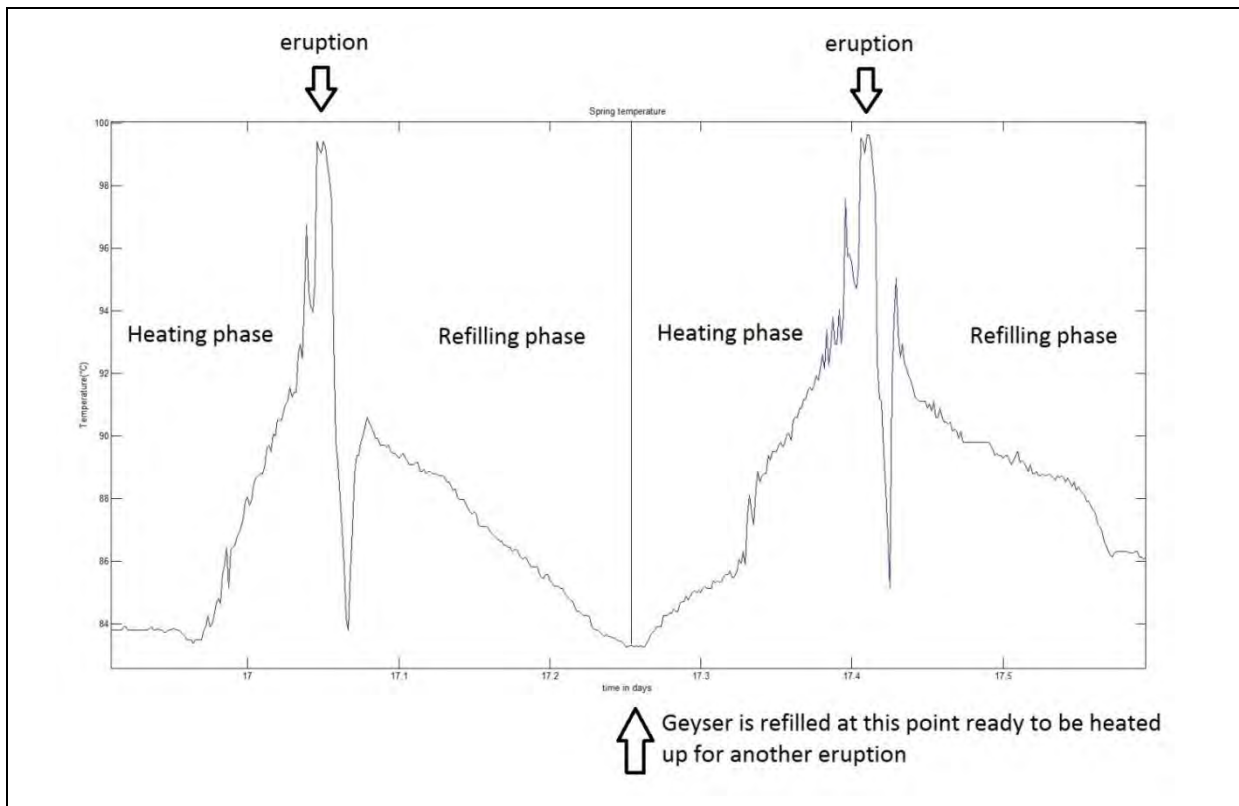


Figure 35. Here a typical cycle is broken into two phases: a refill phase and a heating phase. The eruption is treated as happening instantaneously at the peak of each cycle.

Now we can try to ascertain how the heating time and refill time are affected by air pressure during each cycle.

To test our idea on the data, we devised an algorithm which finds peaks and lows in the data, stores the time interval between them and also computes and stores the average air pressure during each of these periods (Figure 36 gives a picture of how this algorithm works). Note that this was only done for periods when the geyser was active and any irregularities were ignored. Figure 38 shows scatter plots of time against pressure for the two phases; the figure contains separate scatter plots for Datasets 1 to 4, and then a scatter plot for all of the datasets combined.

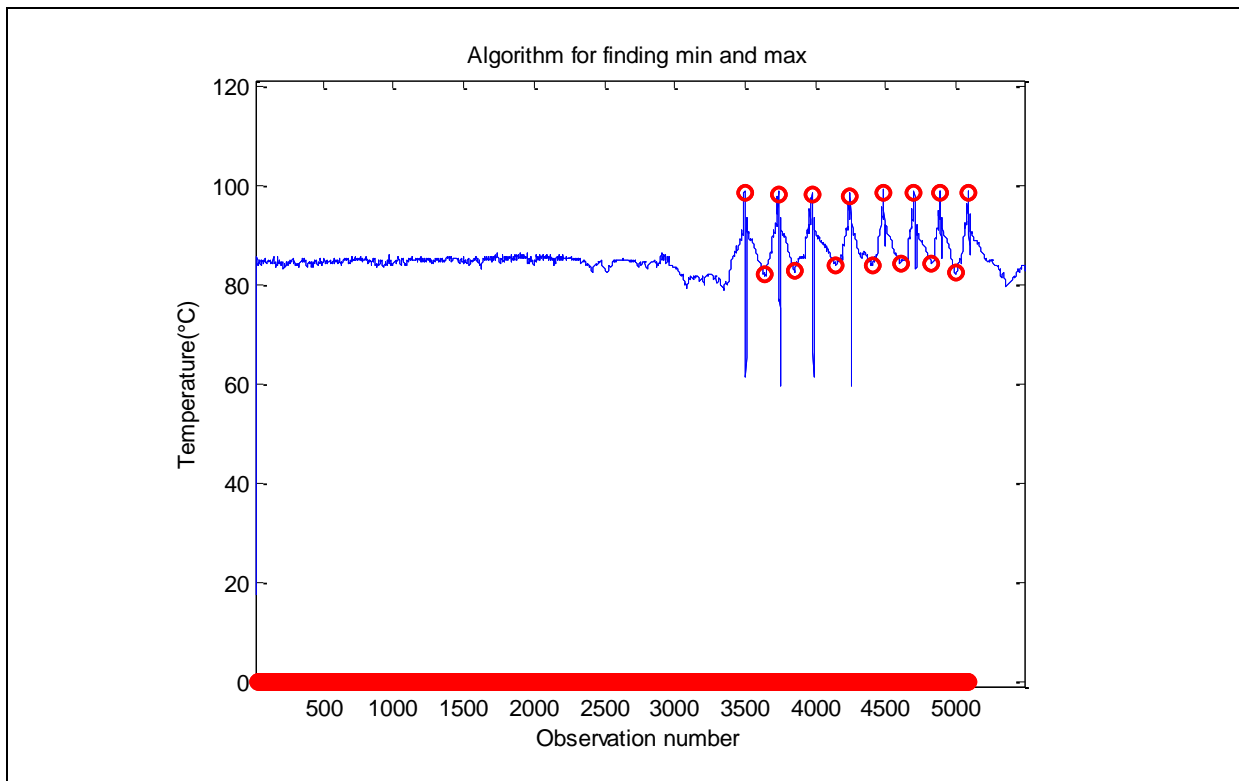


Figure 36. The algorithm finds the peaks and lows in the data (marked by red circles) and stores the time period and average air pressure between them. The blue line represents spring temperature.

Note that

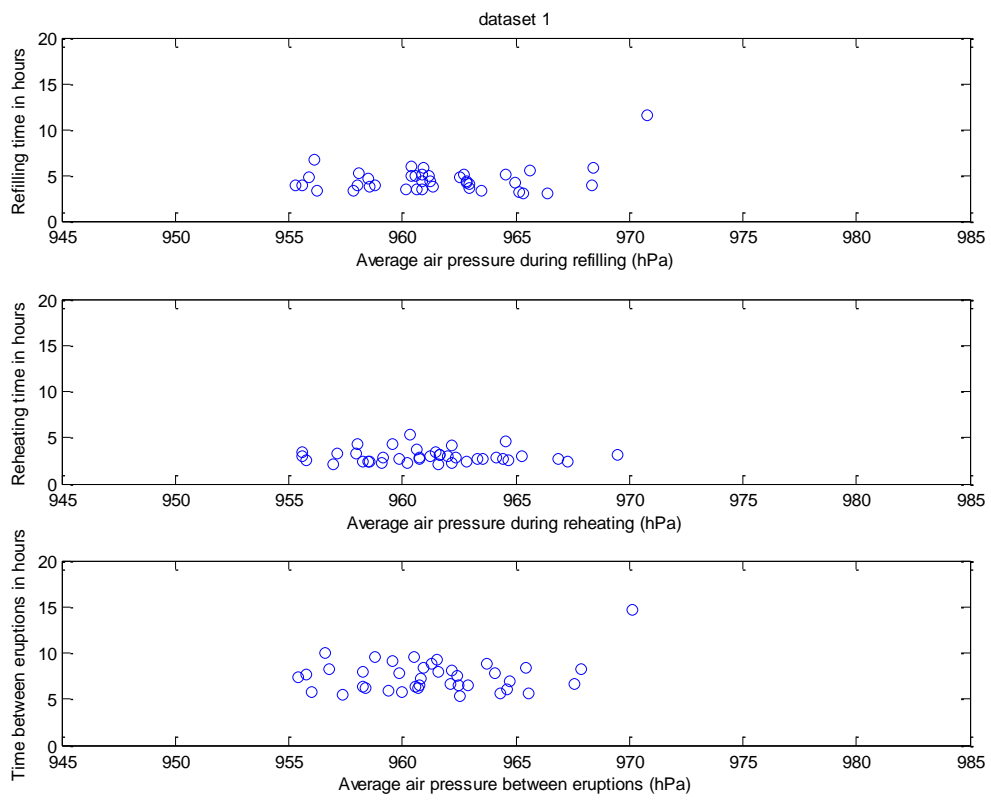
$$\text{refill time} + \text{heating time} = \text{time between two eruptions}$$

and the average air pressure during this period will be the average air-pressure during the filling and heating phases. Using the data we already have we can work out eruption intervals and plot them against average air pressure (see Figure 37 (a) to (e)) to add to the analysis in the frequency and air pressure section. Also note that, in this analysis, only the periods where the geyser was active were analysed, hence no account for zero frequency periods was taken.

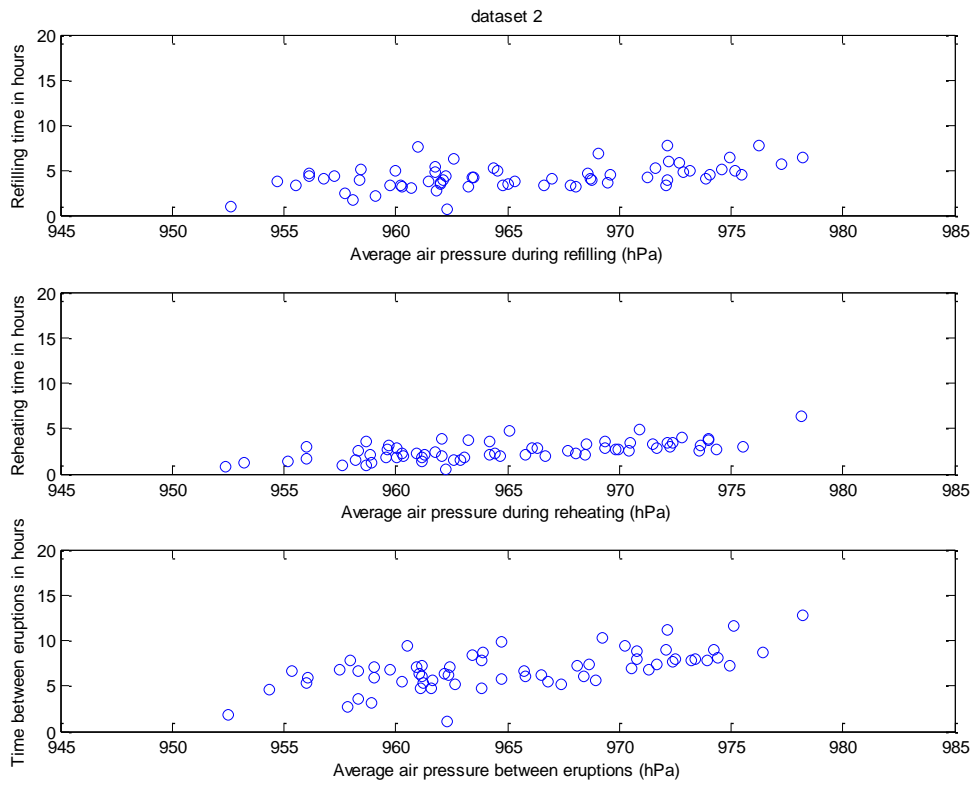
If there is a relationship between air-pressure and heating/refill times then we should expect the scatter plots in Figure 37 to show the relationship (given that our assumptions were correct). All of the graphs, except for Dataset 1 (Figure 37 (a)), show some sort of positive correlation.

To make the relationship more explicit we look at fitting a regression line through the whole dataset (see Figure 38). But first we take the natural logarithm of refill time (Figure 38 (a)), the time between eruptions (Figure 38 (b)) and heating time (Figure 38 (c)); this is due to two reasons: (1) it seems reasonable to assume an exponential relationship⁴ and (2) the log transform greatly improves the fit of the regression model.

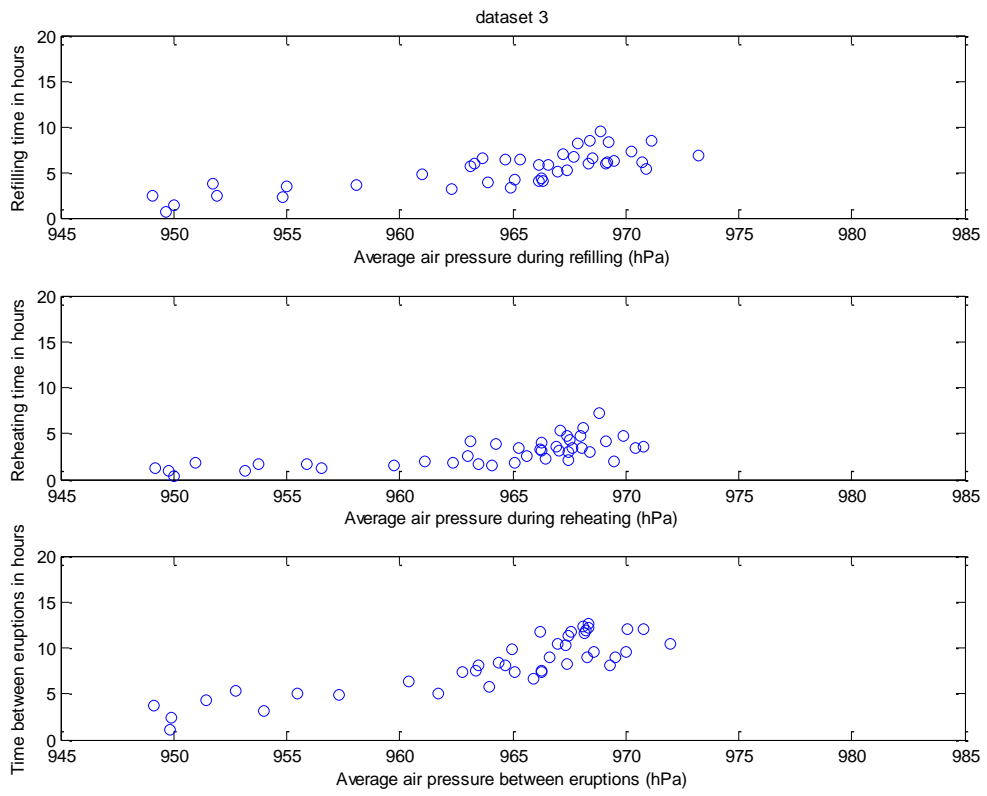
⁴ As air pressure goes to infinity the time between two eruptions (mathematically) becomes infinite and as air pressure goes to negative infinity, the time between two eruptions (mathematically) goes to zero. The same argument applies to heating and filling times.



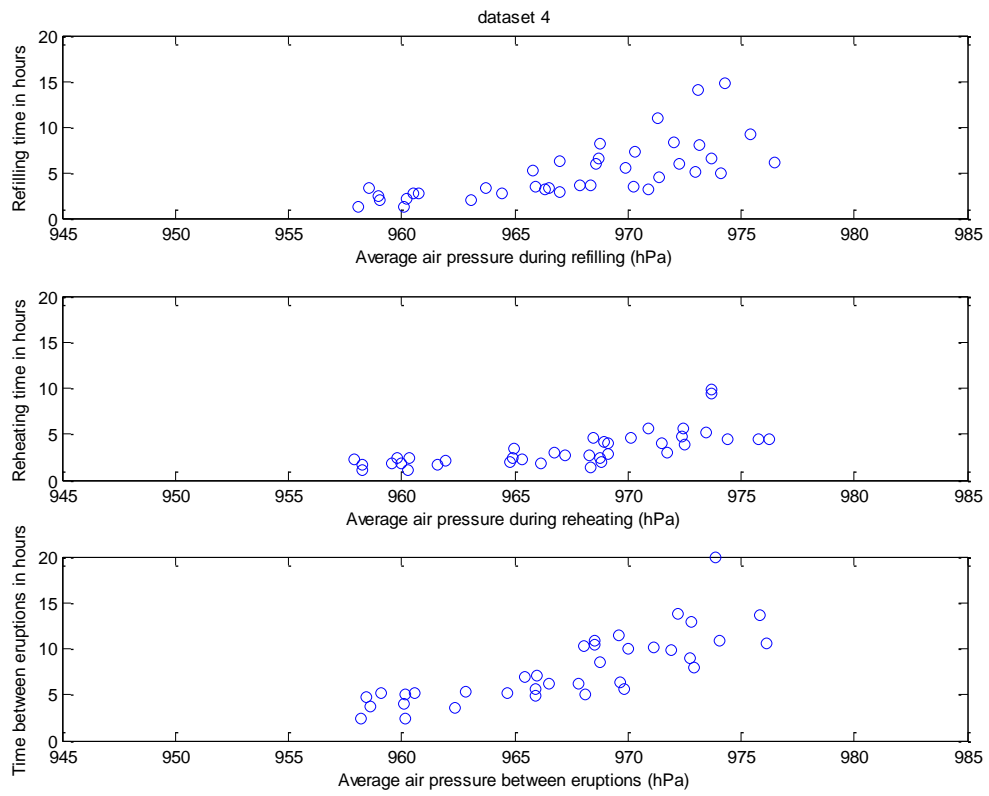
(a)



(b)



(c)



(d)

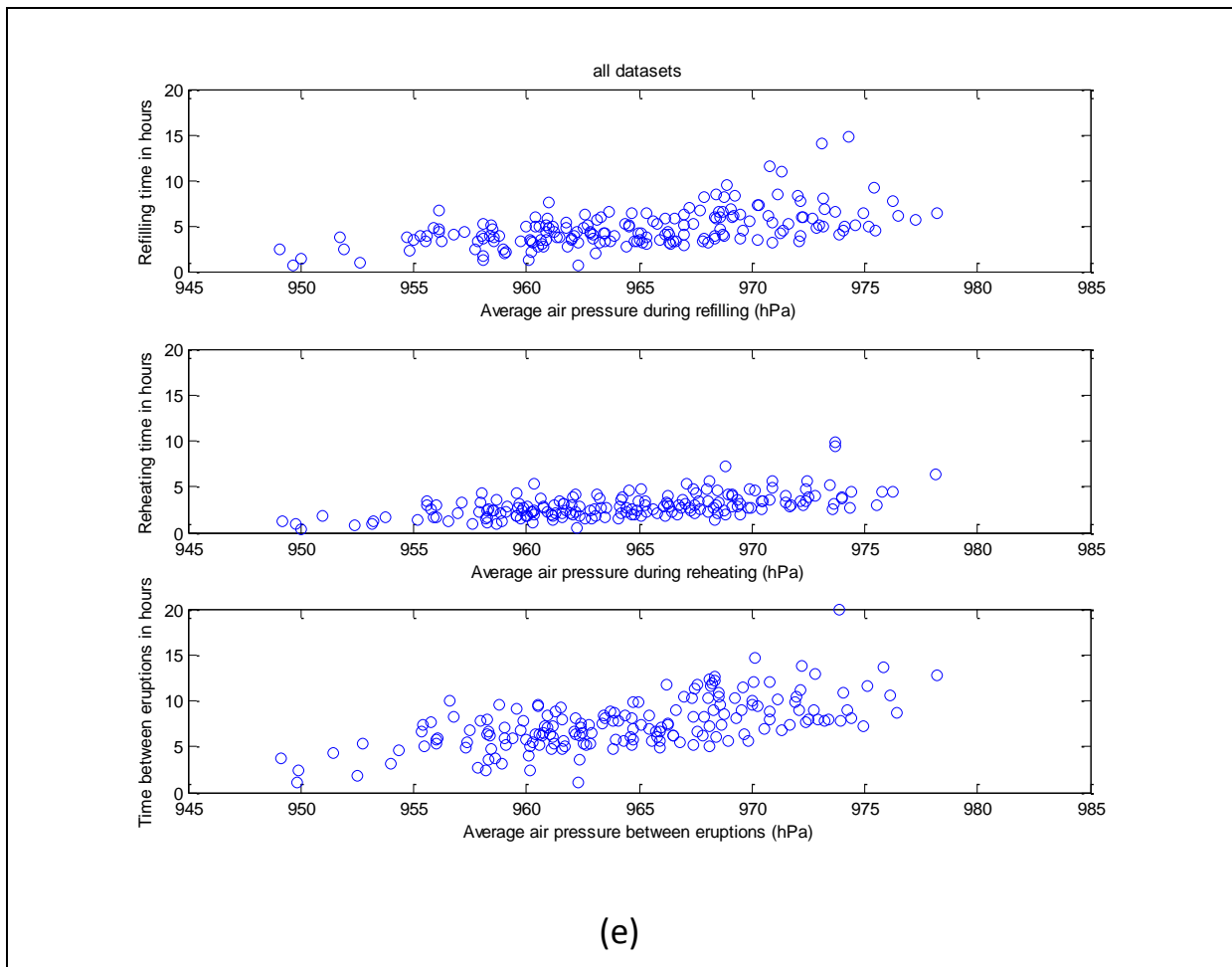
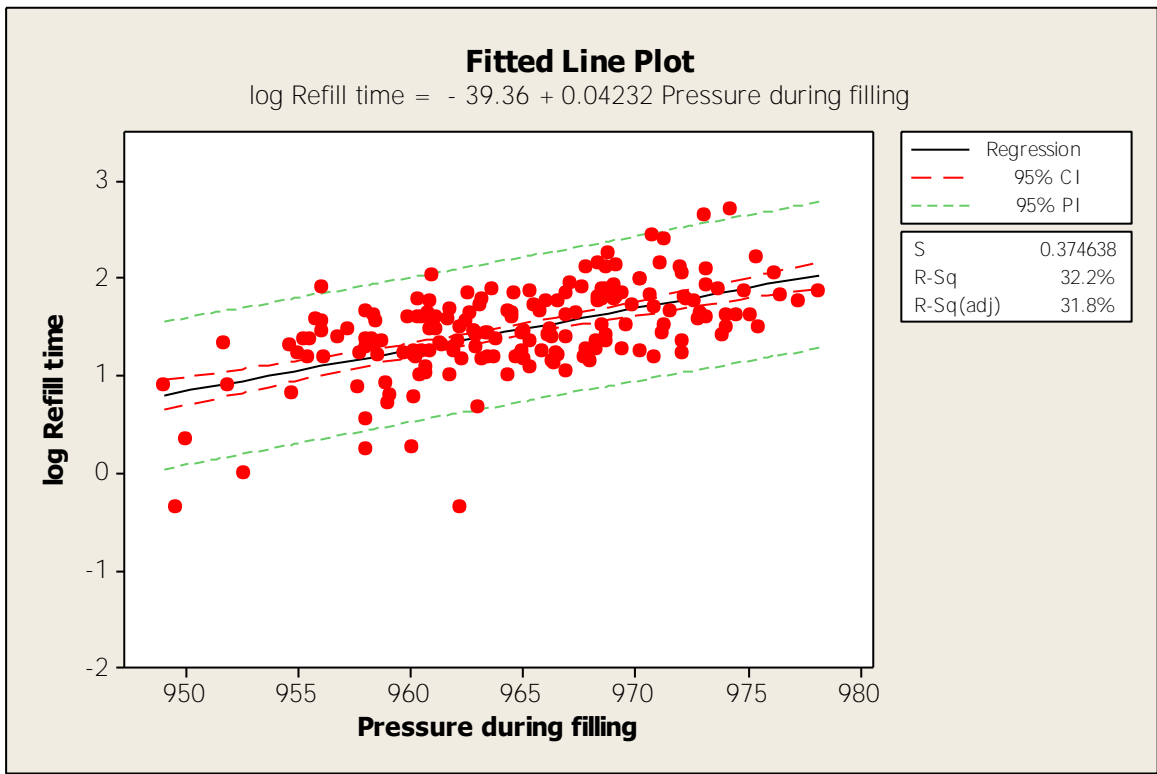


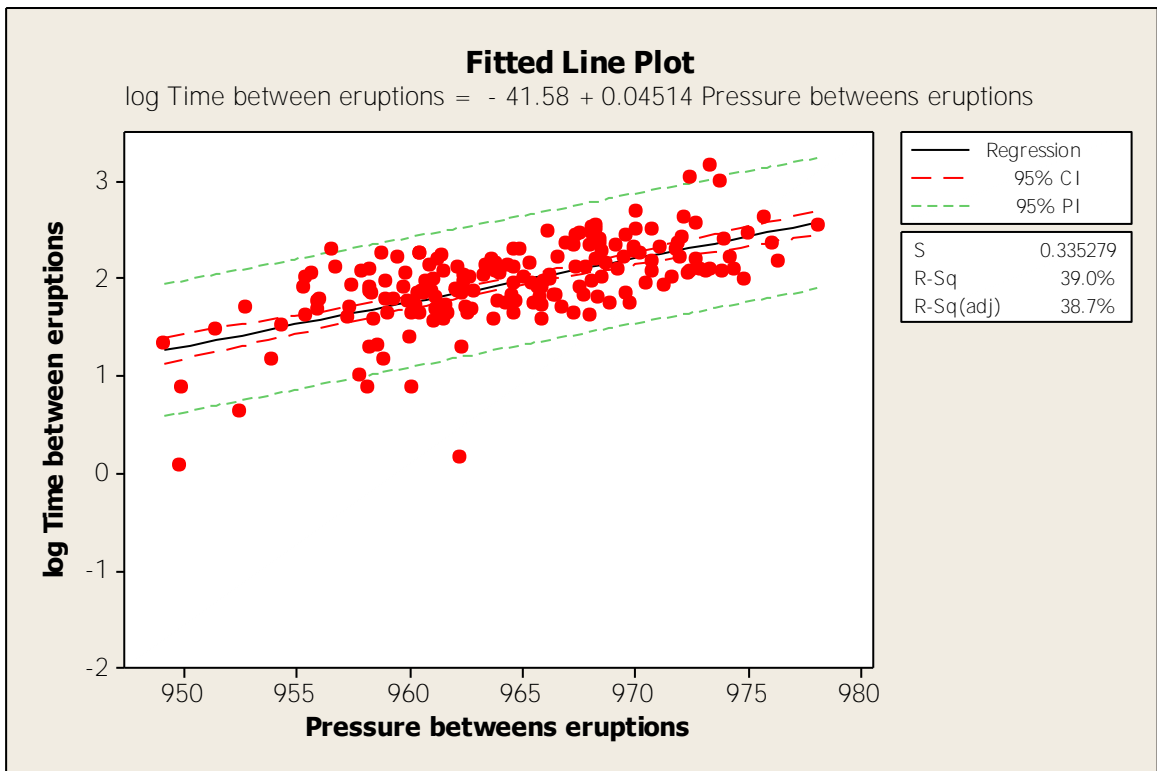
Figure 37. Each graph has three subgraphs: the first is for refill time, the second for heating time and the third for the time between eruptions. These times are plotted against corresponding average air pressure values. (a) Dataset 1. (b) Dataset 2. (c) Dataset 3. (d) Dataset 4. (e) All datasets combined.

The plots in Figure 38 shows there is definitely a relationship between air pressure and spring behaviour, however the R^2 values are quite small making the relationship rather weak. Nevertheless, there is still some information here and the analysis shows that refill time and heating time do indeed depend to some extent on air pressure. If our assumptions used in measuring refill time and heating time are correct, then Figure 38 shows that about 30% of the variation in refill rate and 35% of the variation in heating rate can be explained by the variations in air-pressure.

Finally, when in eruptive mode, about 40% of the variability in eruption frequency (the inverse of the time between two eruptions) can be explained by variations in air-pressure.



(a)



(b)

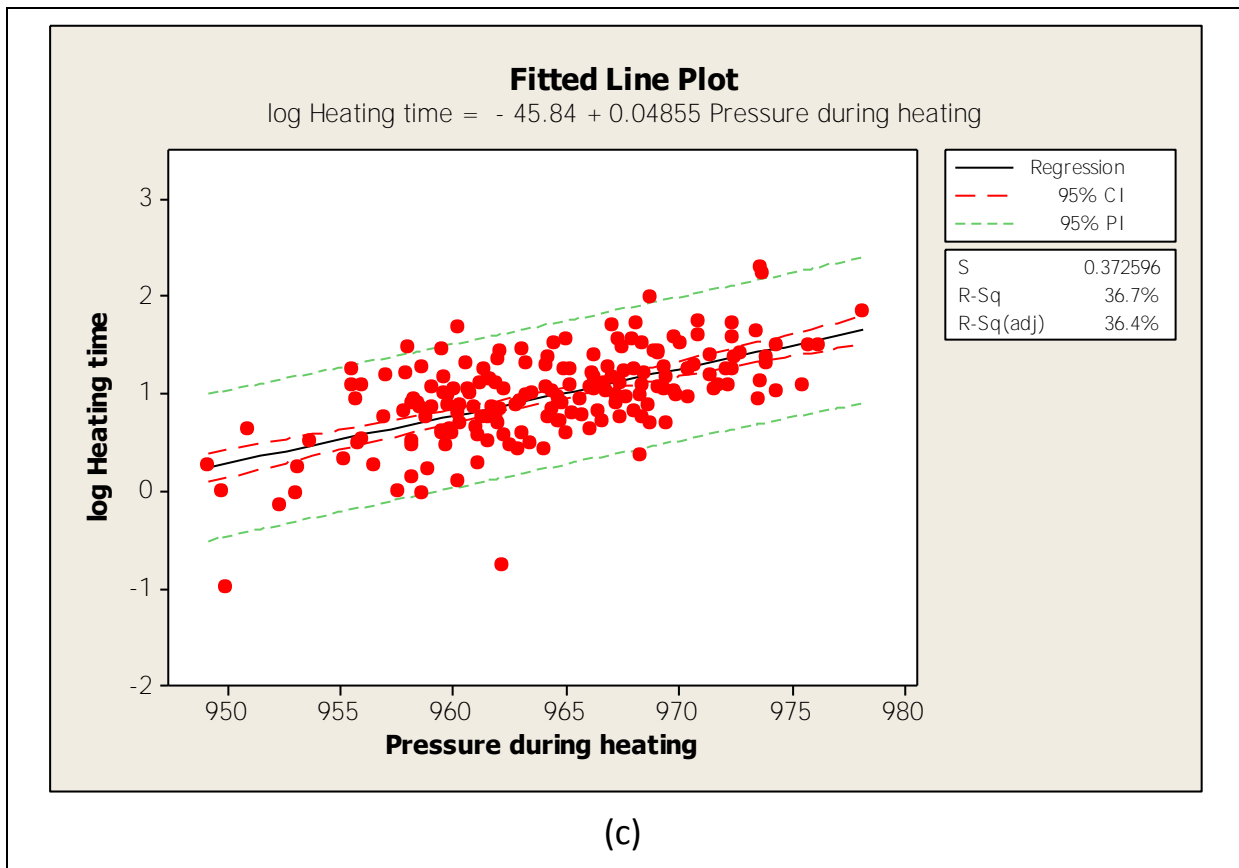


Figure 38. Regression lines fitted to: (a) The log of refill time interval against air pressure; (b) The log of eruption interval against air pressure; (c) The log of heating time interval against air pressure.

2.7.3 Frequency and air pressure revisited

Previously when looking at the frequency of the cycles against air pressure, we used a crude estimate for daily frequencies. Using a slight variation of the algorithm developed in the previous section we can take the peaks of every cycle and calculate the time and average air pressure between them. This would yield a more systematically-obtained and hence, arguably, a more reliable result for assessing the effect of air pressure on eruption frequency.

What we expect based on previous findings is a positive correlation between air pressure and eruption interval. Again, we expect an exponential relationship⁵.

Note that there is a difference between the analysis in this section and the previous ones on frequency and pressure. When analysing the the time between eruptions in the previous section we looked only at periods when the geyser was active. In the section on eruption frequency and air pressure we looked at daily frequencies against average daily pressure, so frequency was zero at times. In this section we look at the entire data collection (ignoring irregular periods) and take the intervals between two eruptions instead of looking at frequency during fixed intervals (like a day) or looking only at active periods.

⁵ As air pressure goes to infinity, the time between two eruptions (mathematically) becomes infinite, and as air pressure goes to negative infinity, the time between two eruptions (mathematically) goes to zero.

The inverse of eruption interval is eruption frequency. Since we expect an exponential relationship, we take the natural log of eruption frequency. (This is the negative of the natural log of eruption interval, so for the rest of the analysis we will work with the natural log of frequency).

Figure 39 shows scatter plots for the log of eruption frequency against air pressure for the four datasets first and then for all of the datasets combined. As before, Dataset 1 does not show a very strong relationship, however the other three data sets show a definite (and seemingly linear) relationship.

Again we fit a linear regression line through the plot for the entire dataset (Figure 40). Here there is a definite relationship but it is not very strong, $R^2 = 38\%$ tells us that only 38% of the variation in eruption frequency is explained by air pressure. Notice that it is not clear whether the relationship is linear since the data seems to fall off the line by a large amount as the pressure gets higher; this may have to do with the pressure threshold mentioned previously so that we may get an asymptote at some unknown point possibly close to 980 hPa.

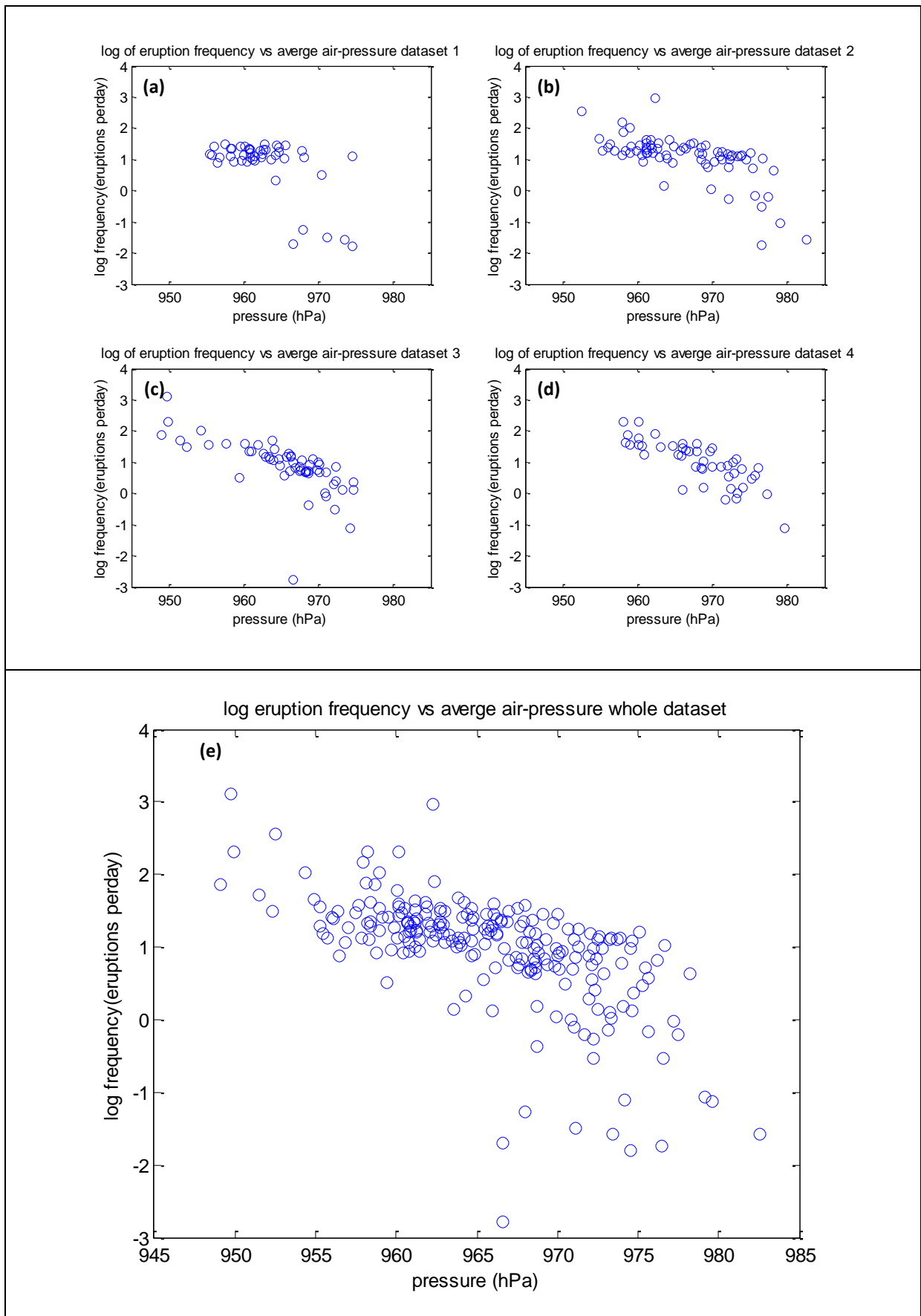


Figure 39. Scatter plots of Log frequency vs air pressure. (a) Dataset 1. (b) Dataset 2. (c) Dataset 3. (d) Dataset 4. (e) All datasets.

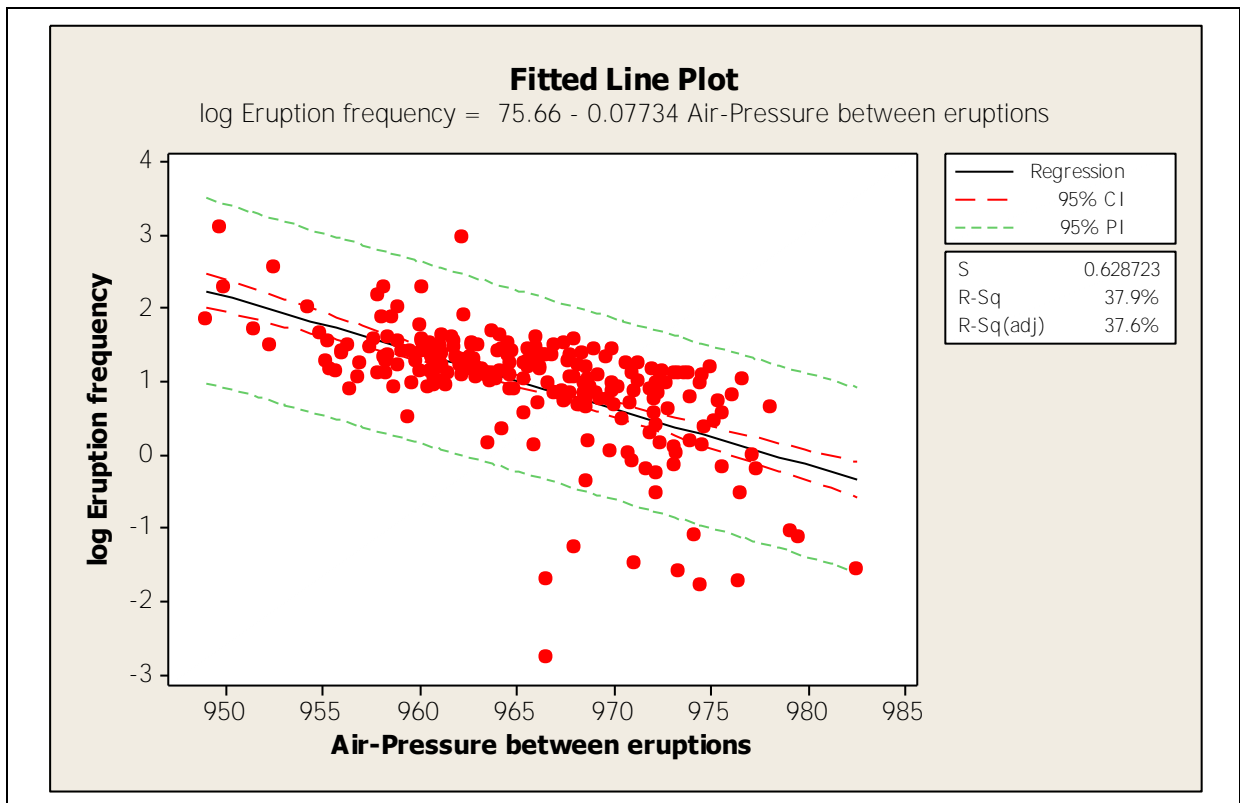


Figure 40. Regression line for log frequency vs air pressure.

2.8 Waiotapu Geyser: Summary and conclusions

While looking at temperature data from the Waiotapu Geyser we identified two modes in the spring's temperature behaviour: a quiescent mode where the temperature was constant (around 80 °C) and an eruptive mode during which the temperature displayed cyclic behaviour, fluctuating between about 80-100 °C. When in this eruptive mode the spring's temperature displayed a distinct pattern which varied in frequency through time.

There were no consistent relationships identified between spring temperature and air temperature or seismic activity throughout the time period analysed. There is possibly a relation between high rainfall events and spring cooling. However a relationship between air pressure and spring temperature was identified. It was observed that periods of high air pressure corresponded with the quiescent mode in the data and periods of low air pressure corresponded with the eruptive mode. It was further observed that lowering the air pressure seemed to increase the temperature cycle's frequency. We tested this idea quantitatively by plotting pressure against frequency as scatter plots and fitting a regression line through them. We found that while there was some definite relationship, it wasn't very strong (R^2 of about 40%) and there were still variations in frequency which were unexplained by air pressure alone.

We speculated that variations in air pressure lead to variations in the filling and/or heating rates of the geyser and hence its eruption frequency. After testing this idea we found some evidence in its favour; however, the evidence we found was not very strong and it rested on the set of assumptions that were made.

From the analysis it is clear that air pressure is definitely a factor affecting the Waiotapu Geyser. But it is also clear that other unidentified factors are also having various effects on the system. It is difficult to say what these other factors might be without further analysis, but in light of the previous studies on geysers they may include things such as tidal forces, the longer-term hydrologic cycle, the internal dynamics of the geyser and precipitation trends. The fact that the water level drops from time to time may also be an indicator that the geyser is connected to some other nearby thermal features.

3 SODA FOUNTAIN

3.1 Introduction

There are five temperature time series datasets from the Soda Fountain, a spring at the Orakei Korako Thermal area (Section 3.2). The data is described in Section 3.3.

In Section 3.4 the data is compared with climate data (air temperature, pressure, and rainfall) to investigate if there is any correlation with short term climate variations. Seismic records from the GNS Science Geonet website are used to examine any relationship between spring behaviour and seismic events (Section 3.5).

Sections of the data, where we are reasonably sure that the probe was measuring water temperature over the entire cycle, are selected for Fourier analysis to show the dominant frequencies of the cycle (Section 3.6). A closer examination of the temperature cycle and air pressure is given in Section 0.

3.2 Description

The Orakei Korako Geothermal Field is an unexploited field consisting of over 30 small active geysers and about 100 hot springs (Leaver *et al.*, 2005). It lies within the Taupo Volcanic Zone (see Figure 1) and straddles the Waikato River at Lake Ohakuri (Lynne & Howe, 2010).

The Soda Fountain is an "erupting hot spring" located at the Orakei Korako Geothermal Field. It consists of dilute $\text{HCO}_3 - \text{Cl}$ water with the water level rising and falling from time to time (Lynne & Howe, 2010). The spring has long dormant periods. "Data from 1995-2009 suggest that the water temperature ... dominantly ranges between 96 to 100 °C. Since 2002, the temperature has not decreased to below 90 °C, however prior to May 2002, on several occasions the temperature decreased to as low as 66 °C" (Lynne & Howe, 2010).

The fourth photograph in figure 42 shows the overflow channel while the Soda Fountain is erupting. A video of the spring erupting can be found on the following link:

<http://www.youtube.com/watch?v=wHpalR-pVIO>.



Figure 41. The Soda Fountain Spring full of water and overflowing. The feed is located in the base of the pool, below the boiling water in the upper right of the photo.



Figure 42. The overflow channel, with flow to the left of the photo.



Figure 43. The Soda Fountain is surrounded by sinter, some of which has a geysirite texture, particularly the exposures near the boiling area of the pool.



Figure 44. A view of the Soda Fountain showing the path of the overflow channel.

3.3 The Data

There were five sets of data collected from the Soda Fountain; each dataset is 45 days long with temperature recorded at 2-minute intervals. We will refer to a certain day in a dataset as the number of days after the first observation for that dataset. The dates of collection are as follows:

Dataset 1: 15/06/2010 08:58:24 a.m. – 30/07/2010 12:42:24 p.m.

Dataset 2: 16/08/2010 04:04:17 p.m. – 30/09/2010 07:48:17 p.m.

Dataset 3: 4/10/2010 08:48:51 a.m. – 18/11/2010 12:32:51 p.m.

Dataset 4: 30/12/2010 09:02:38 a.m. – 13/02/2011 12:46:38 p.m.

Dataset 5: 3/03/2011 02:10:40 p.m. – 17/04/2011 05:54:40 p.m.

Each dataset is broken into two halves; plots of the resulting 10 figures give us an overview of the spring temperature over time (see Figure 46).

3.3.1 Data description

Although difficult to see from the plots in Figure 46 due to the high frequency oscillations, the temperature shows periodic patterns. There are two main types of cycle, described below, and shown in Figure 45.

3.3.1.1 Low amplitude and high temperature cycle:

An example of this type of cycle is Interval A, shown in Figure 45. Over the interval, the temperature oscillates over approximately 5 °C, with an average temperature above 90 °C. These low amplitude high temperature intervals are used for the Fourier analysis.

3.3.1.2 Large amplitude cycle:

There are periods when the temperature cycles between near-boiling and less than 70 °C; at times it drops below 40 °C. An example of this behaviour is shown by Interval B in Figure 45. The process that causes this large fluctuation in the temperature is unknown, but it is possibly caused by the water level dropping below the level of the probe. This means that the data consists of water temperature and air temperature measurements. Although this is one possible explanation, until further investigations can demonstrate the reason for the large fluctuations, the data cannot be used for Fourier analysis. However, it is reasonable to investigate any possible correlation between climatic factors and the interval of these large temperature fluctuations.

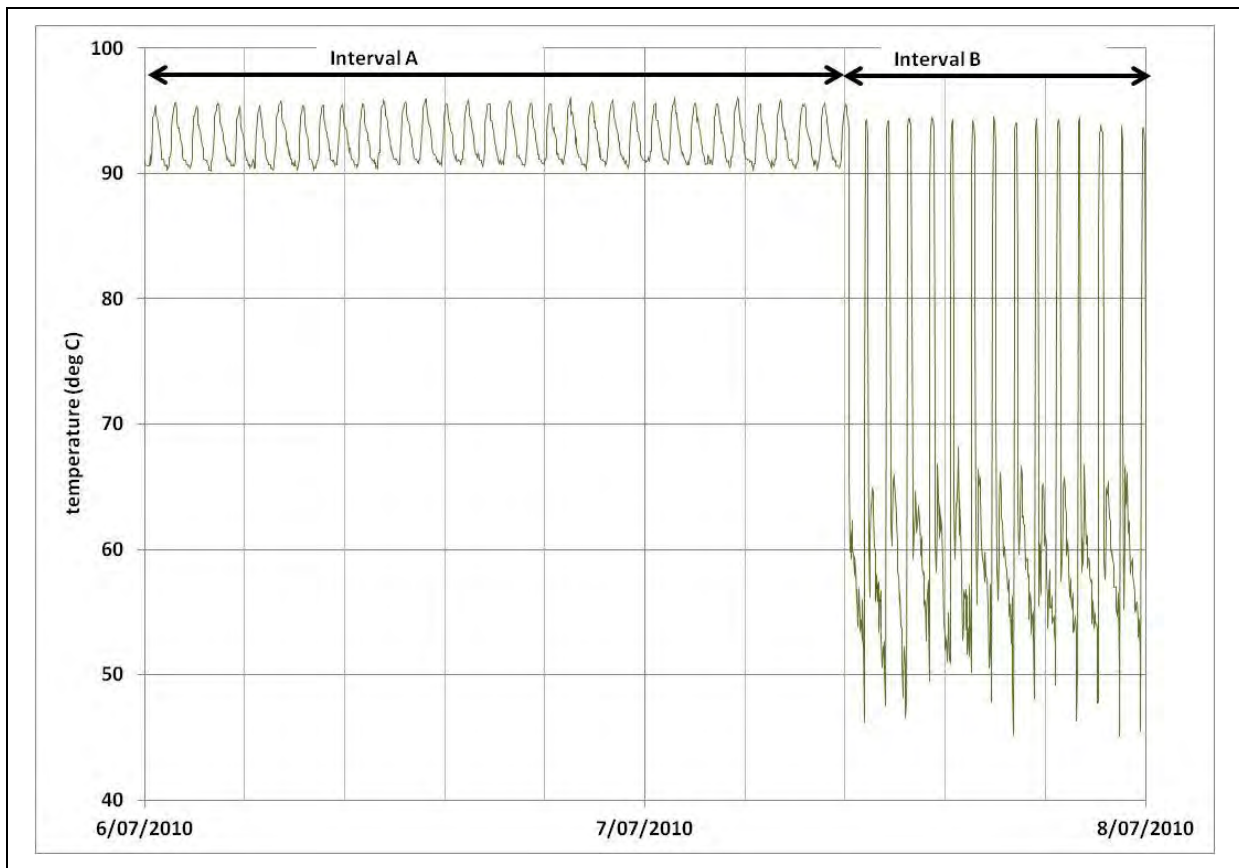


Figure 45. Interval A is an example of low amplitude, high temperature cycle, and Interval B is an example of large amplitude fluctuations in temperature.

3.3.1.3 Maximum temperatures

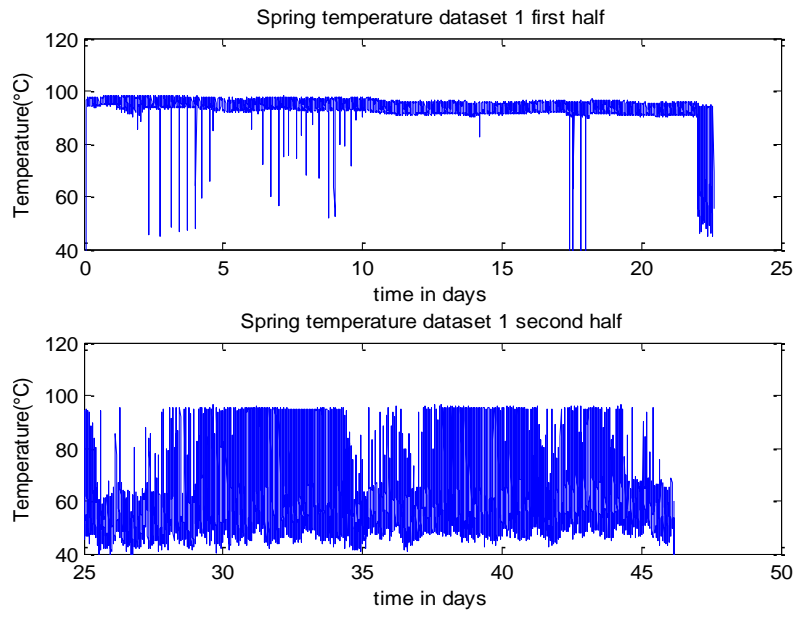
Datasets 3, 4, and 5 all contain time intervals where the temperature peaks in the cycle are above boiling point at atmospheric pressure (approximately 1 bar).

After about Day 15 on Dataset 5 we observe that the peak temperature is 120 °C. This data requires some scrutiny because 120 °C is significantly above boiling point at atmospheric pressure.

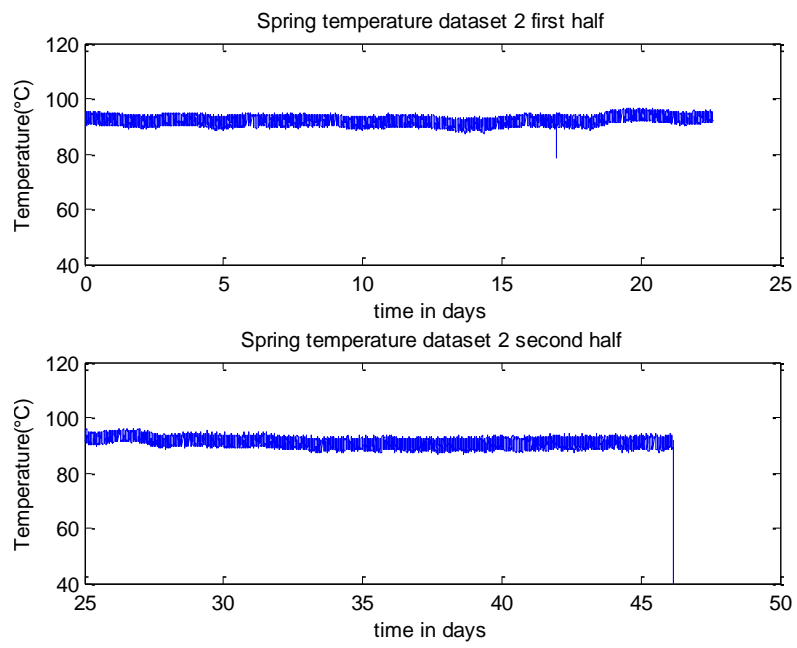
There are no observations of the geyser during this period. There are two possible explanations for the high temperature data; either the records are real, suggesting there was strong geysering, or the datalogger was failing. These possibilities are discussed below.

Geysering is suggested because of the high temperature (and high heat flow), and because the data shows cyclic temperatures with approximately the same frequency as the rest of the data. The probe was at least 0.5 m below the floor of the pool, in the relatively constricted feed channel, where there may be intermittent high pressure during an eruption. If the water temperature was 120 °C the pressure would be approximately 2 bar. The problem with this proposed situation is that the probe might be expected to be thrown out of the feed unless it was wedged. For Dataset 5, the frequency and amplitude of the cycle look similar to the other datasets, lending weight to the proposition that the data is real.

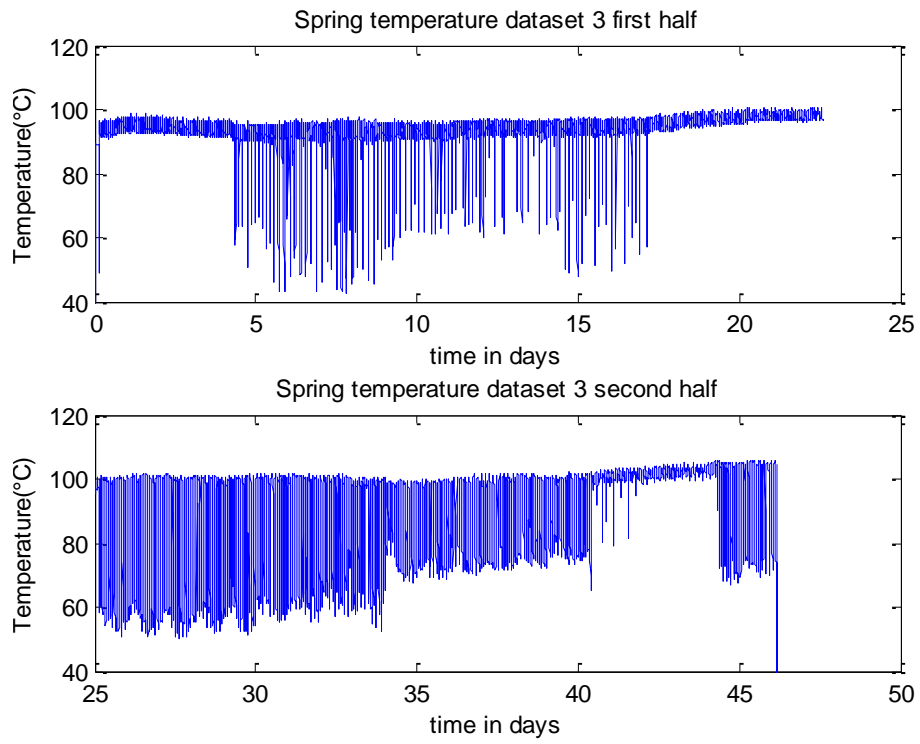
This brings us to the alternative: equipment failure. This is suggested because the datalogger did indeed fail to work after this deployment.



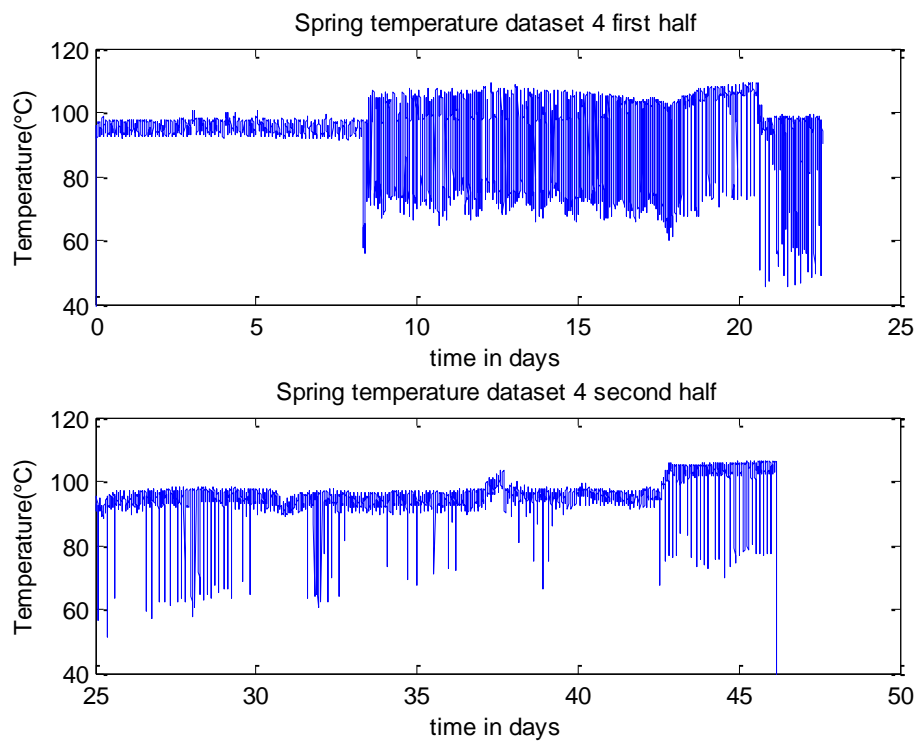
(a)



(b)



(c)



(d)

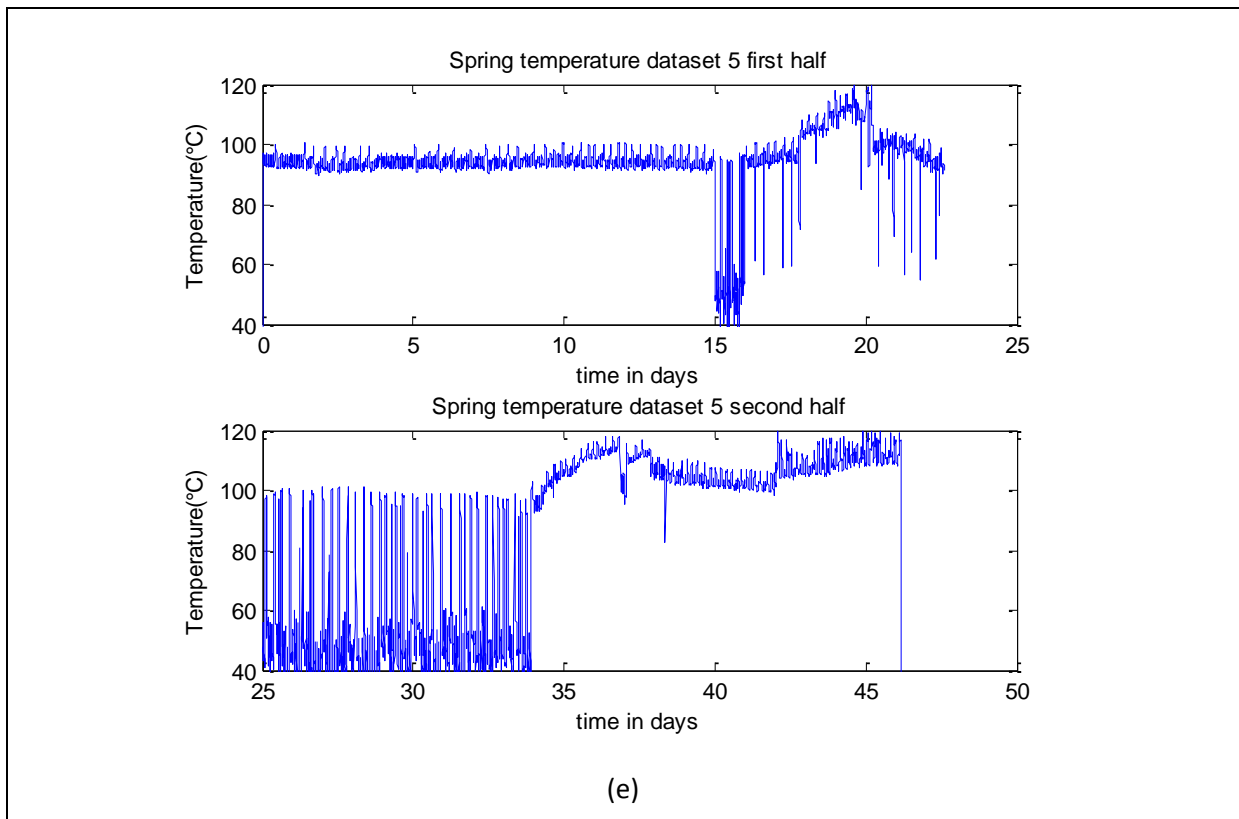


Figure 46. Temperature vs time plots for Soda Spring. Datasets 1–5 are broken down into two halves and are plotted from top to bottom in order. (a) Dataset 1. (b) Dataset 2. (c) Dataset 3. (d) Dataset 4. (e) Dataset 5.

3.4 Examining the effects of climate factors

In this section, the rainfall, air pressure and air temperature data obtained from the database on the NIWA website (Taupo AWS station) are analysed in order to find a relationship (or lack of relationship) between these variables and the spring temperature. Note that the air temperature data presented here is an average of the hourly high and low temperatures taken from the NIWA database.

Figure 47 and Figure 48 indicate that there are no apparent relationships between any of the variables and spring temperature. Dataset 2, which is the most well-behaved of all the datasets, does not seem to show any sort of special response to variations in any of the climate factors. We will analyse the effects of air pressure and air temperature further in following sections.

The comments made with respect to the Waiotapu Geyser and climatic factors also apply here; that the nature of the datasets (discrete intervals rather than continuous) limit the investigation to only short term climatic conditions.

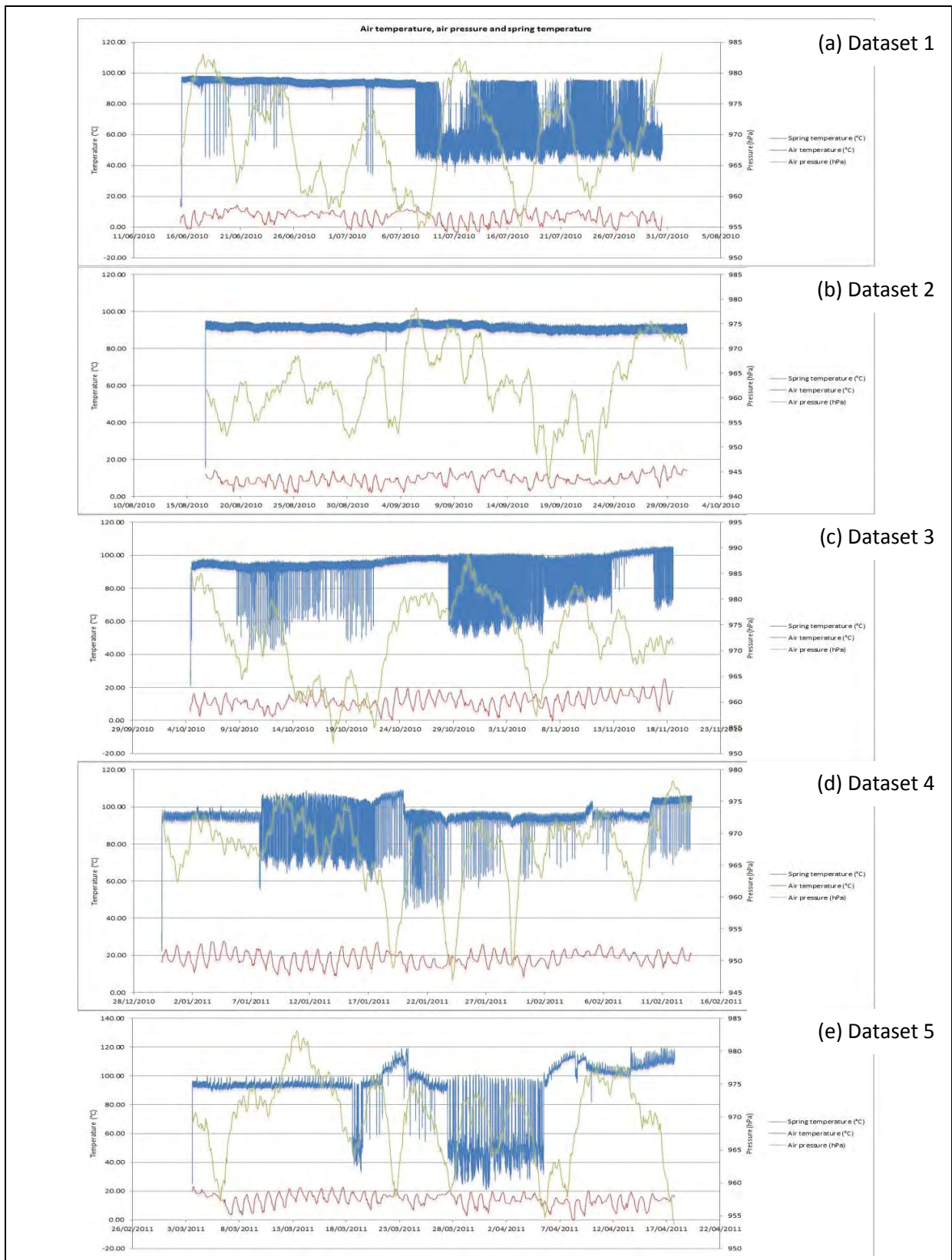


Figure 47. Soda Fountain spring temperature, air pressure and air temperature as time series. In each case, the red line is the air temperature, the green line the air pressure and the blue line is spring temperature. Pressure (right axis) is measured in hectopascals while temperature (left axis) is measured in degrees Celsius (°C). (a) Dataset 1. (b) Dataset 2. (c) Dataset 3. (d) Dataset 4. (e) Dataset 5.

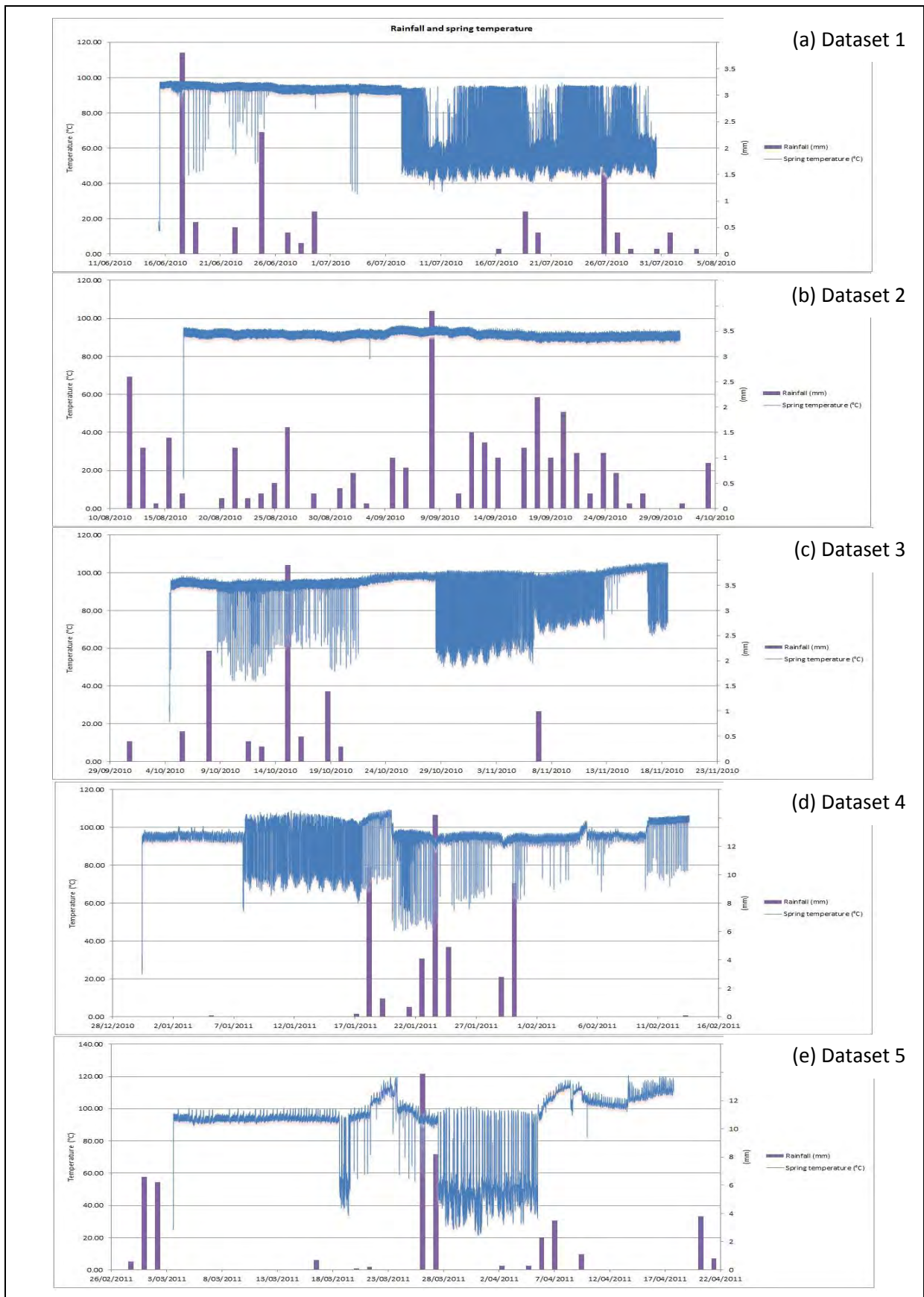
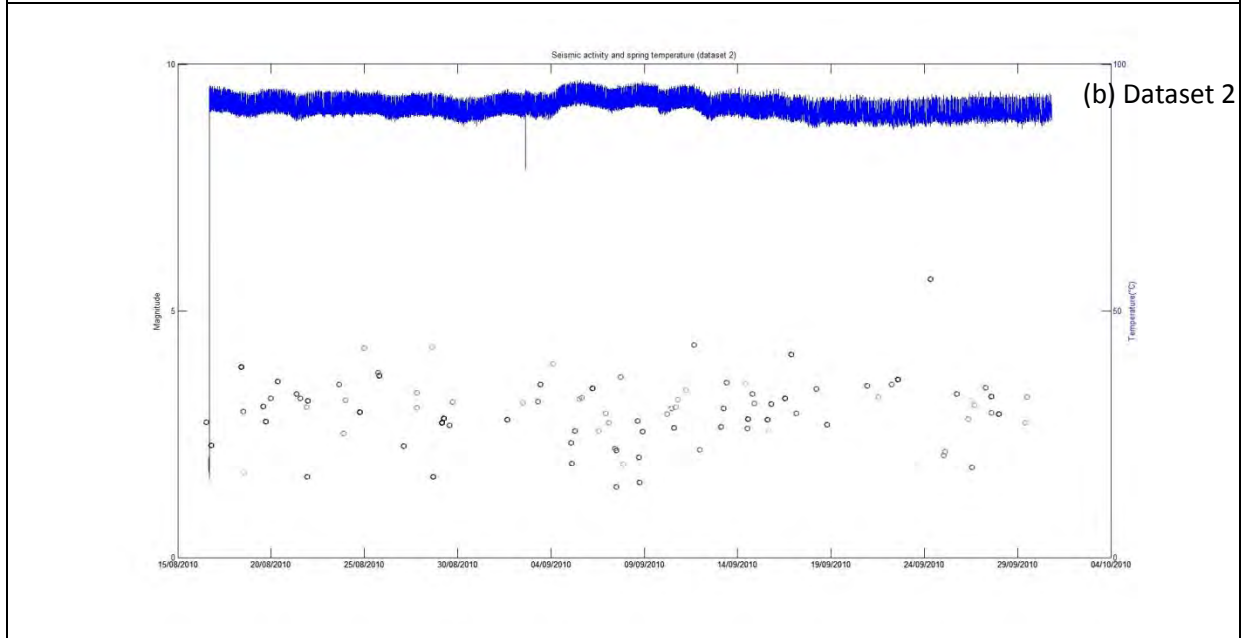
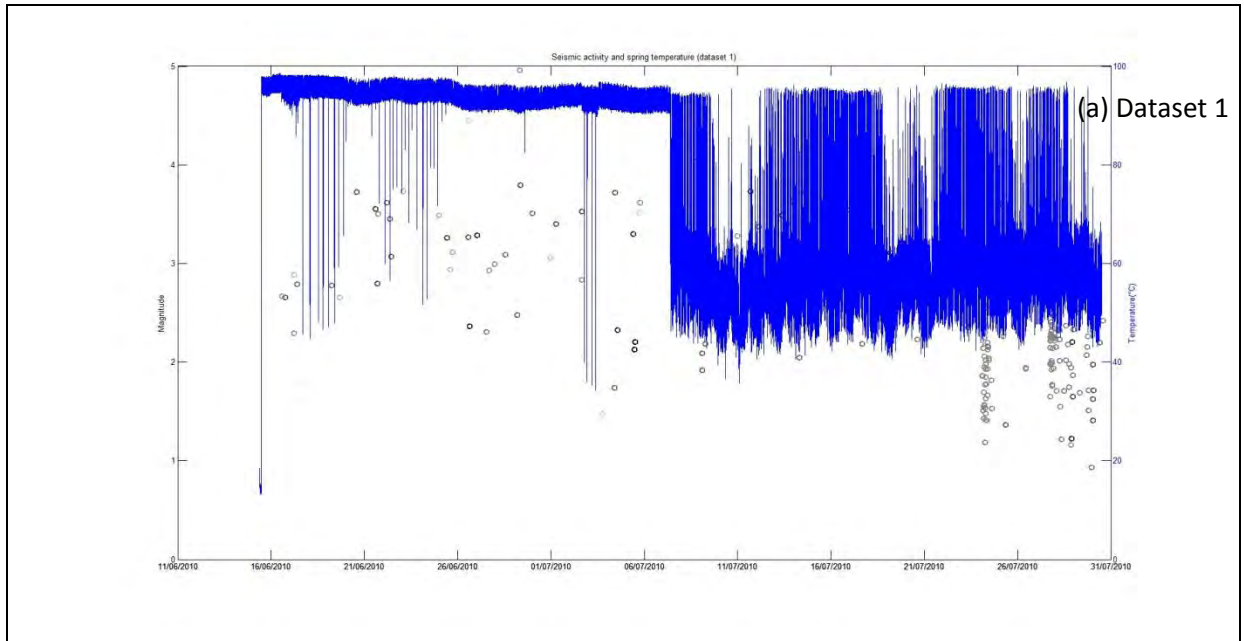


Figure 48. Soda Fountain spring temperature (°C) in blue and rainfall (mm) in purple.
 (a) Dataset 1. (b) Dataset 2. (c) Dataset 3. (d) Dataset 4. (e) Dataset 5.

3.5 Seismic activity

Seismic data obtained from GeoNet – Quake Search is presented in this section along with spring temperature. Figure 49 shows the plots for seismic activity and spring temperature. Spring temperature (the blue line) is plotted on the right axis and the magnitude of seismic activity (black circles) is plotted on the left axis. The colour of the circles indicates the distance of the seismic event from the Soda Fountain: the darker the circles the closer the seismic event.

Although there are changes in the way the spring temperature behaves with time, there seems to be seismic activity occurring continually making it difficult to pinpoint one specific event which may be causing these these changes. It is not clear whether there is any effect associated with seismic activity on the spring temperature.



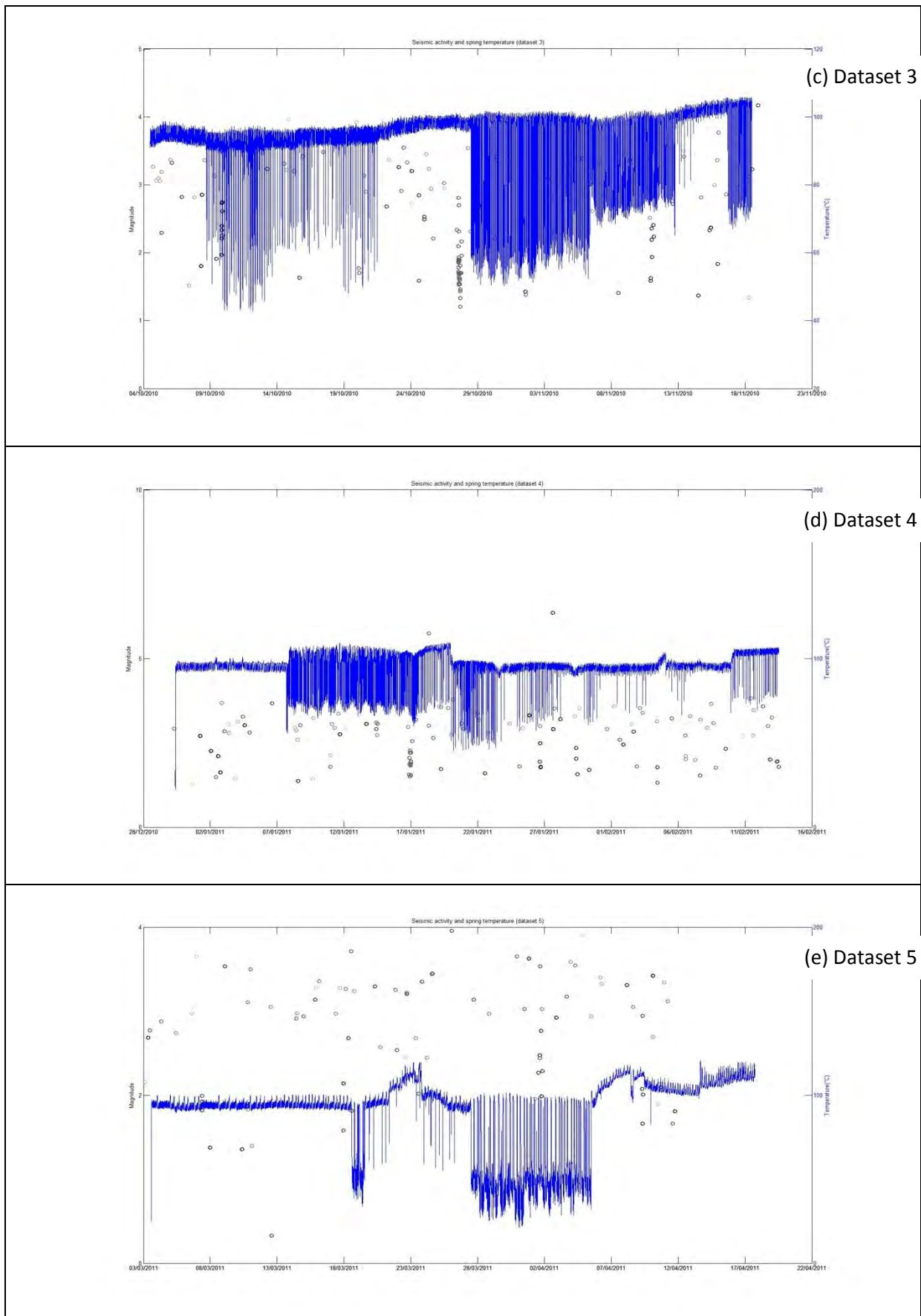


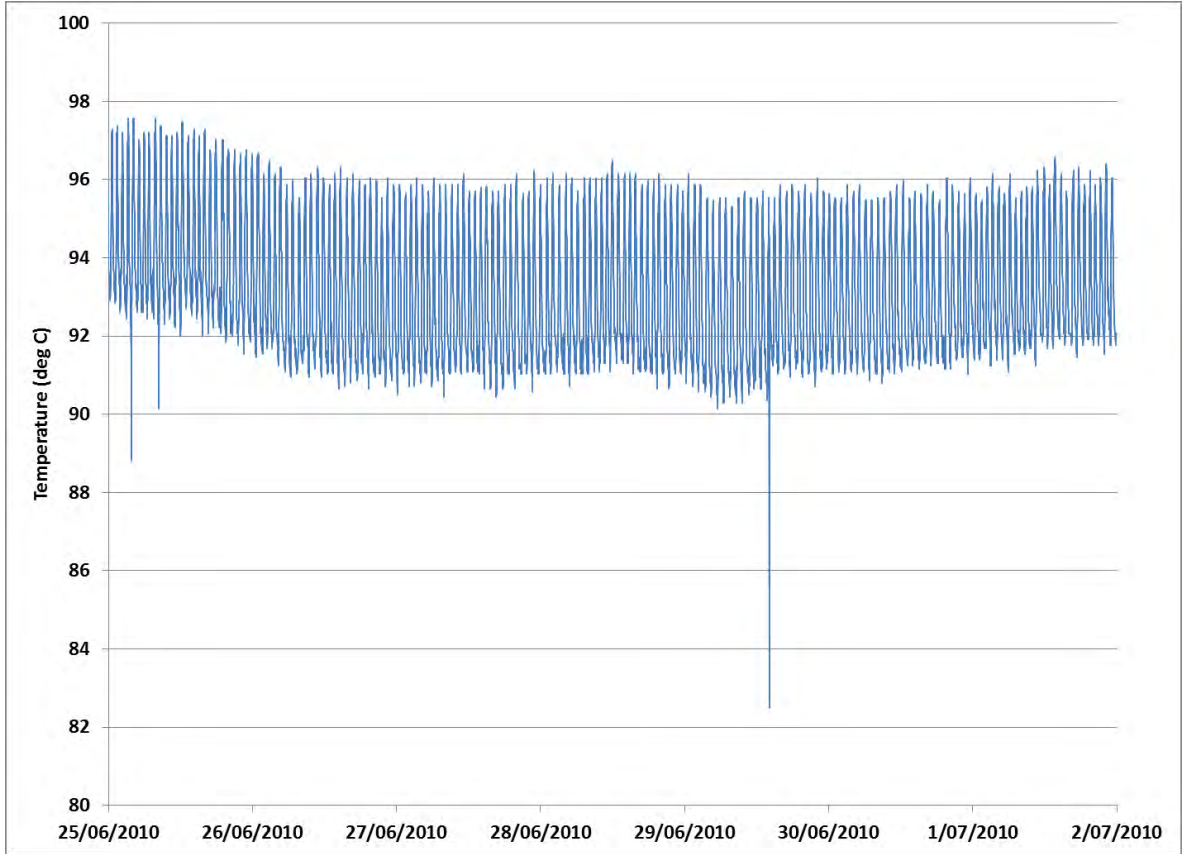
Figure 49. Spring temperature: blue line; seismic activity: black circles. Darker circles indicate that the seismic event was closer to the Soda Fountain. (a) Dataset 1. (b) Dataset 2. (c) Dataset 3. (d) Dataset 4. (e) Dataset 5.

3.6 *Fourier Analysis*

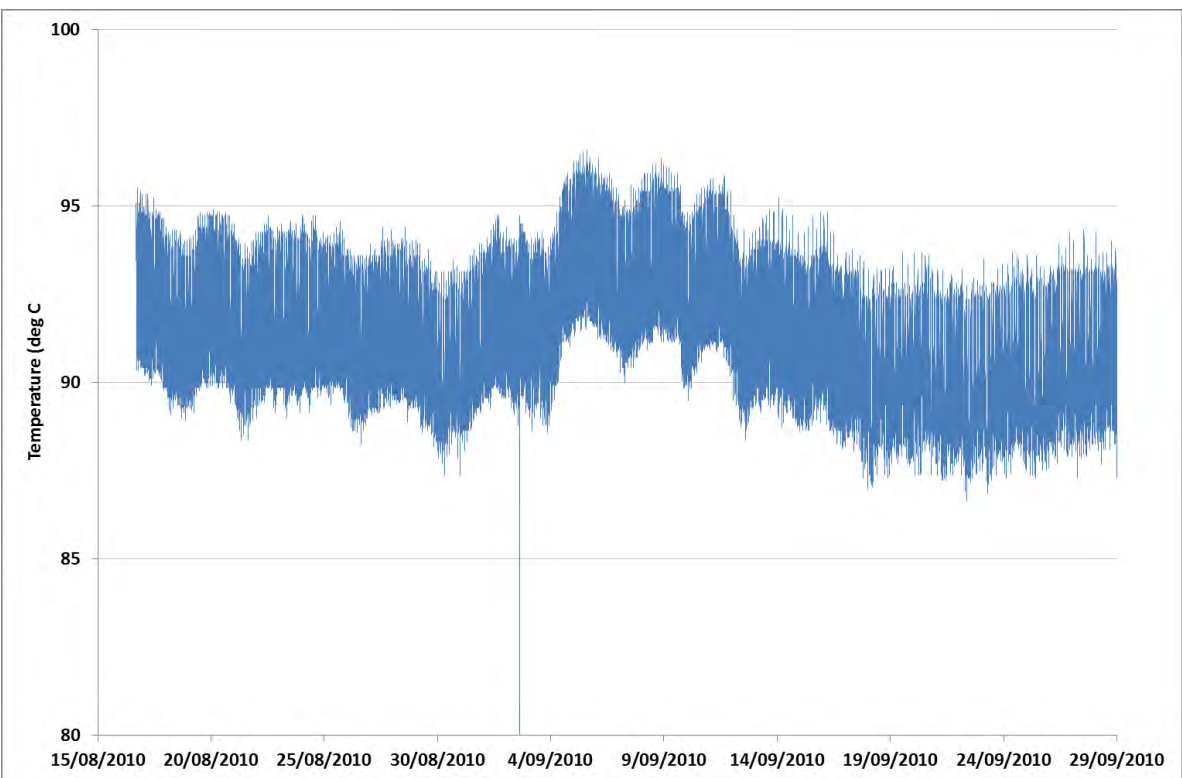
In order to analyse the frequency components of the temperature cycles we use the same Discrete Fourier Transform procedure we applied to the Waiotapu Geyser.

The datasets have been broken down into intervals which display regular cyclic temperature variation of less than 10 degrees, and a high average temperature (greater than 90 °C) shown in Figure 50 (a) to (f). This ensures that the analysis is applied to water temperature, and not to intervals where the datalogger may have recorded air temperature over part of the cycle as discussed in the previous section. This provides eight suitable time intervals; one interval from Dataset 1, the entire interval of Dataset 2 (16th August to 30 September), three intervals from Dataset 3, one from Dataset 4, and two from Dataset 5.

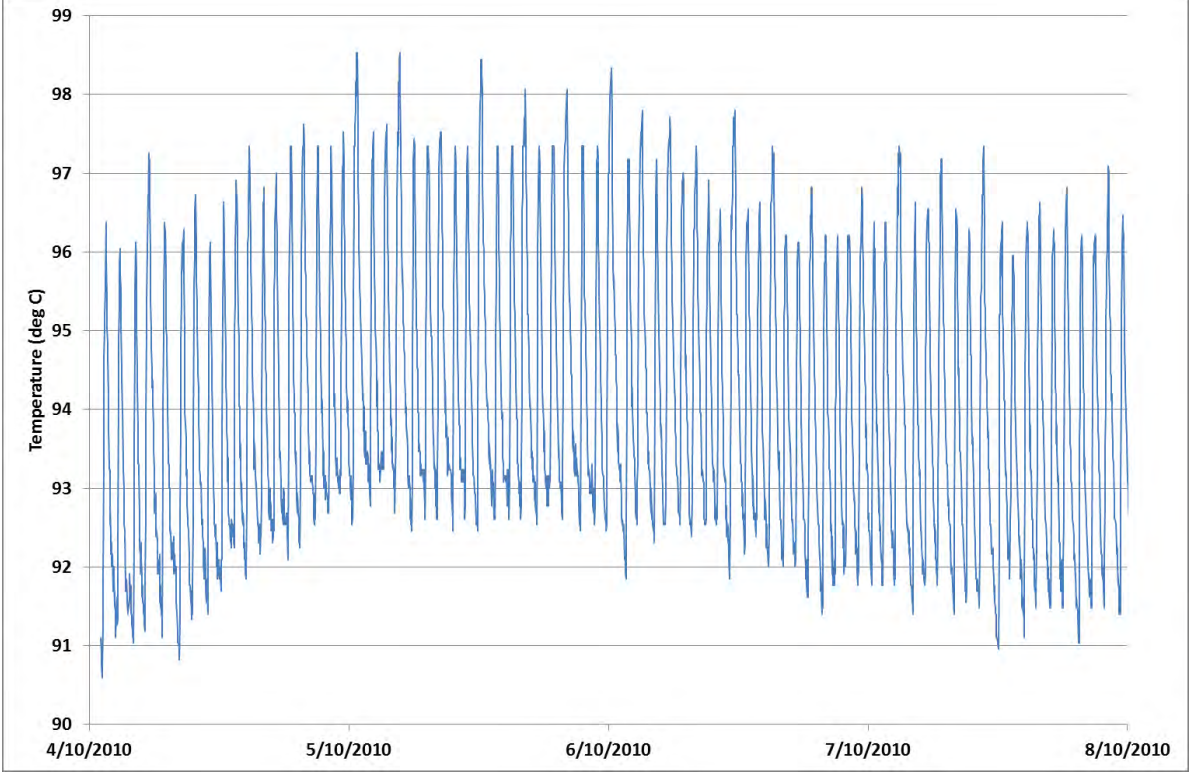
The data details and results of the analysis are given in Table 1 and shown graphically in Figure 51.



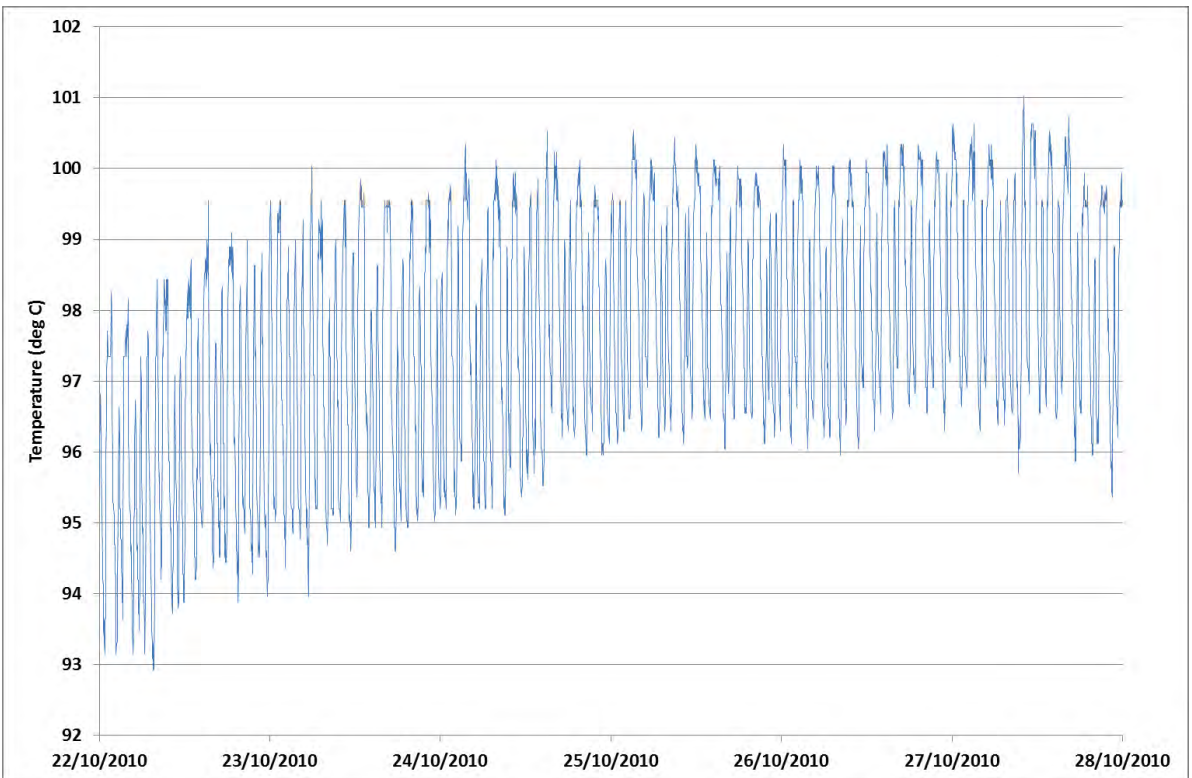
(a)



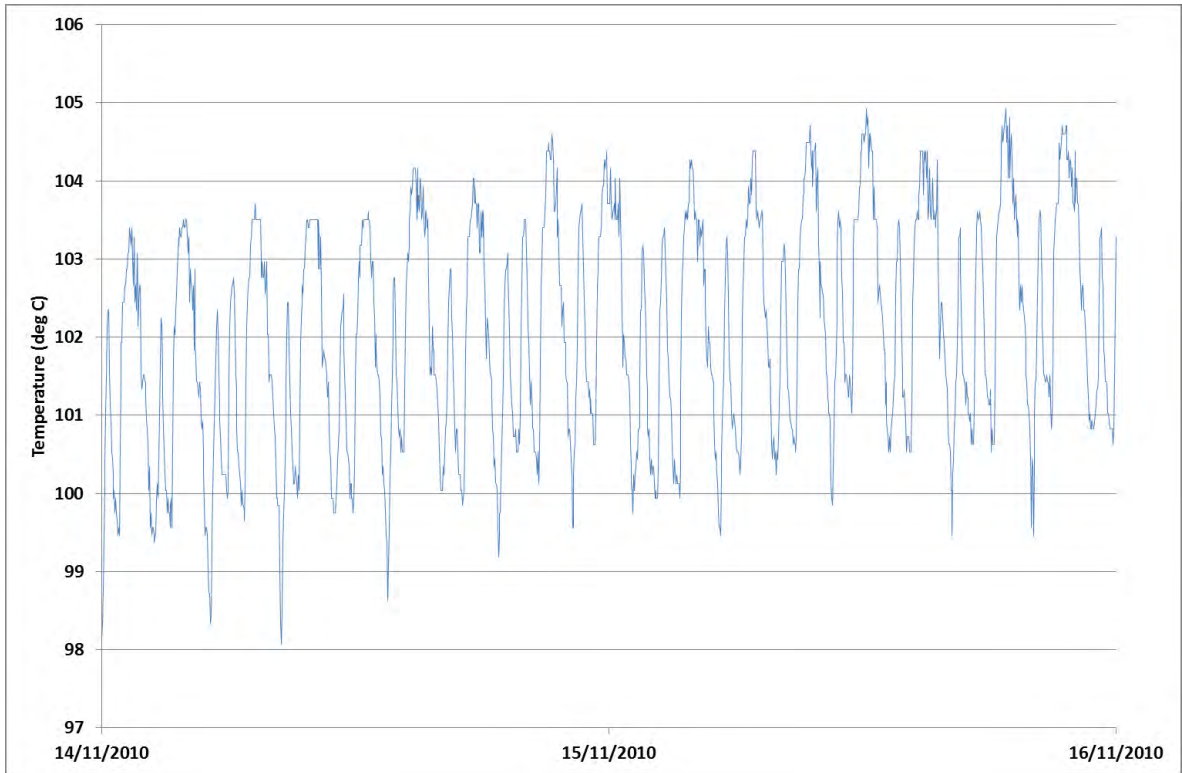
(b)



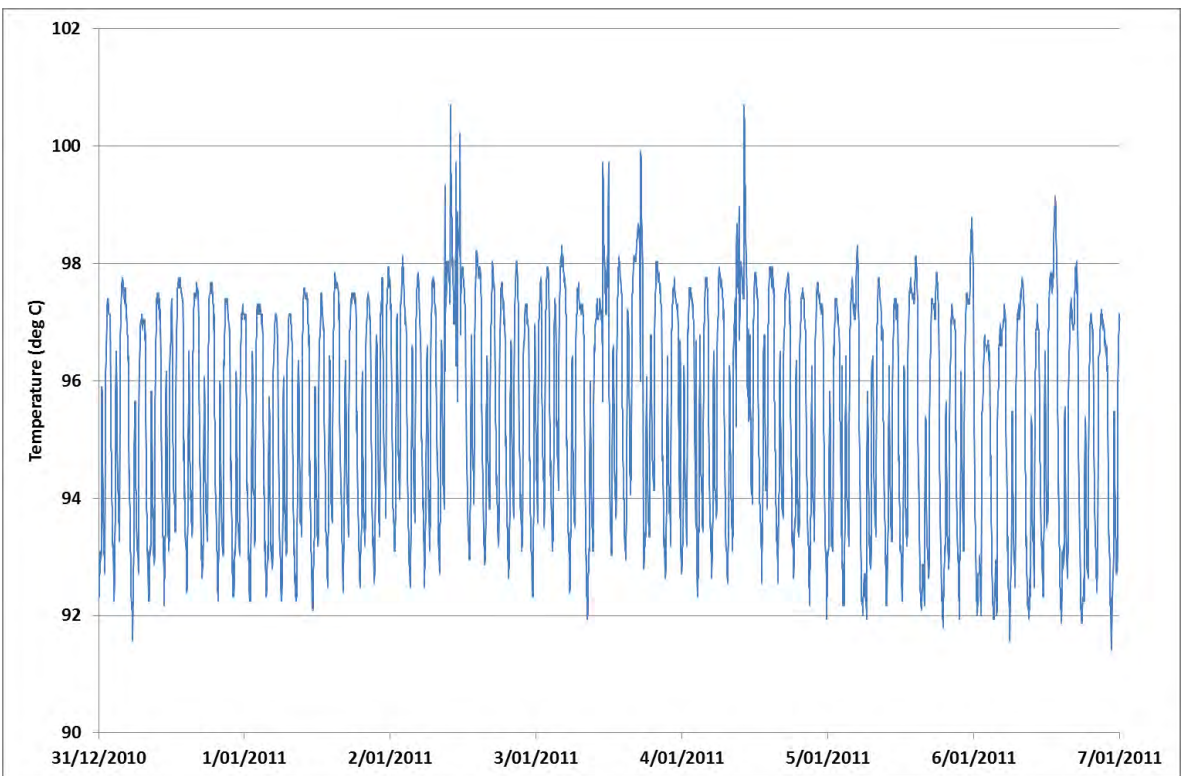
(c)



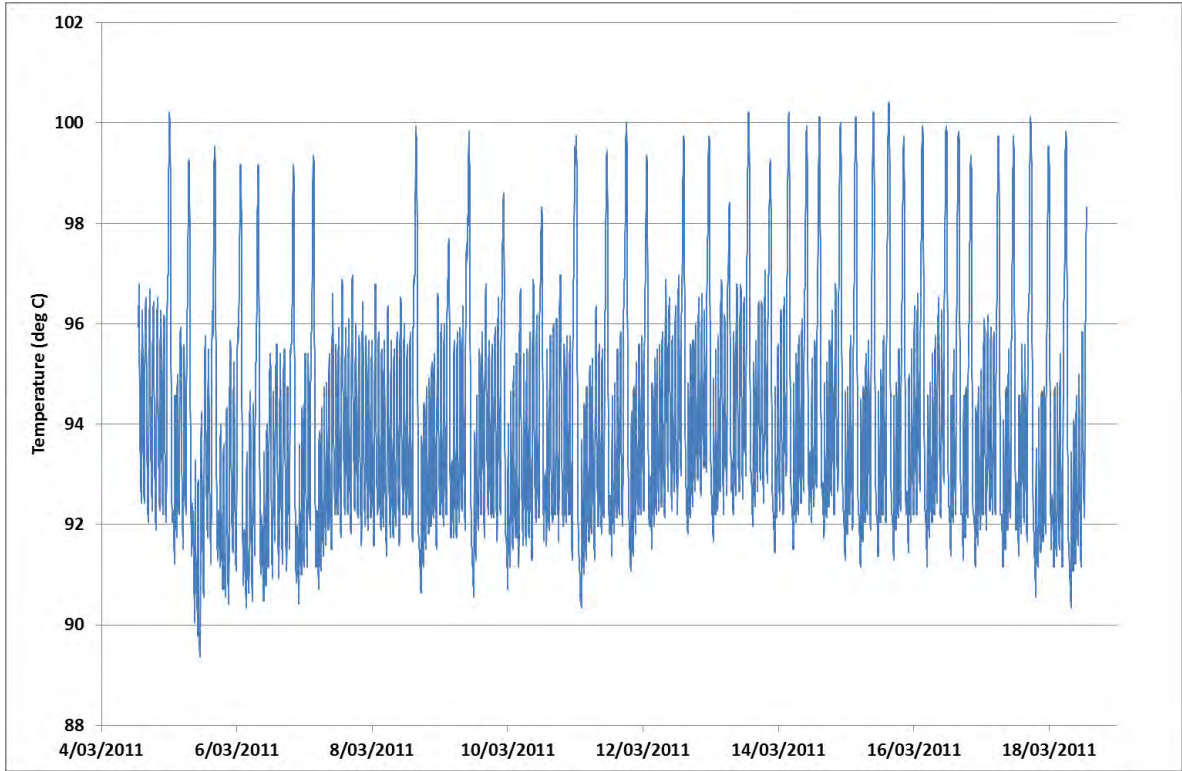
(d)



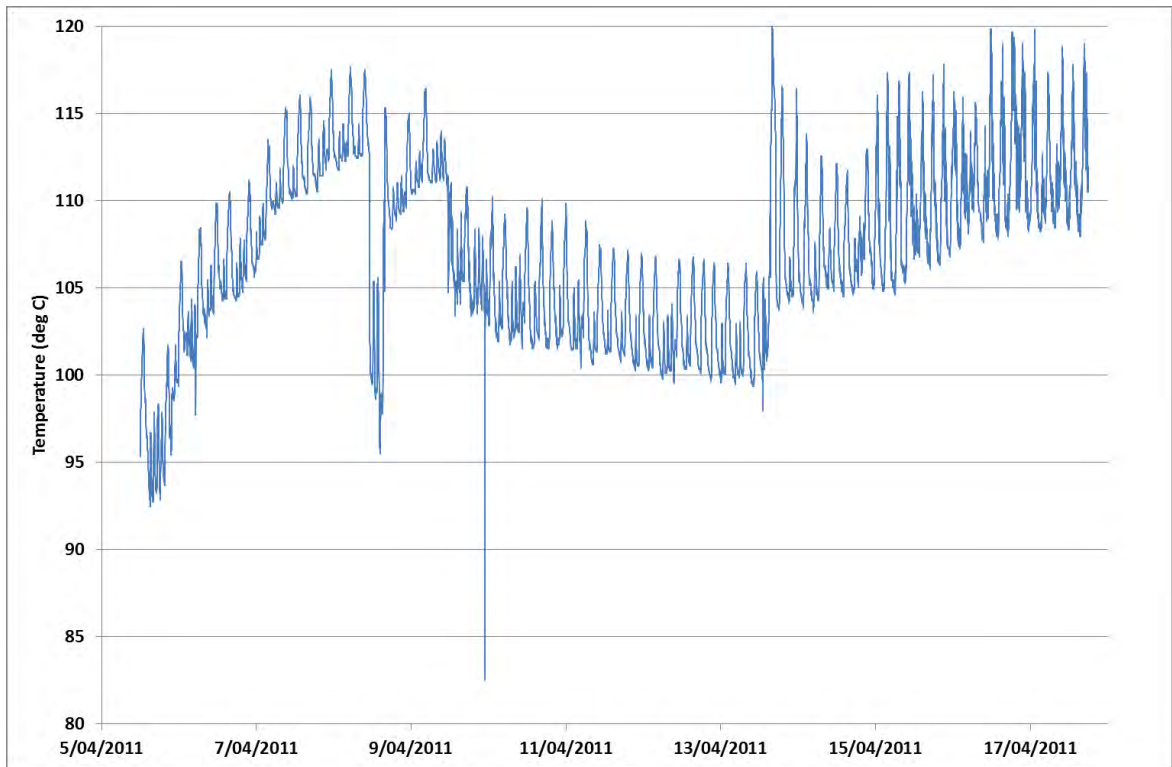
(e)



(f)



(g)



(h)

Figure 50. Plots of the subsets of Soda Fountain Datasets that have regular temperature variation and are suitable for a Fourier analysis. The entire dataset for Dataset 2 is suitable, while Datasets 3 and 4 have shorter time intervals within each dataset. (a) Dataset 1, Subset 1. (b) Dataset 2, entire dataset. (c) Dataset 3, Subset 1. (d) Dataset 3, Subset 2. (e) Dataset 3, Subset 3. (f) Dataset 4, Subset 1. (g) Dataset 5, Subset 1. (h) Dataset 5, Subset 2.

Table 1. Details and Results of Fourier analysis for all datasets.

Dataset	Subset	Interval	Length (days)	T _{av} (°C)	Dominant frequency (cycles/hr)	Length of cycle (hr)
Dataset 1						
	Subset 1	25/06/2010 - 02/07/2010	7	92.9	1.02	0.98
Dataset 2						
	Entire dataset	15/08/2010 - 29/09/2010	45	91.1	0.94	1.06
Dataset 3						
	Subset 1	04/10/2010 - 08/10/2010	4	94.0	0.78	1.28
	Subset 2	22/10/2010 - 28/10/2010	6	97.6	0.42	2.38
	Subset 3	14/11/2010 - 16/11/2011	2	102.0	0.33	3.03
Dataset 4						
	Subset 1	31/12/2010 - 07/01/2011	7	95.4	0.38	2.63
Dataset 5						
	Subset 1	04/03/2011 - 18/03/2011	14	94.0	0.16	6.22
	Subset 2	05/04/2011 - 17/04/2011	12	107.0	0.28	3.58

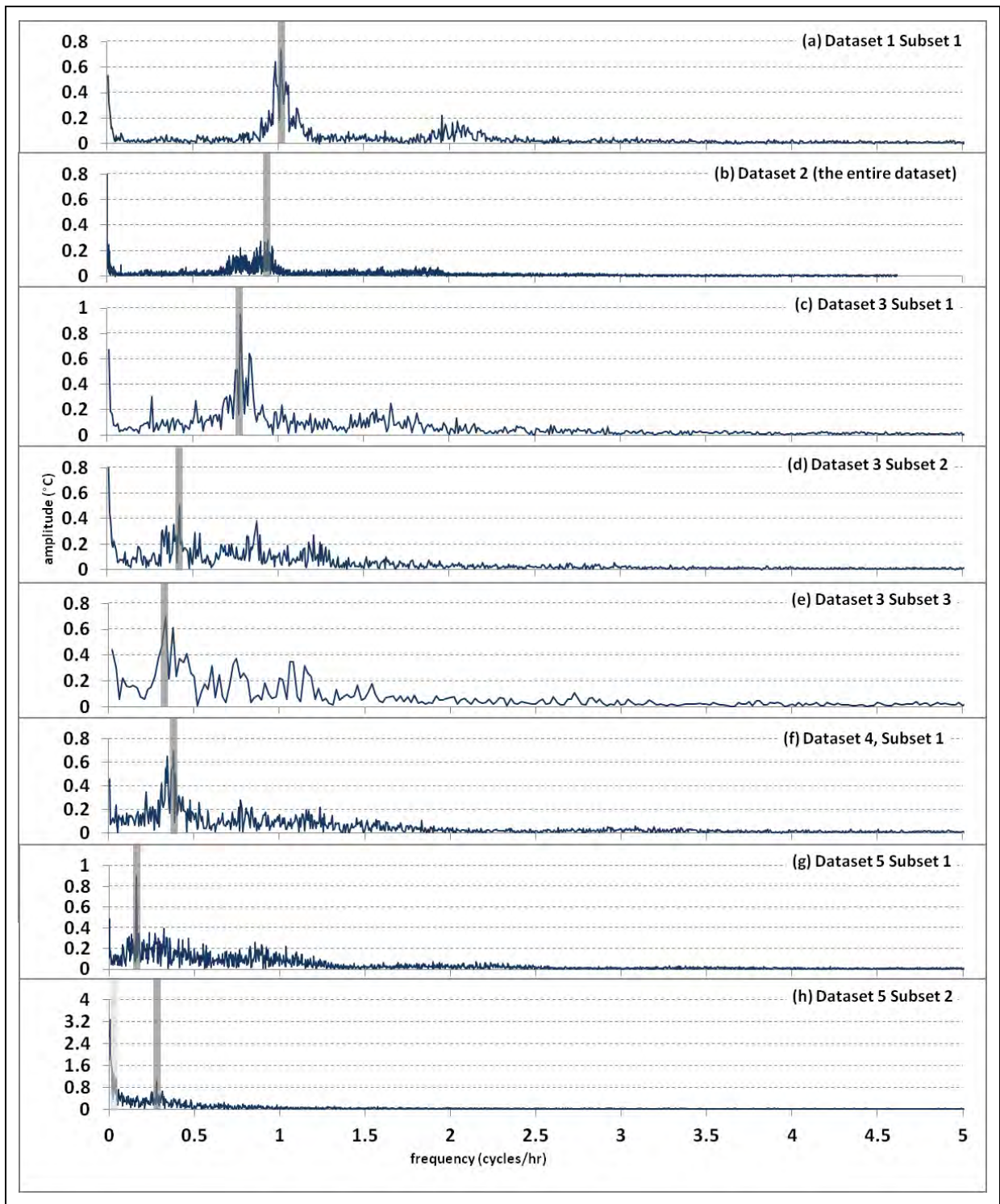


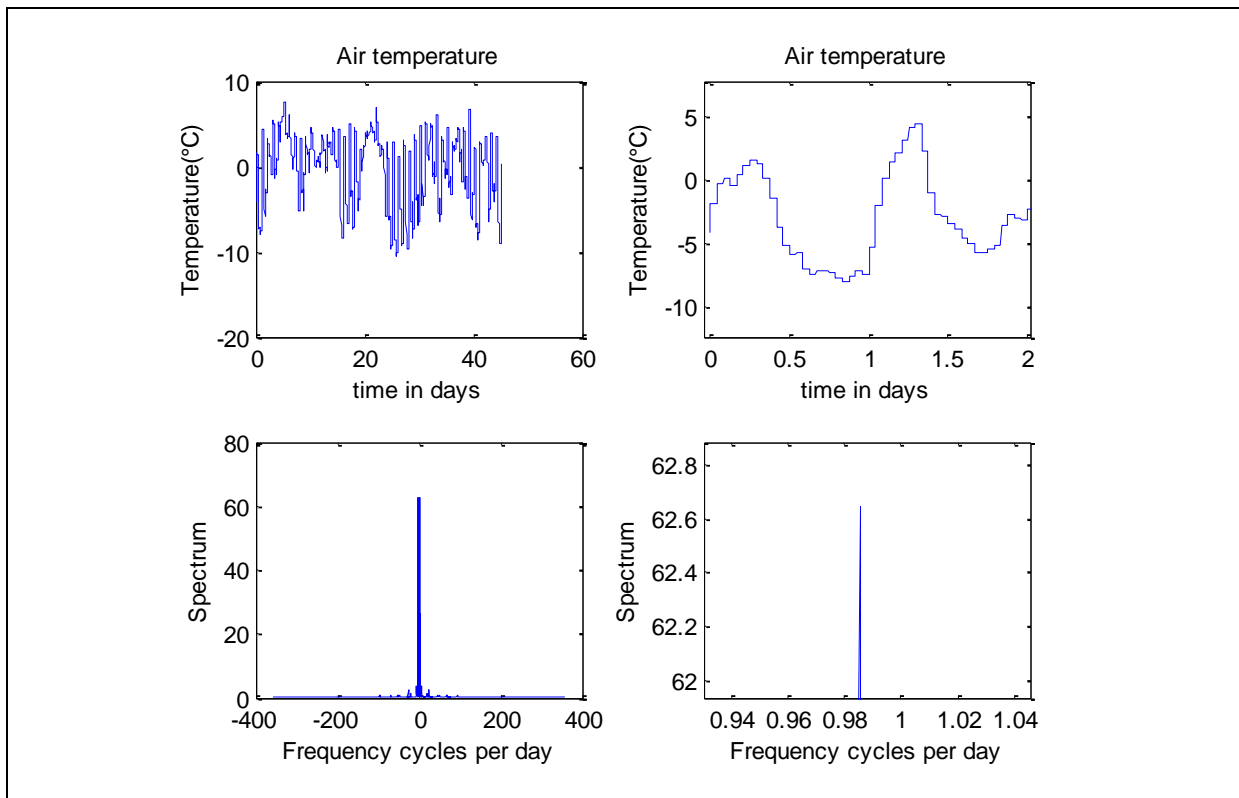
Figure 51. Frequency vs amplitude from the Fourier analysis. The vertical line highlights the dominant frequency for each dataset (also see Table 1). Note that Dataset 5 Subset 2 has a large amplitude, low frequency component, highlighted here by a very light grey line. The frequency of interest, that is comparable to the other datasets, is highlighted by the darker grey line.

3.7 Air pressure and the temperature cycle

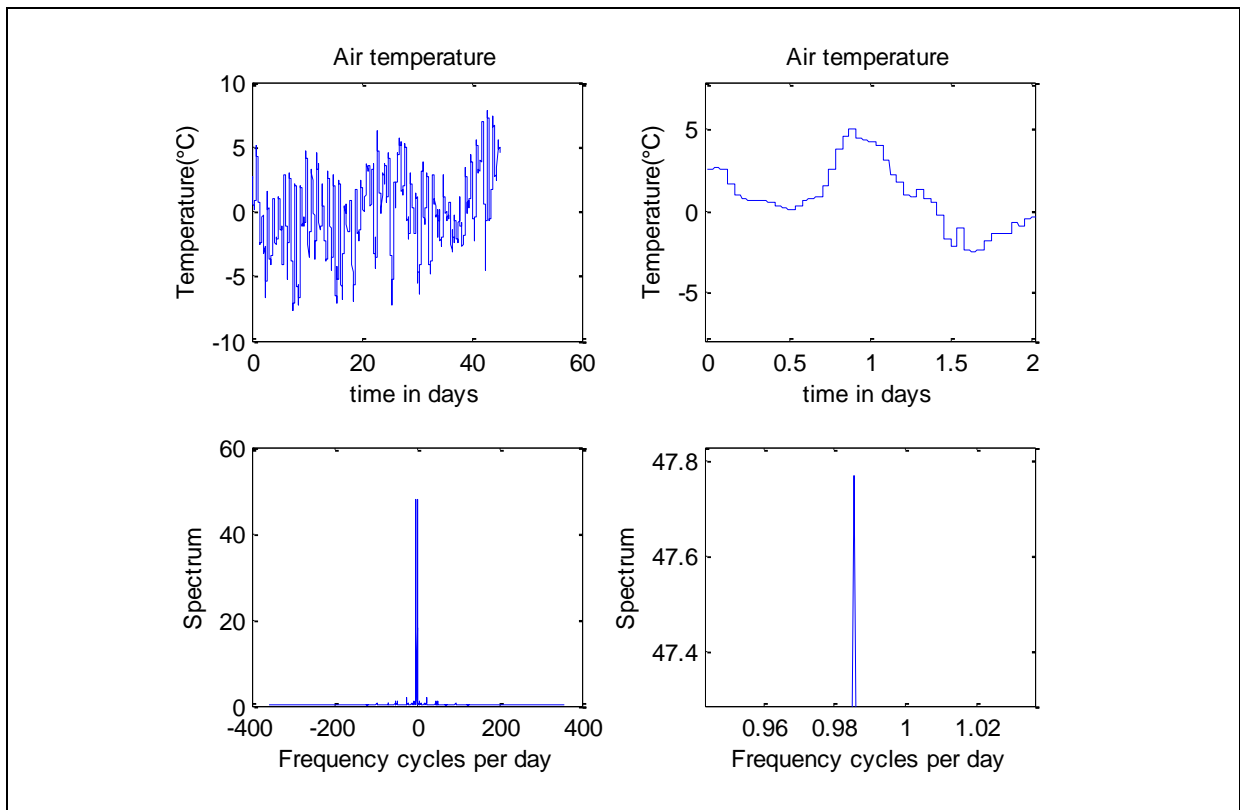
We now turn our attention to air temperature variations. The air temperature is plotted against time for Datasets 1–5 in Figure 52 (a) to (e). In the same way as before, by analysing air temperature data we find dominant frequencies of one cycle per day throughout all the datasets as one would expect. Hence it is reasonable to rule out air temperature as having any significant effect on the system.

When analysing data from the Waiotapu Geysir, we developed an algorithm for picking out the temperature cycle peaks and taking the time intervals and the average air pressure between those peaks. We then took the natural logarithm of these time intervals and plotted them against the average air pressure in order to find some sort of relationship between air pressure and eruption frequency.

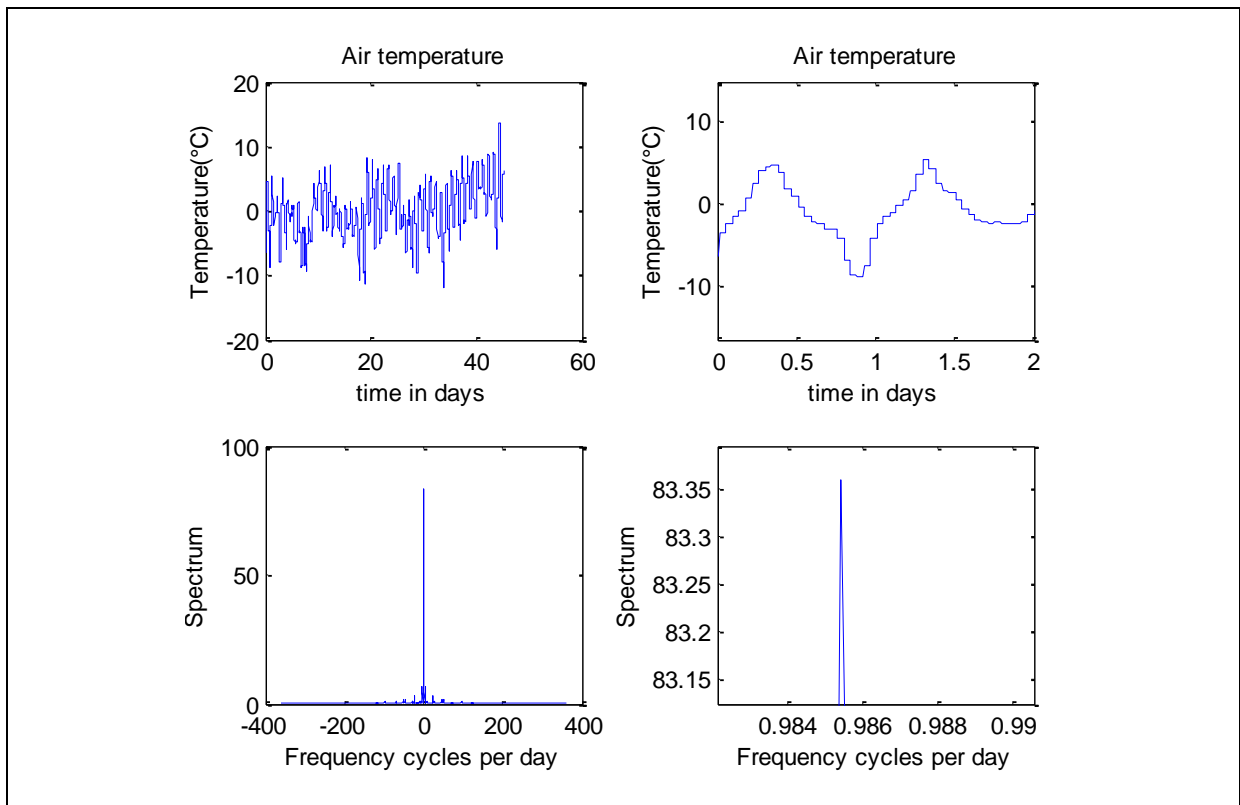
In this section we use the same algorithm (with a small adjustment) and apply it to the Soda Fountain Dataset 2 (since it is the most well behaved of the datasets) to check for any influence air-pressure may be having on the cyclic behaviour of the spring (see Figure 53).



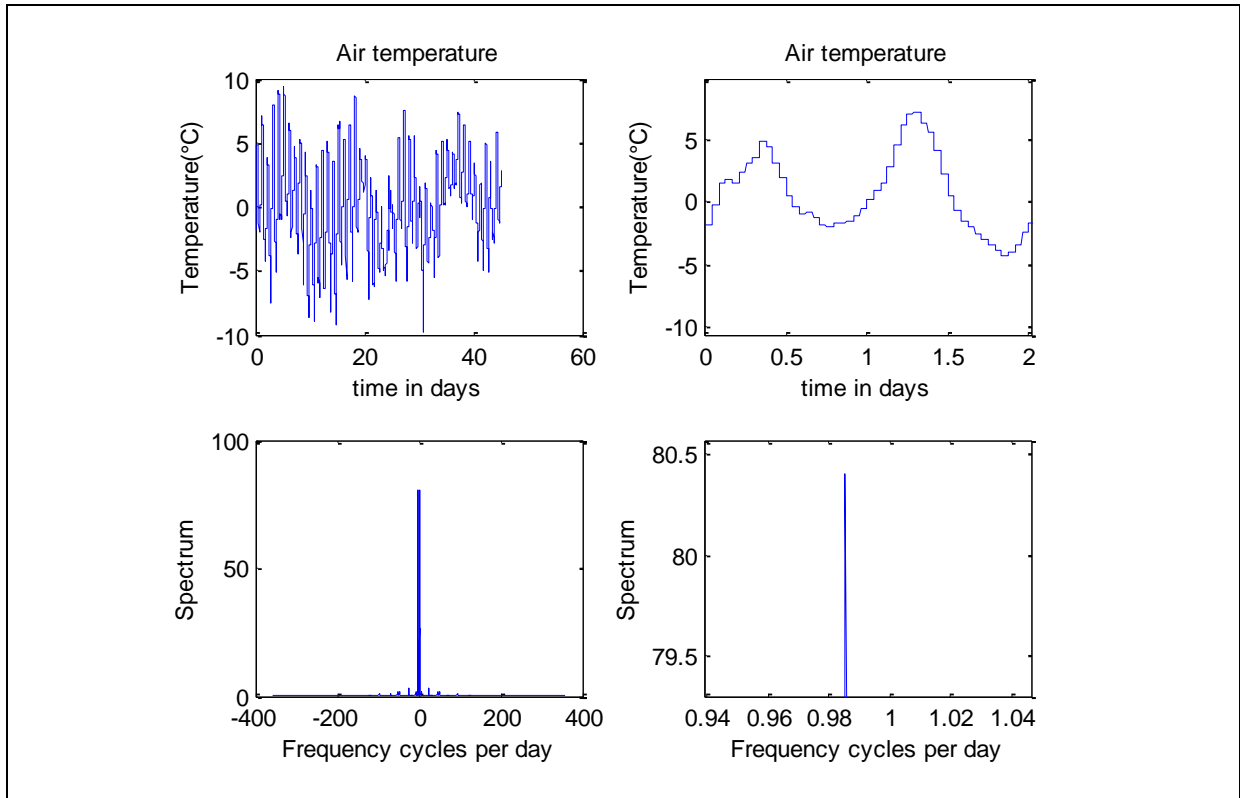
(a)



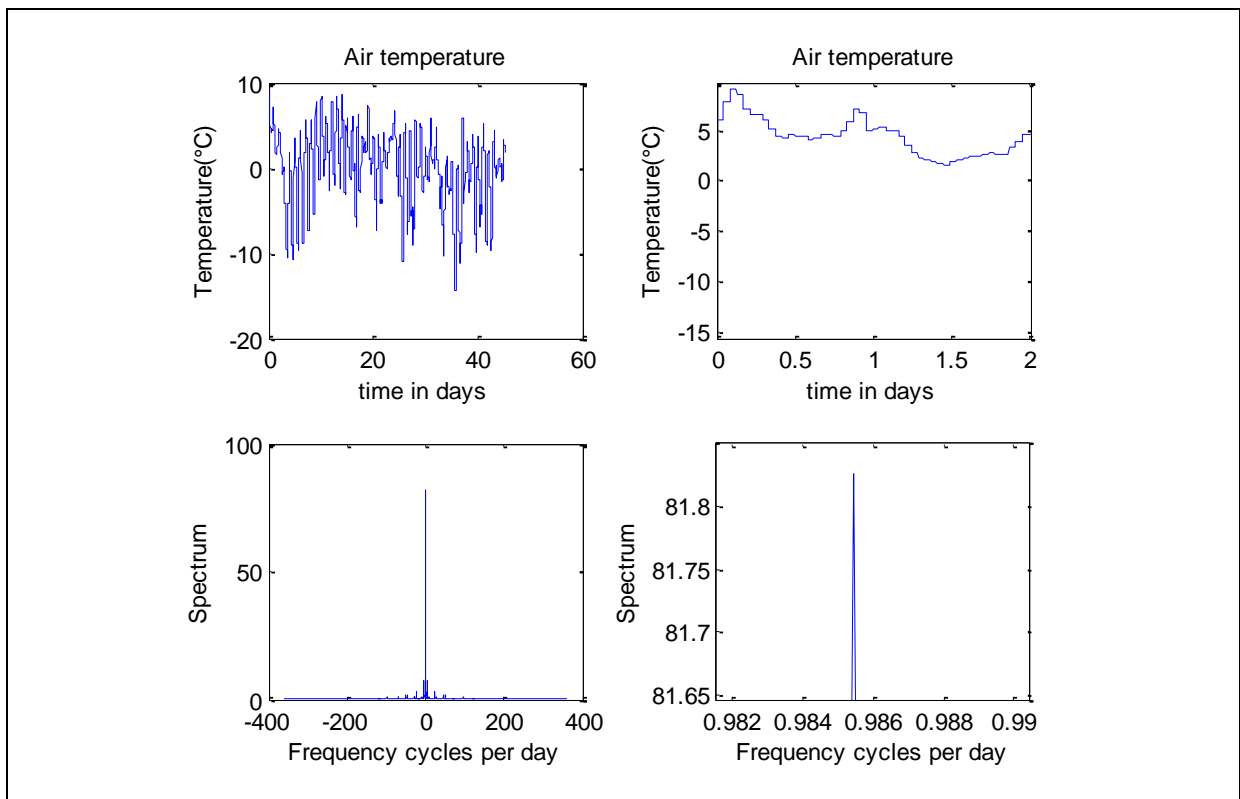
(b)



(c)



(d)



(e)

Figure 52. Air-temperature data for the time intervals for (a) Dataset 1. (b) Dataset 2. (c) Dataset 3. (d) Dataset 4. (e) Dataset 5. The left upper graph shows the air-temperature for the given dataset while the right upper graph shows the temperature on the first two days. The lower left graph is the frequency spectrum and the right lower graph zooms in onto the spectrum to identify the dominant frequencies. The dominant frequencies are around 1 cycle per day.

The plot of time intervals between cycle peaks against the average air pressure between the peaks does not show any apparent correlation (Figure 54). A regression analysis of the natural logarithm of the cycle frequency against air-pressure again shows little correlation (Figure 55). Note that what we refer to as cycle frequency here is the inverse of the time between two peaks.

Some extra information that comes from this analysis is that the average time period between the peaks is about 1 hour 9 minutes. Considering the different methods of analysing the data, this is a good agreement with the Fourier analysis, which gives the dominant period at 1 hr 3.6 min.

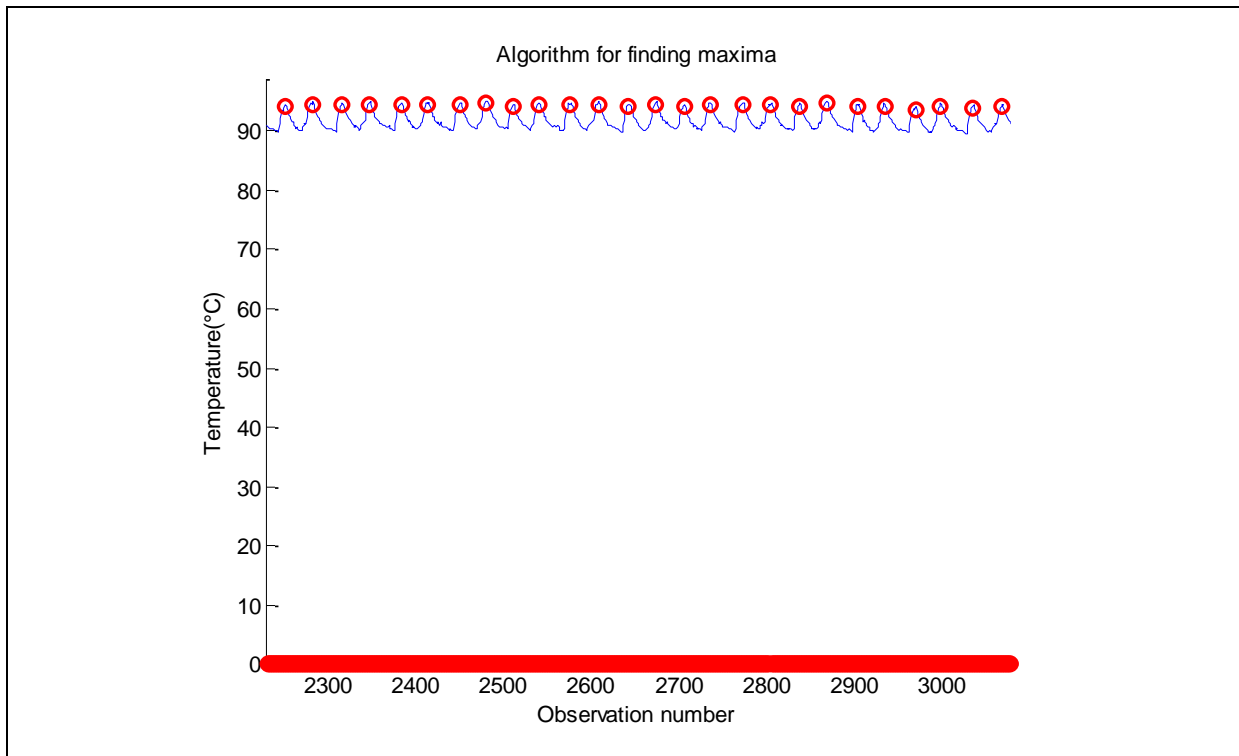


Figure 53. The algorithm picks out the maximum point in each cycle.

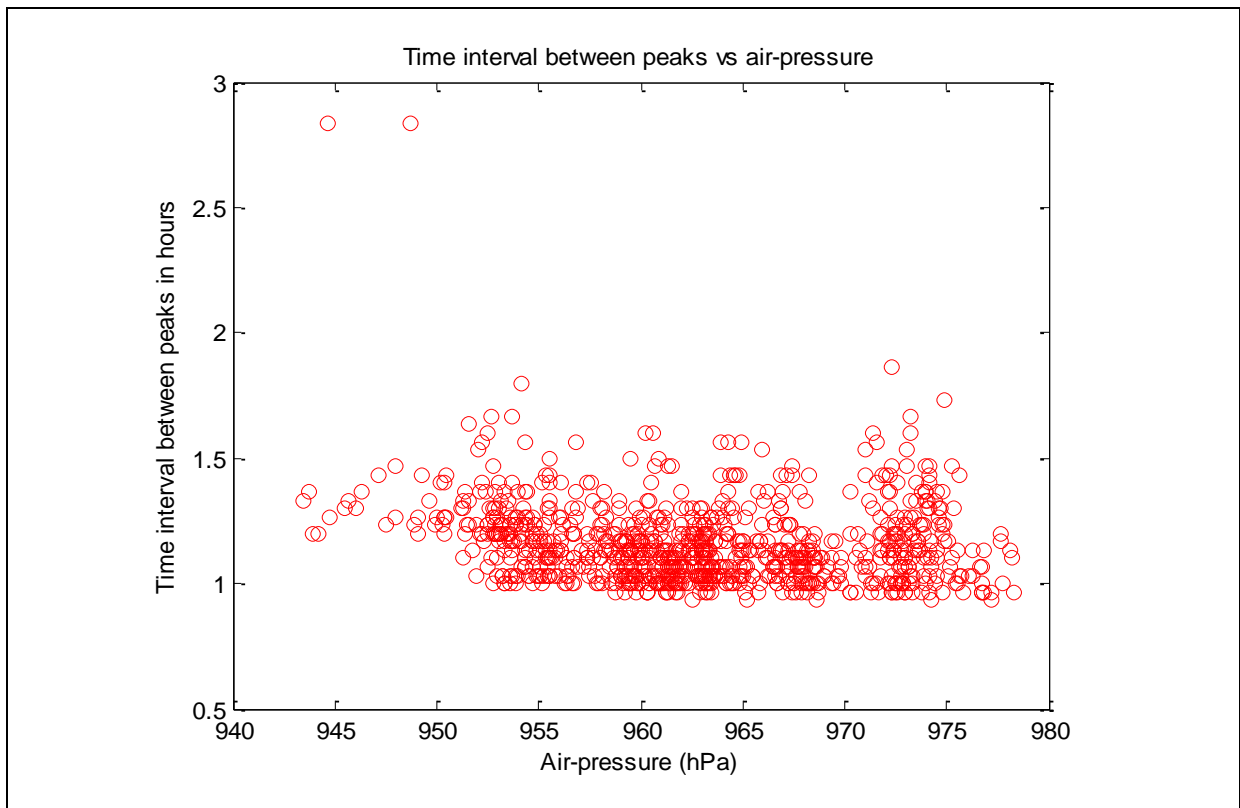


Figure 54. A plot of time between cycle peaks against average air pressure between the peaks.

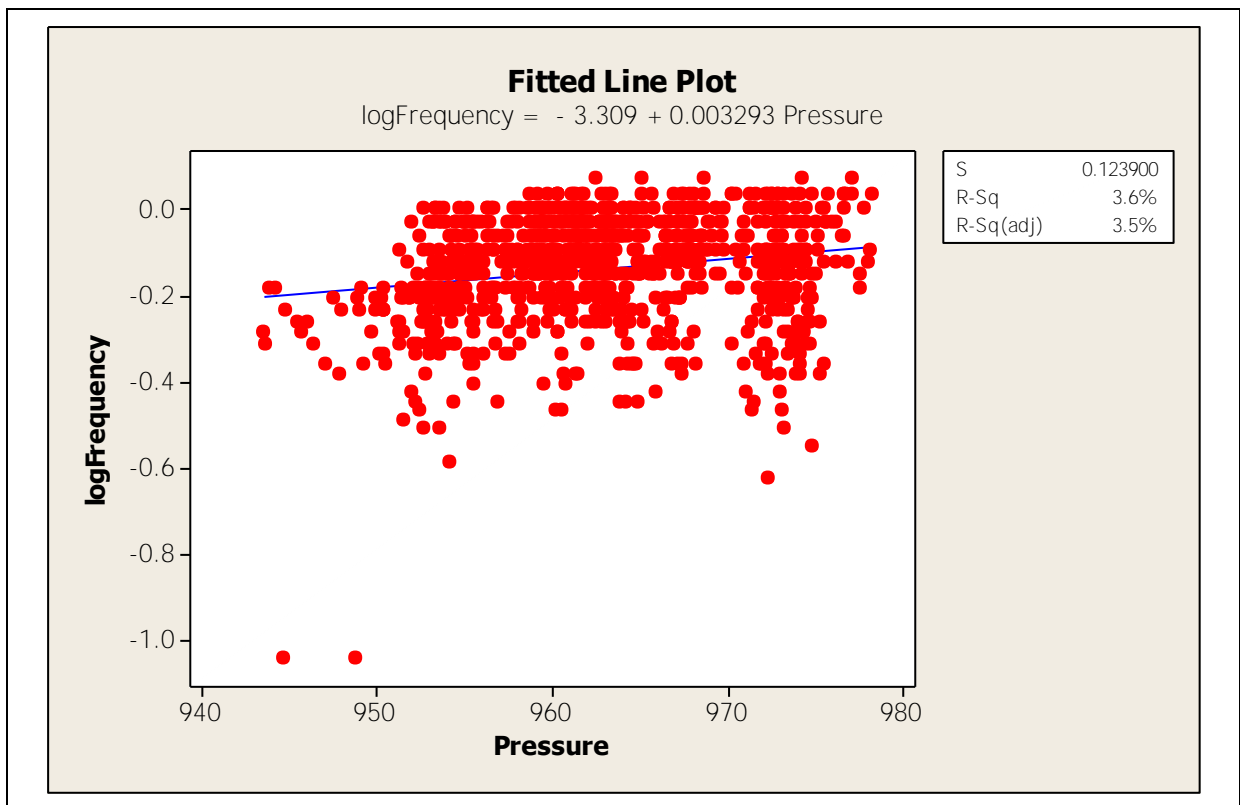


Figure 55. Log (frequency) against average air-pressure: regression plot.

3.8 Soda Fountain: Conclusion

No effects due to air temperature, air pressure, rainfall or seismic events on the Soda Fountain were identified.

A Fourier analysis of temperature data from the Soda Fountain shows that for the time intervals sampled, the temperature cycle was between one and six hours, with an average temperature between 91 and 107 °C. The maximum temperature reaches 120 °C in Dataset 5. There are no observations of spring temperature at this time, but if the temperature recording was accurate, there is a possibility that this could be a period of geysering.

The cause of the cycle is not known. It may be due to the spring's own internal dynamics, other nearby springs or other, as yet unidentified, factors.

There are intervals during which the water level in the spring shows large fluctuations. We suggest that the water level fell below the probe level and the minimum temperature measurements were of air, rather than water temperature.

4 DISCUSSION AND RECOMMENDATIONS FOR FUTURE MONITORING

This study applies a quantitative approach to geothermal temperature time series. While it has produced interesting results in terms of demonstrating a relationship between air pressure and spring activity, and identified the dominant frequencies in cyclic data, it also contains lessons for designing future monitoring programs. Issues that should be addressed are briefly discussed below:

Data continuity

The discontinuity of the datasets means that any relation of spring cyclic activity to climatic variables is limited to short-term response. Continuous data would show, for instance, if there is any seasonal component in activity. There may also be a longer-term response to hydrologic conditions which cannot be identified with short, discrete, datasets.

Hydrology of the surrounding area

Changes in spring behaviour may also indicate human-induced changes in the environment. In the case of Orakei Korako, the adjacent Lake Ohakuri water levels are controlled by electricity generation from hydro dams. Time was too short to include Lake Ohakuri water level data, but this data should be included in (and be readily available for) future studies of Orakei Korako springs.

Water level or pressure data

The springs have been observed to show water level changes, however no data is available. Future data collection should include water level or pressure information. This would enable a better interpretation of temperature data; for instance, whether the recorded temperature is always a water temperature, or if at some point in the cycle, the probe is sensing air temperature.

Multiple temperature measurements

This study is based on temperature time series taken from a single point in each spring. If it is possible to obtain temperature data from multiple levels in the feed channel, this may give information on processes in the feed channel of the springs (for instance boiling, and/or location and timing of inflows).

No correlation with seismic events can be seen in the data used for this study. This is surprising given the correlation with seismic events reported in the literature and reviewed in Section 1. However, the quality of seismic data is not good with respect to location, which may affect the results of this study.

Preservation of natural geothermal features is important for several reasons; because of their intrinsic beauty, their value as a tourist attraction, because they are indicators of heat and mass flow through the geothermal system, and also as indicators of subsurface geothermal conditions. With the continued development of New Zealand's geothermal resources, understanding the natural variability and the response of natural surface features to external inputs is of paramount

importance for resource management, both in terms of protecting the geothermal springs, and understanding the subsurface system.

If the natural variability of spring behaviour is understood, then human induced changes may be easier to identify. For this reason, continuous data collection from selected natural springs which have a component of fluid from the deep reservoir should be an important aspect of geothermal monitoring.

5 REFERENCES

- Hanor, J.S. (1980) Fire in Folded Rocks: geology of Hot Springs National Park. Eastern National Park and Monument Association.
- Hedenquist, J.W. (1991) Boiling and dilution in the shallow portion of the Waiotapu geothermal system, New Zealand. *Geochimica et Cosmochimica Acta* 55(10), 2753-2765.
- Hurwitz, S., Kumar, A., Taylor, R. and Heasler, H. (2008) Climate-induced variations of geyser periodicity in Yellowstone National Park, USA. *Geology* 36(6), 451-454. <doi:10.1130/g24723a.1>
- Husen, S., Taylor, R., Smith, R.B. and Heasler, H. (2004) Changes in geyser eruption behavior and remotely-triggered seismicity in Yellowstone National Park produced by the 2002 M 7.9 Denali fault earthquake, Alaska. *Geology* 32(6), 537-540. <doi:10.1130/g20381.1>
- Ingebritsen, S.E. and Rojstaczer, S.A. (1993) Controls on Geyser Periodicity. *Science* 263(5135), 889-892.
- Ingebritsen, S.E. and Rojstaczer, S.A. (1996) Geyser periodicity and the response of geysers to deformation. *Journal of Geophysical Research*, 101(B10), 21891-21905.
- Leaver, J.D., Borges, K. and Unsworth, C. (2005) Analysis of Contemporaneous Pseudorandom Data from Two Springs in the Orakei Korako Geothermal Field of New Zealand. Proceedings of the World Geothermal Congress, 2005, Antalya, Turkey.
- Lynne, B. and Howe, T. (2010) Surface Activity at Orakei Korako Geothermal Field between 1927 and 2009. Report, *Institute of Earth Science and Engineering*, University of Auckland.
- Newson, J. (2011) Geothermal Features Annual Monitoring Report, July 2011. Waikato Regional Council Technical Report 2012/11, <http://www.waikatoregion.govt.nz/tr201211>
- Newson, J. and Netten, M. (2011) Geothermal Spring Temperature Variation. Presentation at the International Union of Geodesy and Geophysics (IUGG) Annual Assembly, Melbourne 2011.
- Rojstaczer, S., Galloway, D.L., Ingebritsen, S.E. and Rubin, D.M. (2003) Variability in geyser eruptive timing and its causes: Yellowstone National Park. *Geophysical Research Letters* 30(18). <doi: 10.1029/2003GL017853>
- Saptadji, N.M., O'Sullivan, M.J. and Freeston, D.H. (1994) Mathematical Models of Geysers at Rotorua geothermal field, New Zealand. *Geotherm. Sci. & Tech.* 4(1), 37-75.
- Saptadji, N.M. (1995) Modelling of geysers. Unpublished PhD thesis, University of Auckland, Auckland.
- Scott, B. J. (1994) Cyclic activity in the Crater Lakes of Waimangu Hydrothermal System, New Zealand. *Geothermics* Vol 23, No 5/6, 555- .
- Bryan, T.S. (2008) *The Geysers of Yellowstone* (4th ed.). University of Colorado Press .

Steinberg, G.S., Merzhanov, A.G. and Steinberg, A.S. (1981) Geyser process: Its theory, modelling and field experiment. Part 1. Theory of geyser process. *Modern Geology* 8, 67-70.

White, D.E. (1967) Some principles of geyser activity, mainly from Steamboat Springs, Nevada. *American Journal of Science* 265, 641-684.